FUNCTIONAL PROPERTIES OF ACTIVE SITE VARIANTS OF YEAST CYTOCHROME *C*

by

STEVEN PATRICK RAFFERTY

B.Sc., The University of Waterloo, 1986

A THESIS SUBMITTED IN PARTIAL FULFILLMENT OF

THE REQUIREMENTS FOR THE DEGREE OF

DOCTOR OF PHILOSOPHY

in

THE FACULTY OF GRADUATE STUDIES

THE DEPARTMENT OF BIOCHEMISTRY

We accept this thesis as conforming

to the required standard

THE UNIVERSITY OF BRITISH COLUMBIA

April 1992

In presenting this thesis in partial fulfilment of the requirements for an advanced degree at the University of British Columbia, I agree that the Library shall make it freely available for reference and study. I further agree that permission for extensive copying of this thesis for scholarly purposes may be granted by the head of my department or by his or her representatives. It is understood that copying or publication of this thesis for financial gain shall not be allowed without my written permission.

Department of Biochemistry

The University of British Columbia
Vancouver, Canada

Date April 27, 1992

DE-6 (2/88)

ABSTRACT

Mitochondrial cytochromes *c* are small, soluble respiratory proteins which exhibit a high degree of amino acid sequence and tertiary structural homologies across the entire eukaryotic kingdom. The influence of mutations within two conserved regions of yeast-iso-1-cytochrome *c* on the physicochemical properties of this protein were examined. i) Invariant residue Phe82, located at the exposed heme edge on the protein surface, was replaced by Tyr, Leu, Ile, Ala, Ser and Gly. ii) Internal residues Asn52, Tyr67, Thr78 and Ile75 form the environment about WAT166, a buried water molecule near the heme. This region undergoes relatively large oxidation-state linked conformational changes and these residues are collectively referred to as 'water switch' residues. The mutants Asn52Ala, Tyr67Phe, Ile75Met and Thr78Gly were studied. The effects of variation at these conserved positions on i) the oxidation-reduction equilibrium, ii) the electron transfer kinetics with inorganic electron transfer partners, and iii) the equilibrium and kinetics of heme axial ligand Met80 displacement by added azide and alkaline pH of yeast iso-1-cytochrome *c*, were determined.

The reduction potentials (pH 6, 25 °C, μ = 0.1 M) of position 82 mutants decreased by up to 45 mV with decreasing size of the side chain. Small differences in the $\Delta H°$ and $\Delta S°$ of reduction were responsible for the observed reduction potentials. Electron transfer rates (corrected for driving force and electrostatics) with the inorganic electron transfer partners $Fe(edta)^{2-}$ (as reductant) and $Co(phen)_3^{3+}$ (as oxidant) increased up to 17-fold as the size of the mutant side chain decreased (pH 6, 25 °C, μ = 0.1 M). Electron transfer reactivity relative to wild type was dependent on the identity of the inorganic electron transfer partner, indicating that mutations at position 82 change that portion of the surface of the cytochrome that contacts electron transfer partners. Eyring plots of the rate data showed small differences in the activation parameters of the mutants. Mutation decreased the stability of the native Fe(III)-Met80 bond, as the binding constant of the cytochrome for added azide, K_{az}, increased up to 5-fold. Kinetic measurements of azide binding (pH 6, 25 °C, μ = 1.0 M) demonstrated that the higher

affinity for azide was caused by increases in the rate of heme crevice opening, from 74 s^{-1} in wild type to greater than 160 s^{-1} for Leu, Ile, Ser, and Gly variants. Phe82 thus has critical roles in i) maintaining a high reduction potential, ii) maintaining the integrity of the Fe(III)-Met80 bond, and iii) forming part of the contact surface with electron transfer partners.

The reduction potentials (pH 6, 25 °C, μ = 0.1 M) of the water switch mutants were at least 33 mV lower than that of the wild type protein. Electron transfer reactivity using the electron transfer partners $Fe(edta)^{2-}$ and $Co(phen)_3^{3+}$ was up to 10-fold higher than wild type, but unlike the position 82 mutants, reactivity relative to the wild type cytochrome was independent of the identity of the electron transfer partner. This observation indicates that water switch mutations influence the electron transfer reactivity of cytochrome *c* by altering the reorganization energy within the protein rather than changing the nature of the contact surface of the protein with its electron transfer partners. Measurements of the azide affinity and the alkaline isomerization of the water switch variants indicated that the stability of the Fe(III)-Met80 bond of these variants was the same as or greater than wild type, with the exception of the Thr78Gly variant. In spite of the improved heme crevice stability and/or electron transfer reactivity of the water switch variants Tyr67Phe, Asn52Ala, and Ile75Met, such variants are extremely rare in nature. This observation suggests that the primary role of the native water switch residues is to maintain a high reduction potential.

TABLE OF CONTENTS

LIST OF FIGURES

LIST OF TABLES

LIST OF ABBREVIATIONS

Å	angstrom
CAPS	3-cyclohexylamino-1-propanesulfonic acid
CD	circular dichroism
CHES	2-(cyclohexylamino)ethanesulfonic acid
CM	carboxymethyl
CN	cyanide
E_{app}	applied potential
$edta^{4-}$	ethylenediaminetetraacetate
$E_{m,6}$	midpoint reduction potential at pH 6
EPR	electron paramagnetic resonance
IR	infra-red
μ	ionic strength
MCD	magnetic circular dichroism
MES	2-[N-morpholino]ethanesulfonic acid
mV	millivolt
NADH	nicotinamide adenine dinucleotide, reduced
nm	nanometer
NMR	nuclear magnetic resonance
ox	oxalate
phen	*o*-phenanthroline
py	pyridine
UV	ultraviolet

ACKNOWLEDGEMENTS

Although this thesis bears only a single name, it really consists of the contributions of many supportive people. It is my pleasure to acknowledge their roles in my career at UBC. I would first like to thank my supervisor, Professor Grant Mauk, for providing me with the inspiration, the tools, and, most importantly, the freedom to develop the project. My thanks to Professors Gary Brayer and Brian James for the gift of their time and expertise as members of my advisory committee.

For all the members of the Mauk, lab, past and present, I give my warmest regards. Special thanks go to Dr. Marcia Mauk, who generously offered her help whenever I had a problem. I thank Dr. Lindsay Eltis and Dr.[2] Tony Lim for their help in the lab in the early days, in addition to trashing buffets and bashing trolls, and to Bhavini Sishta for putting up with us. Thanks go to the father of fermentation, Dr. Alfred Gärtner, and his successors Jackie, Heather, Laura, and Fred, for providing me with large amounts of cytochrome *c*. Dr. Paul Barker must be singled out for teaching me the fine art of cyclic voltammetry, and for acting as our tour guide around the pubs of Oxford; I look forward to his Cambridge sequel. Since Dr. Juan Ferrer is an excellent scientist and a generous friend, he may be forgiven for his less than accurate Spanish translation lessons. The debt of thanks that I owe Dr. Guy Guillemette would require its own chapter; beyond his generosity with his proteins, his friendship and his wine, I must thank Guy and Sylvie for having their first-born on my birthday.

To those in the Smith lab, especially Jeanette Beatty, who convince yeast cells that it's cool to carry cytochrome *c* mutants, I offer my warmest thanks. To those in the Brayer lab (Albert Berghuis, Mike Murphy, Terry Lo, and the Great Master, Gordon Louie) who persuade cytochrome *c* that it's cool to be a crystal, ditto. To the "new" students in Grant's lab, Dean, Christie, Alex and Fred, good luck; you now see that there is a light at the end of the tunnel and no, it isn't the light of an oncoming train.

Marital Marshal Peter Durovic, Simon "Mr. Sportsman" Eastman, and beatnik Louis Lefebvre have absolutely nothing to do (nor do they want to have anything to do) with biological electron transfer. That's their loss, but since they've been my closest friends and fellow travellers on the Rocky Road to Scientific Success, I thank them anyway.

Finally, my love and thanks are offered to mom and dad, who have provided love and constant support, and who have encouraged my curiosity and desire to learn from the very beginning; this is your thesis as much as it is mine. And for my wife, Janet, I save my greatest appreciation of all, for sharing in my successes and comforting me in my failures. Coming home with you washes away all the cares of the day.

This thesis is dedicated to my grandfather, Mr. Lloyd Ludgate, and to the memories of my grandparents, Vivian Ludgate and Mr. & Mrs. Leo Francis Rafferty.

INTRODUCTION

1.1 Overview

The central role of electron transfer reactions in the energy transducing pathways of photosynthesis, respiration, and in the catalytic cycles of many enzymes makes biological electron transfer a phenomenon that merits the extensive theoretical and experimental effort that has been devoted to this field. The study of biological electron transfer systems is a field in which theory, derived from investigations of inorganic models, can be applied to biochemical systems. Consequently, our present understanding of biological electron transfer reactions represents the combined efforts of a wide range of disciplines, from the highly physical to the highly biological.

In such studies, several small, well characterized electron transfer proteins have served as useful models for investigation. Of these proteins, mitochondrial cytochrome *c* has been perhaps the most widely studied example. The popularity of this protein derives in part from its ready availability in large quantities from many species, which provides an abundance of structural and phylogenetic information. Extensive efforts by a large number of investigators have resulted in the description of a great number of chemically-modified derivatives of cytochrome *c* that have been employed to address a wide range of functional questions. Cytochrome *c* has also been shown to be readily amenable to semi-synthetic techniques that allow substitution of specific amino acid residues with others, including non-naturally occurring residues.

The functional characteristics that have been studied through investigation of various species of cytochrome *c* and various modified or semisynthetic forms of the protein are legion. These include assessment of the structural factors responsible for the reduction potential of the cytochrome, the structural elements responsible for the structural integrity of the protein, the nature of binding between cytochrome *c* and its physiological electron transfer partner proteins, and the basis for the pH-dependent functional properties of the cytochrome.

The application of oligonucleotide-directed site specific mutation of proteins (Zoller & Smith, 1983) to the study of cytochrome *c* was facilitated by the availability of a cloned and sequenced gene encoding the yeast cytochrome (Smith *et al.*, 1979). As a result, cytochrome *c* was the first metalloprotein to be modified by this technique (Pielak *et al.*, 1985). Since this initial work, a multitude of variant cytochromes has been constructed and characterized in functional and structural studies designed to probe the mechanism by which cytochrome *c* functions. The balance of this introduction provides a brief background regarding the structure and function of mitochondrial cytochrome *c* and the methods used in this thesis to assess the physicochemical properties of structural variants of cytochrome *c* prepared by site directed mutagenesis. For a comprehensive treatment of all aspects of cytochrome *c*, the reader is referred to the recent monographs of Moore & Pettigrew (Pettigrew & Moore, 1987; Moore & Pettigrew, 1990).

1.2 Structural Features of Cytochrome c

Cytochrome *c* is a small protein with a molecular weight of approximately 12 500, and possesses 104 to 110 residues depending on the species from which it is isolated. Sequence comparison of more than ninety species reveals a high degree of conservation, particularly among the residues that define the heme environment. Twenty six residues are invariant among 96 known sequences, and many other positions have conservative substitutions (Dayhoff, 1972). Differences in length among different species of cytochrome *c* are due to the presence of extra residues at the N-terminus. In this work, the convention of numbering residue positions according to the sequence of tuna cytochrome *c* is followed. Figure 1 shows the amino acid sequence of yeast iso-1-cytochrome *c* (Narita & Titani, 1969).

Comparisons of the three-dimensional structures of cytochrome *c* from several species show that the tertiary structure of this protein has been highly conserved over one billion years. There are remarkable similarities in the overall protein fold and consequently in the positions of highly conserved residues (Bushnell *et al.*, 1990). The structural features of cytochrome *c* described below are believed to be common to most eukaryotic species, as they occur in the four species of cytochrome *c* that have been characterized by X-ray diffraction analysis: tuna heart (Takano & Dickerson, 1981a,b), rice (Ochi *et al.*, 1983), horse heart (Bushnell *et al.*, 1990), and yeast (Louie & Brayer, 1988, 1989, 1990).

The primary structural feature of cytochrome *c* is that it possesses a heme prosthetic group at its active site (Figure 2). The oxidation state of the iron of cytochrome *c* alternates between +3 (oxidized) and +2 (reduced). As the dianion of the porphyrin coordinates to the iron, the heme alternates between a net charge of +1 (oxidized) and 0 (reduced). At neutral pH the heme of cytochrome *c* remains low spin and six-coordinate in both oxidation states.

Heme is covalently bound to cytochrome *c* through thioether linkages provided by cysteine residues 14 and 17, which react with the vinyl groups located on positions 2 and 4 of the porphyrin ring through the action of the enzyme heme lyase. The constraints imposed on the heme by the thioether

-5	Thr	Glu	Phe	Lys	Ala							
1	**Gly**	Ser	Ala	Lys	Lys	**Gly**	Ala	Thr	Leu	**Phe**	Lys	Thr
13	Arg	Cys	Leu	**Gln**	**Cys**	**His**	Thr	Val	Glu	Lys	Gly	Gly
25	Pro	His	Lys	Val	**Gly**	**Pro**	Asn	**Leu**	His	**Gly**	Ile	Phe
37	Gly	**Arg**	His	Ser	**Gly**	Gln	Ala	Glu	Gly	Tyr	Ser	**Tyr**
49	Thr	Asp	Ala	**Asn**	Ile	Lys	Lys	Asn	Val	Leu	**Trp**	Asp
61	Glu	Asn	Asn	Met	Ser	Glu	Tyr	**Leu**	Thr	Asn	**Pro**	**Lys**
73	**Lys**	Tyr	Ile	**Pro**	**Gly**	Thr	**Lys**	**Met**	Ala	**Phe**	Gly	**Gly**
85	Leu	Lys	Lys	Glu	Lys	Asp	**Arg**	Asn	Asp	Leu	Ile	Thr
97	Tyr	Leu	Lys	Lys	Ala	Cys	Glu					

Figure 1 The amino acid sequence of yeast iso-1-cytochrome *c*, with numbering according to the tuna sequence (Narita & Titani, 1969). Residues shown in bold are invariant among 96 known mitochondrial sequences. Underlined residues are the targets of site directed mutagenesis in this work. Lysine 72 is trimethylated, and the N-terminus is not acetylated.

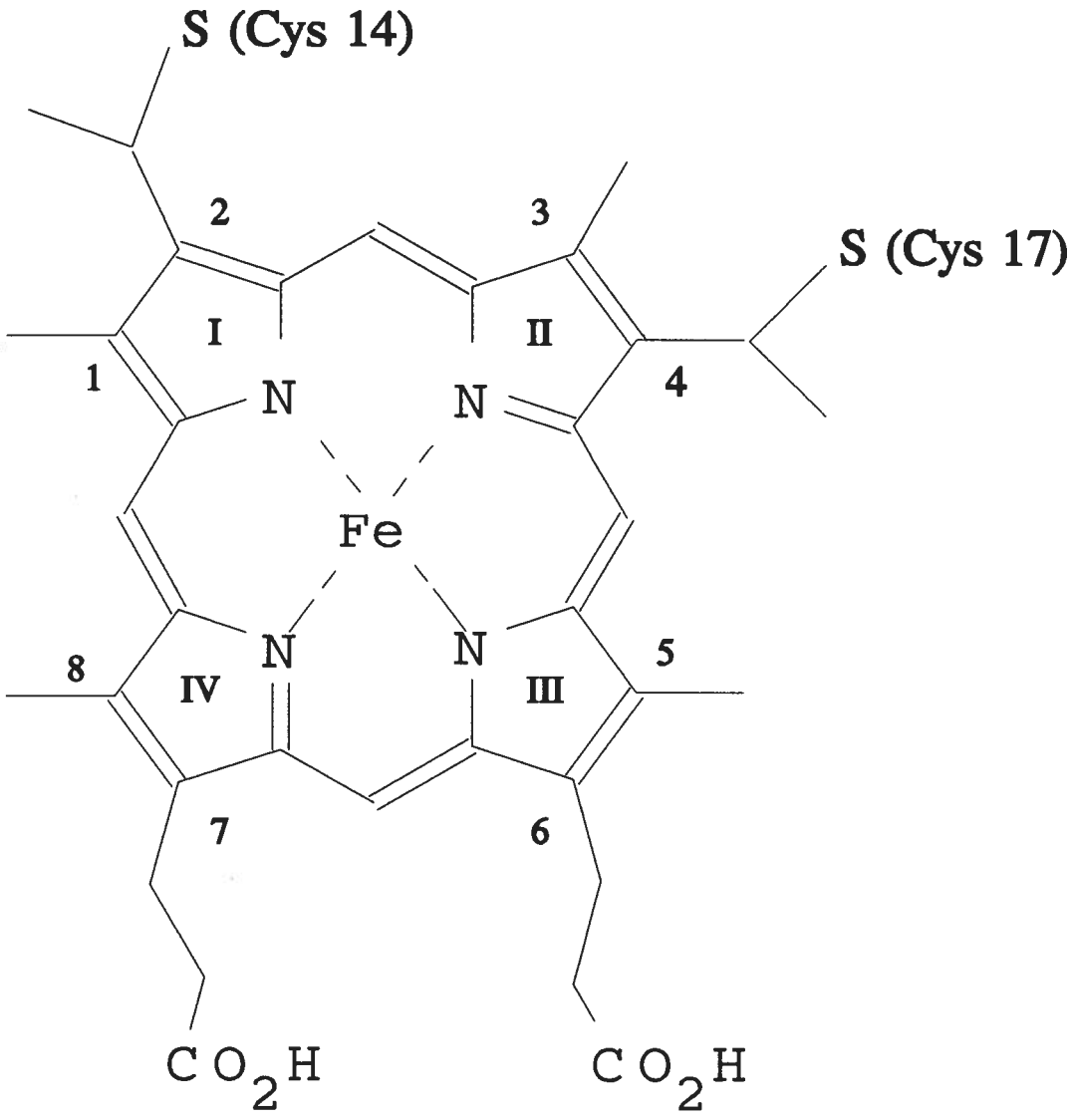

Figure 2 The heme group of cytochrome *c*, showing the numbering schemes of the pyrrole rings (Roman numerals), of the pyrrole ring substituents (Arabic numerals), and the thioether bonds from the protein. Pyrrole rings II and III define the more exposed heme edge of cytochrome *c*.

linkages causes a 'ruffling' of the aromatic ring of the heme. Axial coordination to the heme iron is provided by the $\epsilon 2$ nitrogen of His18 and the sulphur of Met80.

The heme is embedded within the surrounding protein with pyrrole rings II and III closer to the protein surface. This defines the more exposed heme edge. For horse heart and yeast cytochrome *c* respectively, 7.5 and 9.6 percent of the surface area of the heme is solvent accessible, representing about 0.1 percent of the solvent accessible surface area of cytochrome *c* (Bushnell *et al.*, 1990, Louie & Brayer, 1989).

The heme serves as the template about which the polypeptide chain of cytochrome *c* folds. Almost half of the residues occur within the five α-helical segments of the protein. There are six type II reverse turns in cytochrome *c* that cause the direction of the polypeptide chain to change abruptly. The tertiary structure of cytochrome *c* (Figure 3) has dimensions 25 x 25 x 37 Å. Packed against the heme are a set of conserved aromatic residues, which include Trp59, Tyr48, Tyr67 and Phe82.

The heme bears two propionates at positions 6 and 7. As the ionization states of the propionates can influence the oxidation-reduction equilibrium of the heme through electrostatic interactions, an estimate of their pK_as has long been sought. The NMR and IR signals of heme propionates of bacterial cytochromes *c* are sensitive to changes in pH, and pH titrations monitoring these signals have been successful in determining propionate pK_as in these proteins (reviewed in Moore & Pettigrew, 1990). In this manner heme propionate pK_as in the range 6.2 to 8.5 have been measured. The lack of similar pH dependent spectral changes in mitochondrial cytochromes *c* suggests that the dissociation constants of their heme propionates are outside the pH interval 4.5 to 9. An experiment comparing the urea induced proton uptake of oxidized and reduced horse heart cytochrome *c* suggests that one of the pK_as is above 9 while the other is below 4.5 (Hartshorn & Moore, 1989). IR spectroscopy (Tonge *et al.*, 1989) provides evidence for an unusual carboxylate ionization with a pK_a of 9.35. Although the results of these experiments indicate that the two propionates differ in their pK_as by more than 4 pH units, it has not been possible to determine which of the two propionates possesses the higher pK_a. One proposal assigns the

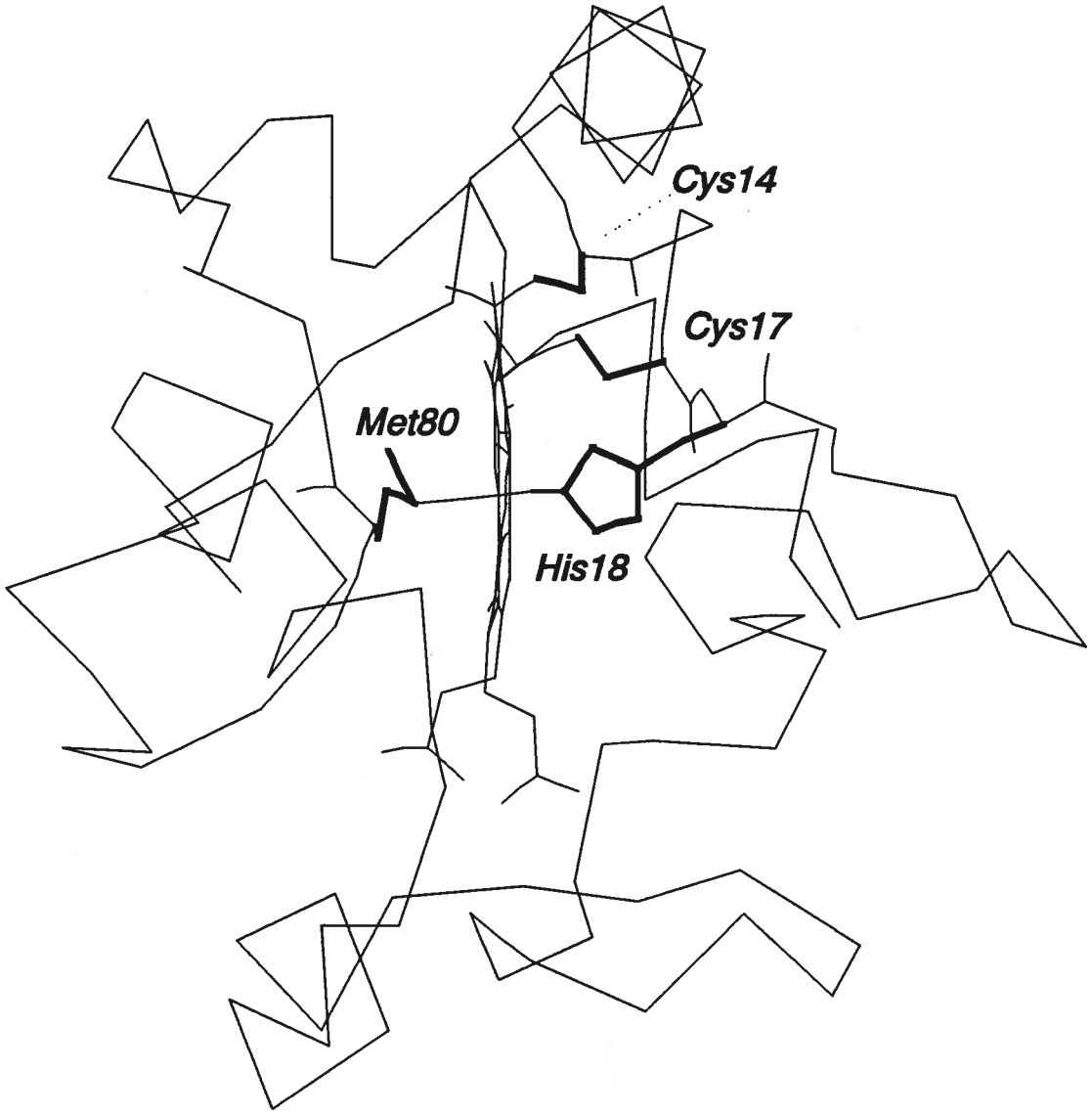

Figure 3 The polypeptide fold of yeast iso-1-cytochrome *c*, showing the heme, the covalent bonds between heme and protein, and the axial ligands (Louie & Brayer, 1990).

pK_a below 4.5 to heme propionate-7, as this group is in contact with the invariant residue Arg38 which is proposed to stabilize the propionate anion through electrostatic interactions (Moore *et al.*, 1984). Heme propionate-6 has thus been assigned the abnormally high pK_a above 9 (Moore & Pettigrew, 1990). However, the proposal that Arg38 is responsible for maintaining the pK_a of heme propionate-7 below 4.5 is not supported by results obtained with position-38 variants of cytochrome *c*, which show no change in either the pH dependence of their reduction potentials[1] or their NMR spectra (Cutler *et al.*, 1989).

Both propionates are buried within the protein, and the residues forming their environment are highly conserved, providing for potential electrostatic and hydrogen bonding interactions. These residues include Thr49, Thr78 and Asn52 about heme propionate-6, and Arg38, Tyr48, Asn52, and Trp59 about heme propionate-7. As it is not possible for all of these potential hydrogen bond partners to interact simultaneously with the propionates, a dynamic equilibrium among hydrogen bonding networks about the heme propionates has been suggested (Moore & Pettigrew, 1990).

Of the three solvent molecules buried within the yeast protein, the one that forms hydrogen bonds with the side chains of the conserved residues Thr78, Tyr67 and Asn52 is of particular interest (Figure 4). This is the site of the largest conformational differences between oxidized and reduced cytochrome *c*. The position of this water molecule (WAT166 by the numbering of Takano & Dickerson, 1981a,b) and its attendant hydrogen bonding partners have been remarkably well conserved in all known structures of native cytochromes *c* (reviewed in Bushnell *et al.*, 1990). Because of the relatively large oxidation-state-linked conformational changes occurring in this hydrogen bond network, the three residues involved will be collectively referred to as the 'water switch' residues in the balance of this work . This term also includes the conserved residue Ile75, which, although not part of the hydrogen bond network, shields this region from exposure to the solvent.

---

[1] Replacement of Arg38 by Lys, Ala, Asn, Gln, His, and Leu resulted in reduction potentials as much as 50 mV lower than the native protein but did not significantly change the pH dependence of reduction potential in the pH interval between 5.5 and 8.5 (Cutler *et al.*, 1989).

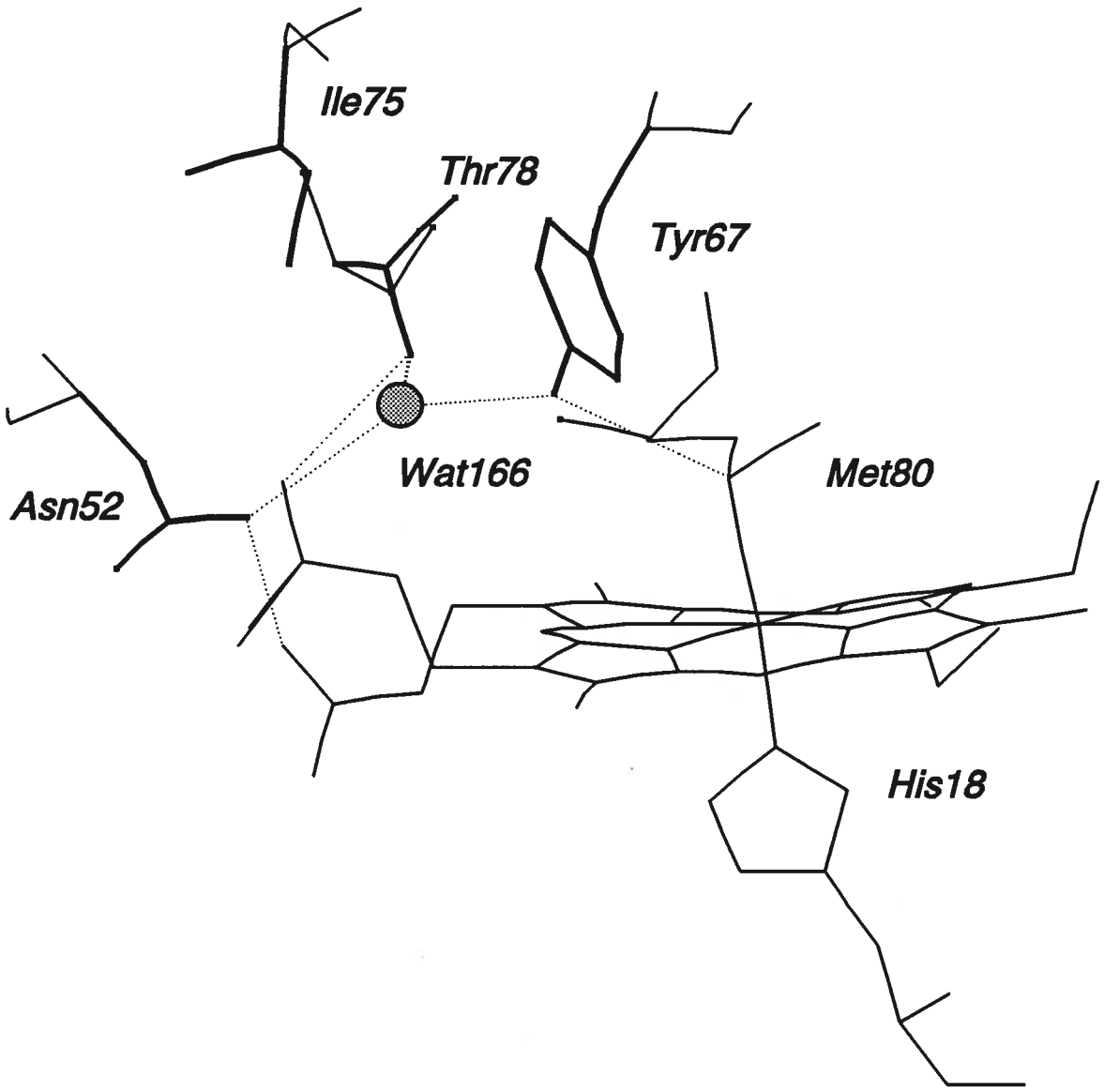

Figure 4 The structure of reduced yeast iso-1-cytochrome *c* about WAT166, with the hydrogen bonding partners to this water molecule indicated by the heavy lines (Louie & Brayer, 1990). Dotted lines indicate hydrogen bonds.

Mitochondrial cytochromes *c* are highly basic proteins owing to an abundance of positively charged residues that are located mainly on the protein surface. Yeast iso-1 cytochrome *c* is a typical example of these proteins, with three arginines, sixteen lysines and four histidines. The surface distribution of these basic groups is asymmetrical, and several of the most conserved such residues encircle the exposed heme edge. Within this 'ring' of basic residues and adjacent to the exposed heme edge is the invariant residue Phe82 (Figure 5). In the crystal structures of cytochrome *c*, the phenyl ring of Phe82 is approximately coplanar with the heme. This residue has been the target of several structural (Louie & Brayer, 1988, 1989) and functional (Michel *et al.*, 1989; Pearce *et al.*, 1989) studies. It is believed to have roles in maintaining a high reduction potential (Kassner, 1972, 1973) and in facilitating electron transfer (Poulos & Kraut, 1980). NMR spectroscopy and molecular dynamics simulations have indicated that this residue may be highly mobile. The rate at which the phenyl ring rotates about the C_β-C_γ bond is estimated to be greater than 10^4 s^{-1} (Williams *et al.*, 1985). By comparison, aromatic residues whose rotation is restrained have rate constants for ring flips on the order of 10 s^{-1} (Moore & Williams, 1980). In a molecular dynamics simulation of the cytochrome b_5 - cytochrome *c* complex, Wendoloski *et al.* (1987) observed large movement of the Phe82 side chain about its C_α-C_β bond that suggested a role for this side chain as an aromatic bridge between the two hemes and providing a facile path for electron transfer. However, this proposal was not supported by an NMR investigation of the cytochrome b_5 - cytochrome *c* complex (Burch *et al.*, 1990), which found no evidence for significant movement of Phe82 about this bond.

Cytochrome *c* undergoes several post-translational modifications to its structure, the most important of which is the covalent attachment of heme to apocytochrome *c*. This step is catalyzed by the enzyme heme lyase, and it is coupled to the translocation of cytochrome *c* across the mitochondrial outer membrane (Hennig & Neupert, 1981, Hennig *et al.*, 1983). Two additional alterations are often observed in mitochondrial cytochromes *c*. N-terminal acetylation in vertebrate and plant cytochromes *c* is catalyzed by an acetyl-coenzyme A / N-acetyl transferase (Tsunasawa & Sakujama, 1984). This modification is

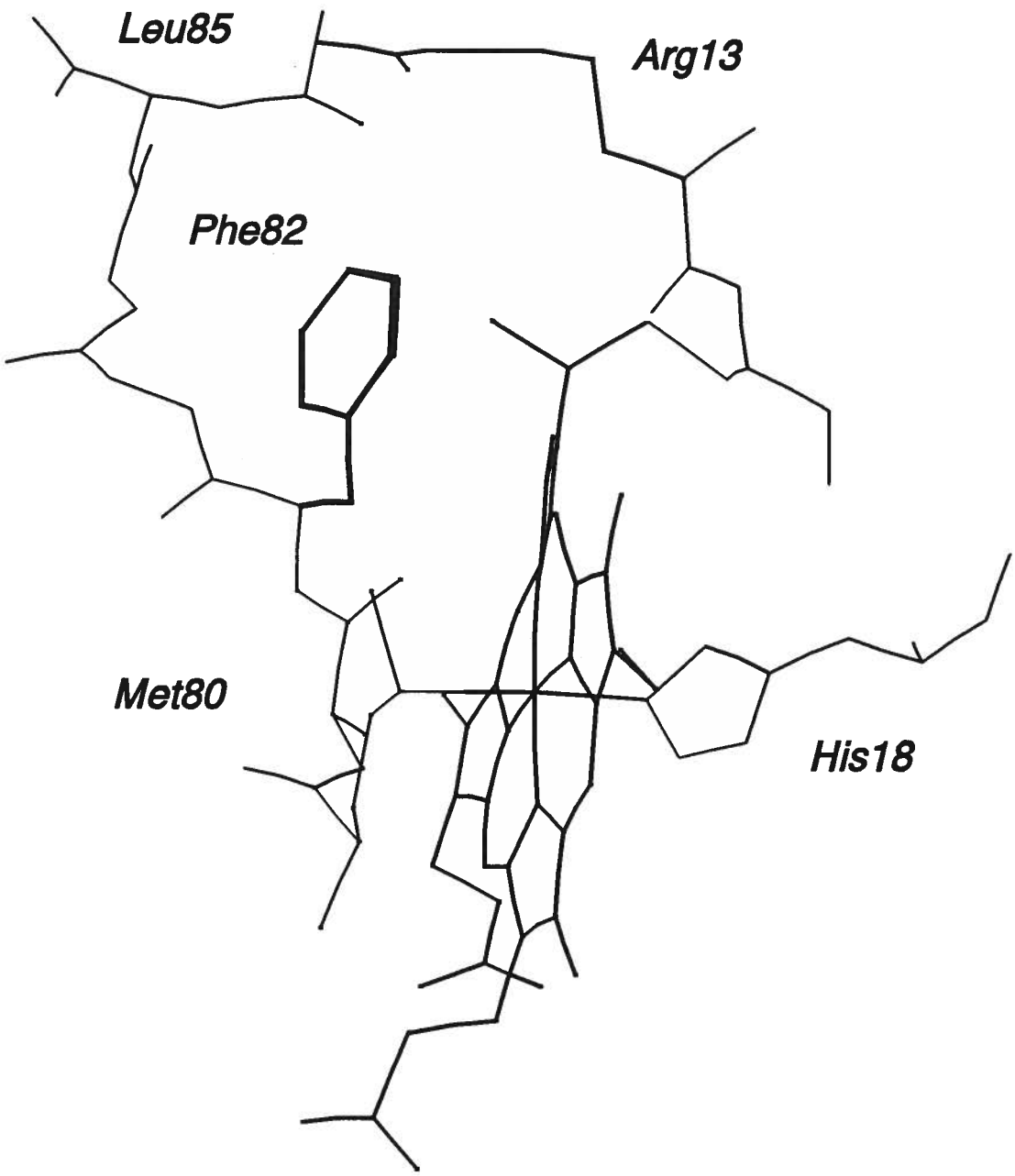

Figure 5 The environment of the invariant residue Phe82 (Louie & Brayer, 1990).

believed to increase the resistance of cytochrome *c* to proteolysis by aminopeptidases (Jörnvall, 1975). Trimethylation of specific lysine residues of plant and fungal cytochromes *c* is catalyzed by an S-adenosyl methionine-dependent lysine methyl transferase specific for cytochrome *c* (Dimaria *et al.*, 1979). The reason for this modification is not clear, although trimethylated cytochrome *c* binds three times more tightly to the mitochondrial inner membrane than unmodified cytochrome *c* (Polastro *et al.*, 1978).

1.3 Structural Differences Between Oxidized and Reduced Cytochrome c

Long before crystal structures of cytochrome *c* were available, differences in the physicochemical properties between the two oxidation states of cytochrome *c* suggested that they exhibit structural differences. Oxidized yeast and bovine cytochromes *c* are readily digested by trypsin and subtilisin, while their reduced counterparts are completely resistant (Nozaki *et al.*, 1958; Yamanaka *et al.*, 1959). The reduced protein is also more resistant to denaturation by heat, guanidine hydrochloride, alcohols, and urea (Myer, 1968; Urry, 1965; Kaminsky *et al.*, 1972). Ulmer and Kagi (1968) used IR spectroscopy to monitor the hydrogen-deuterium exchange of amide groups in horse heart cytochrome *c* and detected oxidation-state dependent differences in the extent of exchange which indicated a more rigid reduced structure. The temperature dependence of the reduction potential of horse heart cytochrome *c* has a small negative entropy of reduction indicating that the reduced state is relatively more ordered than the oxidized state (Taniguchi *et al.*, 1982b). Reichlin and coworkers (1966) observed a small but reproducible difference in the immunological response of reduced and oxidized horse heart cytochrome *c* to anticytochrome *c* sera.

Direct evidence for structural differences between oxidized and reduced forms of cytochrome *c* is revealed by comparison of the crystal structures of the two forms of the protein. Oxidized and reduced structures are available for tuna (Takano & Dickerson, 1981a,b) and yeast iso-1 cytochromes *c* (Louie & Brayer, 1990; Berghuis & Brayer, in preparation). There are no significant changes in the position of the atoms of the polypeptide backbone between the two oxidation states, and side chain movements

are restricted to only a few locations. These include WAT166 and its hydrogen bond network and the hydrogen bond network about heme propionate-7. The largest changes occur in the vicinity of WAT166, which moves 1.7 Å towards the heme upon oxidation (Figure 6). Other changes occurring with oxidation include breakage of the hydrogen bonds between Met80 and Tyr67 and the hydrogen bonds between WAT166 / Asn52 and Asn52 / heme propionate-7.

Although the oxidation-state linked conformational changes are similar in tuna and yeast cytochromes *c*, there are subtle differences between the two species. WAT166 of yeast cytochrome *c* moves 1.7 Å towards the heme upon oxidation, compared to 1 Å in the tuna protein. The larger displacement of WAT166 in yeast cytochrome *c* leads to the loss of its hydrogen bond with Asn52 in the oxidized structure, while this bond is retained in the oxidized tuna protein. In both species of cytochrome *c*, the conformational changes are consistent with stabilization of the positive charge on the oxidized heme through charge-dipole interactions.

1.4 Physiological Roles of Cytochrome c

Cytochrome *c* is a reversible, single electron carrier of the mitochondrial intermembrane space (Figure 7). The major function of this protein is to transfer electrons from ubiquinol-cytochrome *c* oxidoreductase to cytochrome *c* oxidase without significant loss of free energy.

Cytochrome *c* also channels electrons from two other pathways to cytochrome *c* oxidase. In yeast, cytochrome *c* accepts electrons from flavocytochrome b_2, which catalyzes the oxidation of L-lactate to pyruvate (Bach *et al.*, 1942a,b). Reducing equivalents from NADH can also be transferred to cytochrome *c* through a NADH cytochrome b_5 oxidoreductase / cytochrome b_5 complex bound to the mitochondrial outer membrane. (Ito, 1980a,b; Lederer *et al.*, 1983).

Cytochrome *c* also takes part in two detoxification pathways. In one of these, cytochrome *c* accepts electrons from sulphite oxidase, which is the terminal detoxification enzyme in the catabolism of sulphur containing amino acids (McLeod *et al.*, 1961, Cohen & Fridovich, 1971). In the other, cytochrome *c*

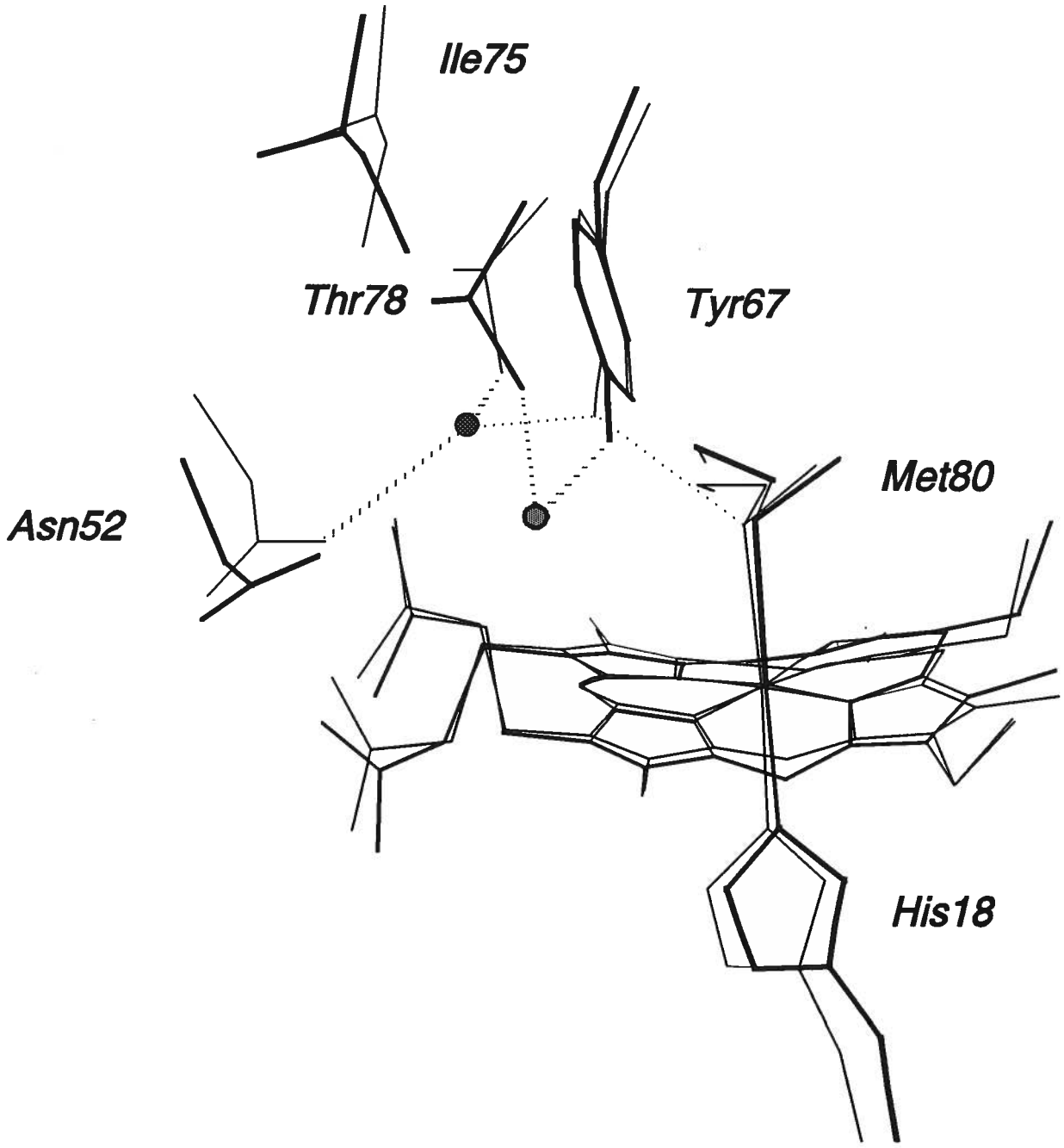

Figure 6 The oxidation state-linked conformational changes about WAT166 in yeast iso-1-cytochrome *c* (Louie & Brayer, 1990; Berghuis & Brayer, in preparation). Thin lines, reduced; thick lines, oxidized. The dashed lines represent hydrogen bonds to WAT166, which is represented by the circles.

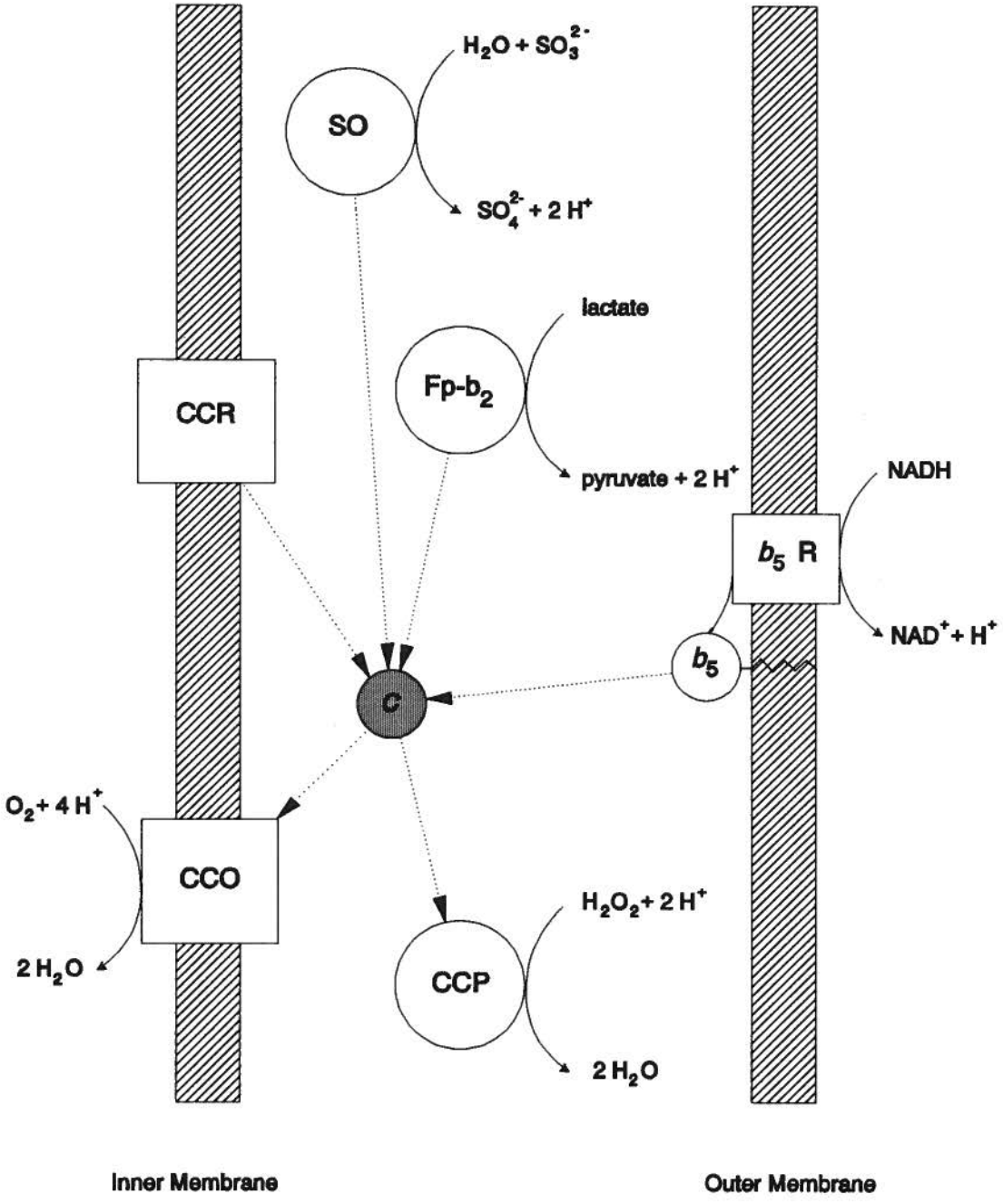

Figure 7 The physiological electron transfer partners of cytochrome *c* and their location within the mitochondrial membranes (Pettigrew & Moore, 1987). Arrowheads denote the direction of electron transfer. (Abbreviations: CCR, ubiquinol-cytochrome *c* oxidoreductase; CCO, cytochrome *c* oxidase; CCP, cytochrome *c* peroxidase; *c*, cytochrome *c*; b_5, cytochrome b_5; b_5R, NADH-cytochrome b_5 oxidoreductase; Fp-b_2, flavocytochrome b_2; SO, sulfite oxidase.)

donates electrons to cytochrome *c* peroxidase, which catalyzes the reduction of peroxide to water (Altschul *et al.*, 1940; Abrams *et al.*, 1942).

The ability of cytochrome *c* to interact with partners located on both of the mitochondrial membranes and in the intermembrane space indicates that this protein is mobile and not completely bound to the mitochondrial inner membrane, as are other members of the respiratory chain. Cytochrome *c* forms stable complexes with all of its natural electron transfer partners with dissociation constants on the order of 10^{-7} M at low ionic strength (reviewed in Pettigrew & Moore, 1987).

1.5 Physicochemical Properties of Cytochrome c

1.5.1 UV-Visible Spectra

The UV-visible spectra of cytochrome *c* (Figure 8) are largely due to the electronic structure of the heme and its axial ligands. The majority of the observed bands are due to $\pi \rightarrow \pi^*$ electronic transitions in the porphyrin orbitals. Reduced cytochrome *c* is characterized by three intense absorbance bands arising from porphyrin $\pi \rightarrow \pi^*$ transitions, typically located near 550 nm, 520 nm, and 416 nm. These bands are known respectively as the α, β, and γ bands; the last band is the most intense and is also called the Soret band. In the oxidized protein, the α and β bands merge to produce a broad band centred at 528 nm, while the Soret band decreases in intensity and shifts to 409.5 nm. Also present in the spectra of both oxidation states are bands near 280 nm arising from $\pi \rightarrow \pi^*$ transitions of the aromatic amino acids tyrosine and tryptophan.

The oxidized cytochrome also exhibits a weak absorption band at 695 nm believed to be caused by a porphyrin π to iron(III) *d* transition (reviewed in Moore & Pettigrew, 1990). The presence of this band is characteristic of methionine as one of the axial ligands (Shechter & Saludjian, 1967). Schejter *et al.* (1991) demonstrated that a band of similar position and intensity can be reproduced by the addition of soft ligands to cytochrome *c* in which the Met80 sulphur has been chemically modified to prevent its coordination to the heme.

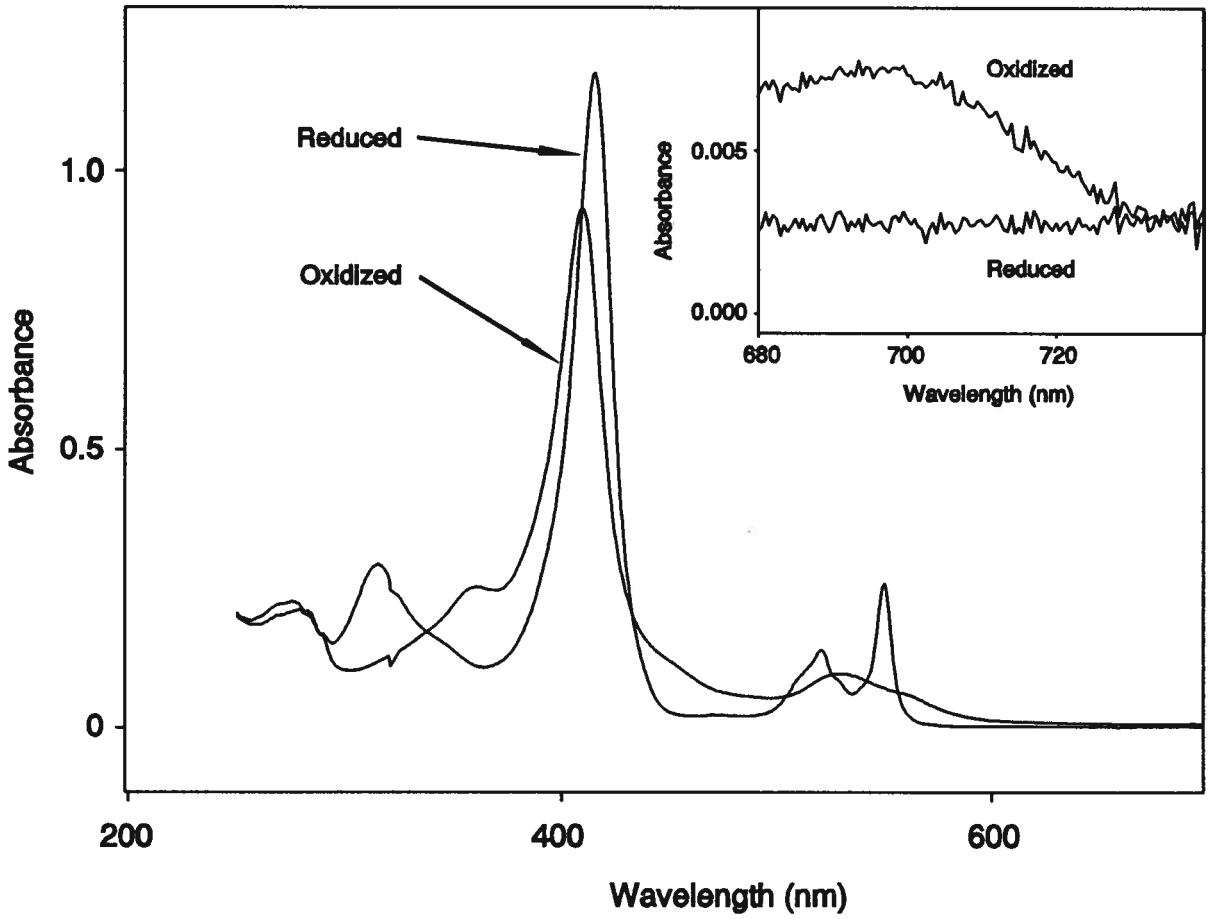

Figure 8 The UV-visible spectra of oxidized and reduced yeast iso-1-cytochrome *c* (25 °C, pH 6, μ = 0.1 M). The reduced protein has absorbance maxima at 550, 521, and 416 nm. The oxidized protein has maxima at 695 (inset), 528, and 409.5 nm.

1.5.2 Electrochemistry

1.5.2.1 Reduction Potential and Its Measurement

The position of the oxidation-reduction equilibrium between two electroactive species (1) is governed by the Nernst equation (2):

$$A_{oxidized} + B_{reduced} \rightleftharpoons A_{reduced} + B_{oxidized} \quad (1)$$

$$E_{cell} = E^0 - \frac{RT}{nF} \ln \frac{[A_{reduced}][B_{oxidized}]}{[A_{oxidized}][B_{reduced}]} \quad (2)$$

In the above expression, A and B are the two electroactive species, E_{cell} is the measured cell potential, R is the gas constant, F is Faraday's constant, T is the absolute temperature in Kelvin, and n is the stoichiometry of electrons in the reaction. E^0 is the cell potential when all cell components have unit activity. The two electroactive species need not be in physical contact as long as there is electrical contact through a salt bridge (for ionic movement) and a wire (for electronic movement). This arrangement allows the complete cell to be subdivided into two 'half cells', one of which can be chosen as a convenient reference against which all half cell potentials are measured. Assigning a potential of 0 Volts to the reference simplifies the Nernst equation (3):

$$E_{half\ cell} = E^0 + \frac{RT}{nF} \ln \frac{[A_{oxidized}]}{[A_{reduced}]} \quad (3)$$

The standard hydrogen electrode (SHE), composed of an inert platinum wire in a 1 M solution of HCl in equilibrium with 1 atm of H_2 gas, serves as this standard reference. By convention, electrochemical half cell reactions are expressed as reductions. Those half reactions with potentials greater than zero have a greater tendency to be reduced relative to the SHE reference. In practice, the SHE is rarely used; experimentally more convenient reference electrodes, such as the saturated calomel electrode, or SCE [composition $Hg/Hg_2Cl_2/KCl$ (saturated), E^0 = 244.4 mV vs SHE] are employed.

By equating the Nernst equation to the expression for the concentration dependence of free energy, the following relation is obtained.

$$\Delta G^0 = -nFE^0 \qquad (4)$$

Thus reduction potentials are direct measurements of the free energy of the oxidation-reduction equilibrium.

Reduction potentials can be measured in several ways. In equilibrium measurements, the cell potential can be controlled by a potentiostat and the ratio of the oxidation states of the species of interest measured. Spectroelectrochemistry is an example of this technique, in which species concentrations are determined spectrophotometrically and the potential is controlled at a semitransparent working electrode (Murray *et al.*, 1967). Electron transfer proteins do not readily transfer electrons with bare metal electrodes even under thermodynamically favourable conditions because their active sites are often buried within the protein. Small inorganic mediators are often necessary to shuttle electrons between the electrode and the protein. Ideally the mediator should only catalyze the attainment of thermodynamic equilibrium between the electrode and the electron transfer protein. Spectroelectrochemistry has been used to measure the reduction potentials of many electron transfer proteins, including cytochrome b_5 (Reid *et al.*, 1982), and cytochromes *c* from various species (Taniguchi *et al.*, 1982b, Cutler *et al.*, 1987).

A second common experiment used to determine reduction potentials is cyclic voltammetry (Bard & Faulkner, 1980; Evans *et al.*, 1983). In this technique, the potential of the working electrode is varied linearly, and current is monitored as a function of potential. Under conditions where electron transfer between the electrode and the electroactive species in solution is rapid, the observed current is proportional to the rate of mass transfer of the reactant to the electrode surface, which in turn depends on the concentration gradient of the electroactive species at the electrode. Although electron transfer proteins interact poorly with bare metal electrode surfaces, the latter can be modified to promote rapid electron transfer (*vide infra*).

Cyclic voltammetry is best understood by describing the events that occur during the experiment, as shown in Figure 9 (Maloy, 1983). Consider an electroactive species that is initially in the oxidized state. The applied potential of the working electrode is initially at a positive value relative to the reduction potential of the species of interest such that no net electrochemical reaction occurs (1). As the potential of the working electrode is lowered and approaches the reduction potential of the electroactive species, a cathodic current i_c begins to flow as electrons are transferred to the oxidized species from the electrode (2). This process causes a depletion of the oxidized species at the working electrode surface and the establishment of a concentration gradient of the oxidized species between its value at the electrode surface and its value in bulk solution far from the electrode surface. The volume between the working electrode surface and the bulk solution is called the depletion layer, which also corresponds to an accumulation layer of the reduced species.

The observed current will be sensitive to this concentration gradient at the working electrode surface. As the reduction proceeds, the concentration gradient and the current both increase. The concentration gradient will be steepest when the applied potential is 28.5 mV beyond the reduction potential of the electroactive species, and at this point the cathodic current reaches a maximum, denoted i_{pc} (3). The current does not increase beyond this point because the concentration gradient of the oxidized species becomes shallower as the depletion layer expands. As the working electrode is taken to more reducing potentials, the current begins to fall in a manner independent of the electrode potential (4). When the direction of the potential sweep is reversed such that the potential of the working electrode is now made more positive, an anodic current i_a begins to flow in the cell as the reduced species accumulated during the first half of the experiment is oxidized. This process gives a current *vs* potential curve similar to that obtained during the sweep to low electrode potentials for the reasons already discussed. The result of this experiment is the current *vs* potential plot known as a cyclic voltammogram. The anodic and cathodic peak currents are symmetrically located about the reduction potential of the electroactive species, and their positions are used to calculate the reduction potential.

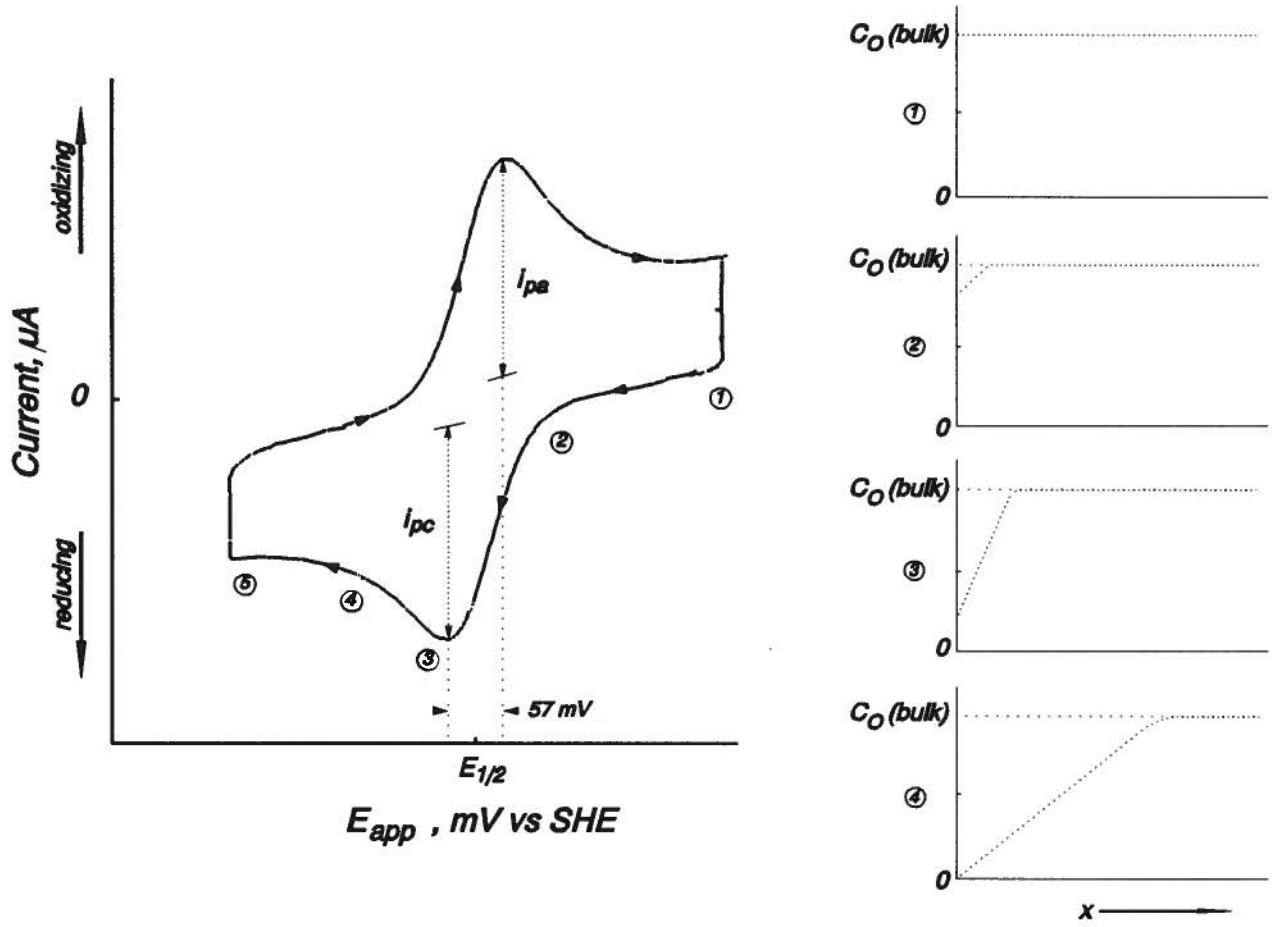

a) b)

Figure 9 a) A cyclic voltammogram obtained for a reversible electrochemical system (25 °C). The terms ip_c and ip_a refer to the peak cathodic and anodic currents, respectively. b) The concentration gradient of the electroactive species at the electrode surface at different points along the voltammogram. The electroactive species is initially in the completely oxidized state, with a concentration of C_O *(bulk)* far from the electrode surface. The *x*-axis represents the distance from the electrode surface. Adapted from Maloy, 1983.

For cyclic voltammetry to be useful in determining reduction potentials, electron transfer between the electrode and the electroactive couple must be reversible. Reversibility requires the heterogeneous electron transfer rate between the electroactive species in solution and the working electrode surface to be sufficiently rapid such that the Nernst equation is obeyed at the surface of the electrode. If this condition is met, the faradaic current will depend only on the rate of mass transfer of the electroactive species to the electrode.

There are three means of mass transfer to the working electrode surface: migration of the charged electroactive species in response to the electric field at the electrode surface, bulk movement of the solution (or convection), and diffusion of the electroactive species in response to a concentration gradient. For determination of reduction potentials by cyclic voltammetry it is desirable that the predominant means of mass transfer is diffusion. Migration is repressed by the presence of a supporting electrolyte in solution, and convection is avoided by performing the experiment in an unstirred solution.

The experimental challenge is to make the heterogeneous electron transfer rates of electron transfer proteins fast. Electron transfer between metal electrode surfaces and proteins is hampered by lower heterogeneous rates of electron transfer as well as denaturation of the protein on the electrode surface. However, in the last fifteen years, techniques have been developed to modify electrode surfaces in a manner that promotes rapid, heterogeneous electron transfer (reviewed by Frew & Hill, 1988). Surface modifiers promote reversible association of the protein and the electrode by making the electrode surface more hydrophilic and providing for favourable electrostatic and hydrogen bonding interactions. Surface modifiers are bifunctional compounds, with one region used for binding to the electrode surface while the other region faces the solution and interacts with the electron transfer protein. An example of a surface modifier is the compound 4,4'-bipyridine (Eddowes & Hill, 1977). The electrode-facing region is frequently a sulphur containing group, while the solution-facing group can be tailored to provide a favourable interaction site for the redox protein to be studied (Taniguchi *et al.*, 1982a; Allen *et al.*, 1984). Peptides can be used as surface modifiers, with cysteine residues used to anchor the modifier to

the electrode surface while hydrophilic charged residues provide the interaction site for the protein. In addition, some electrode surfaces such as pyrolytic edge graphite (Armstrong *et al.*, 1984) and tin doped indium oxide (Yeh & Kuwana, 1977) are 'naturally modified' and promote reversible electron transfer with proteins.

1.5.2.2 Factors Affecting The Reduction Potential of Cytochrome c

Under physiological conditions, the reduction potentials of mitochondrial cytochromes *c* are in the range +260 to +290 mV (Pettigrew & Moore, 1987). These reduction potentials are about halfway between that of the NAD^+/NADH couple (-320 mV) that is the electron donor to the respiratory chain, and O_2/H_2O (+820 mV), which is the terminal electron acceptor for this system.

The reduction potential of a heme containing protein will depend upon the nature of the porphyrin, the axial ligands, and the dielectric environment surrounding the heme (Bottomly *et al.*, 1982; Moore & Williams, 1977; Moore *et al.*, 1986). As all mitochondrial cytochromes *c* possess the same porphyrin and axial ligands, any differences in their reduction potentials are due to differences in the surrounding environment. The medium surrounding an electroactive centre can have a considerable influence on its oxidation-reduction equilibrium. The reduction potential of bipyridine mesoheme methyl ester is 300 mV higher in benzene than in water (Kassner, 1972, 1973). Heme octapeptide[2] in the presence of N-acetyl methionine has the same ligands as cytochrome *c*, yet its reduction potential is 300 mV lower than that of the intact protein (Harbury *et al.*, 1965).

The charge difference between reduced and oxidized heme is a single positive unit. Thus electrostatic interactions between the heme charge and the charges and dipoles in the surrounding medium will be the predominant factors in determining the reduction potential of cytochromes *c*. The stability of a particular oxidation state will depend on the ability of surrounding dipoles and charges to orient themselves in

[2] Heme octapeptide is a species prepared from tryptic digestion of cytochrome *c*. The heme is bound to the peptide through thioether linkages from Cys14 and Cys17 (Tuppy & Paleus, 1955). His18 provides one of the axial ligands.

response to the charge at the heme. The most influential groups will be those located nearest the heme. Consequently, Moore and colleagues have directed attention to Arg38 and the heme propionates (Moore, 1983; Moore *et al.*, 1984; Cutler *et al.*, 1989). Dipoles from peptide bonds and the side chains of polar residues, and nearby solvent molecules, including WAT166, will also contribute to the stabilization of the heme charge (Churg & Warshel, 1986).

The movement of groups adjacent to the heme upon a change in the oxidation state of cytochrome *c* is consistent with a response to the altered charge on the heme, as previously discussed. However, the structural changes are comparatively small, with no significant changes in the positions of the main chain dipoles or the surface charges of the protein. The environment about oxidized heme in cytochrome *c* provides only partial stabilization of the positive charge, far less stabilization than if the heme were immersed in water, where the surrounding solvent dipoles would be free to move in response to the charge. The inability of the protein to solvate the positive charge on oxidized heme as effectively as water is the cause of the difference in potential between cytochrome *c* and N-acetyl methionine / heme octapeptide (Churg & Warshel, 1986).

Measurements of reduction potentials of cytochrome *c* variants are useful because they are sensitive indicators of alterations to the heme environment which influence its ability to stabilize a positive charge on the heme. In addition, reduction potential measurements can be used to determine the thermodynamic parameters associated with reduction (by measurement of the temperature dependence of reduction potentials) and the dissociation constants of titratable groups whose ionization states are sensitive to the oxidation state of the protein (by measurement of the pH dependence of the reduction potential).

1.5.3 Electron Transfer Kinetics

1.5.3.1 Electron Transfer Theory

The relative simplicity of electron transfer reactions compared to other chemical transformations has lead to extensive experimental and theoretical work aimed at determining the factors contributing to observed rates and the magnitude of their contributions. Early work in this field emphasized analysis of reactions between substitutionally inert inorganic complexes and has been useful in identifying the factors that contribute to observed biological electron transfer rates (reviewed by Sutin, 1973; Marcus & Sutin, 1985)

Electron transfer reactions are generally classified as one of two types, according to the involvement of the ligands surrounding the electron transfer centres. 'Inner sphere' electron transfer proceeds through an intermediate in which the reactants share a ligand in their inner coordination shells. This mechanism requires coordination bond breakage and reformation. In contrast, 'outer sphere' electron transfer occurs without changes in the coordination shells of the reactants. Theories for outer sphere electron transfer reactions are easier to consider because such reactions do not involve bond breakage or reformation. The balance of this discussion will be concerned with outer sphere mechanisms. Most electron transfer reactions involving cytochrome *c* occur by an outer sphere mechanism (*vide infra*). Outer sphere electron transfer is believed to occur in the series of steps shown in Figure 10. In the first step, the electron donor and acceptor form a noncovalent precursor complex. Formation of the precursor complex may be influenced by electrostatic interactions between the reactants. The nature of the electrostatic interactions in a particular reacting pair can be determined from the ionic strength dependence of the reaction rate constant. If the reaction is between species of opposite charge, the observed reaction rate will diminish with increasing ionic strength.

Outer sphere electron transfer theory has been developed from activated complex theory (Eyring, 1935), which describes a reaction as proceeding through an intermediate, transitory state of maximum free energy (the activated complex). The expression for the rate constant of an outer sphere reaction

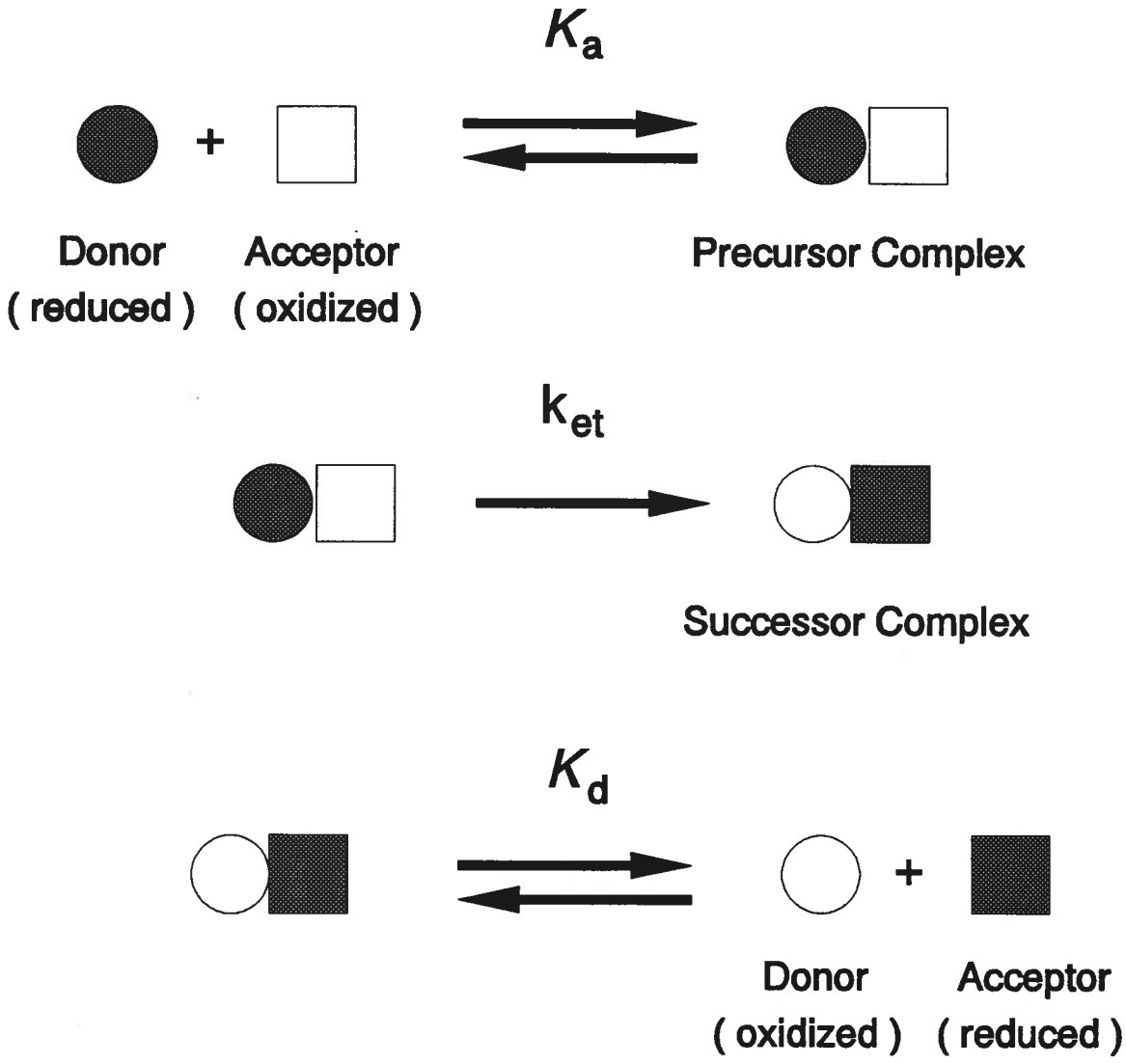

Figure 10 Schematic diagram of the steps involved in outer sphere, intermolecular electron transfer (Scott *et al.*, 1985). The reactants form the precursor complex without a change in the coordination state of the metal centers. K_a is the association constant of the precursor complex; K_d is the dissociation constant of the successor complex. Shaded and unshaded symbols indicate reduced and oxidized components, respectively.

according to this theory is given by

$$k = \kappa Z \exp(\frac{-\Delta G^*}{RT}) \quad (5)$$

In this equation, Z is the collision frequency (10^{11} $M^{-1}s^{-1}$ for bimolecular reactions, 10^{13} s^{-1} for unimolecular reactions). κ is the probability of electron transfer occurring when the precursor complex is at the transition state and is dependent on the distance between the electron transfer sites as well as their relative orientation and the nature of the intervening medium. κ may have values between zero and unity, representing low to high probability respectively of electron transfer occurring when the precursor complex is at the transition state. Reactions for which κ is unity are referred to as being adiabatic.

$\Delta G^{\ddagger}$ is the free energy difference between the ground state and transition state within the precursor complex. The free energy of the precursor complex is a function of its nuclear coordinates. Each possible conformation has associated with it a free energy, giving rise to a multidimensional free energy surface for all possible conformations. There is a similar surface for the successor complex. For illustrative purposes, these surfaces are frequently shown as two dimensional curves, with free energy along the ordinate and the abscissa representing the nuclear coordinate (Figure 11). The parabolic relation between potential energy and nuclear coordinates assumes that the participating chemical bonds can be described as simple harmonic oscillators that obey Hooke's law. The wells of the energy curves are the equilibrium nuclear coordinates about which the nuclei fluctuate in the precursor and successor complexes.

Libby (1952) proposed that the Franck-Condon principal applied to electron transfer within the precursor complex, as the positions and momenta of the relatively massive nuclei can be considered to be unchanged during electron transfer. This premise demands nuclear reorganization of the precursor complex to a conformation that is energetically accessible to the successor complex before electron transfer occurs. This condition is satisfied at the point where the free energy surfaces of the precursor and successor complexes intersect. This point is at the free energy maximum on the reaction coordinate,

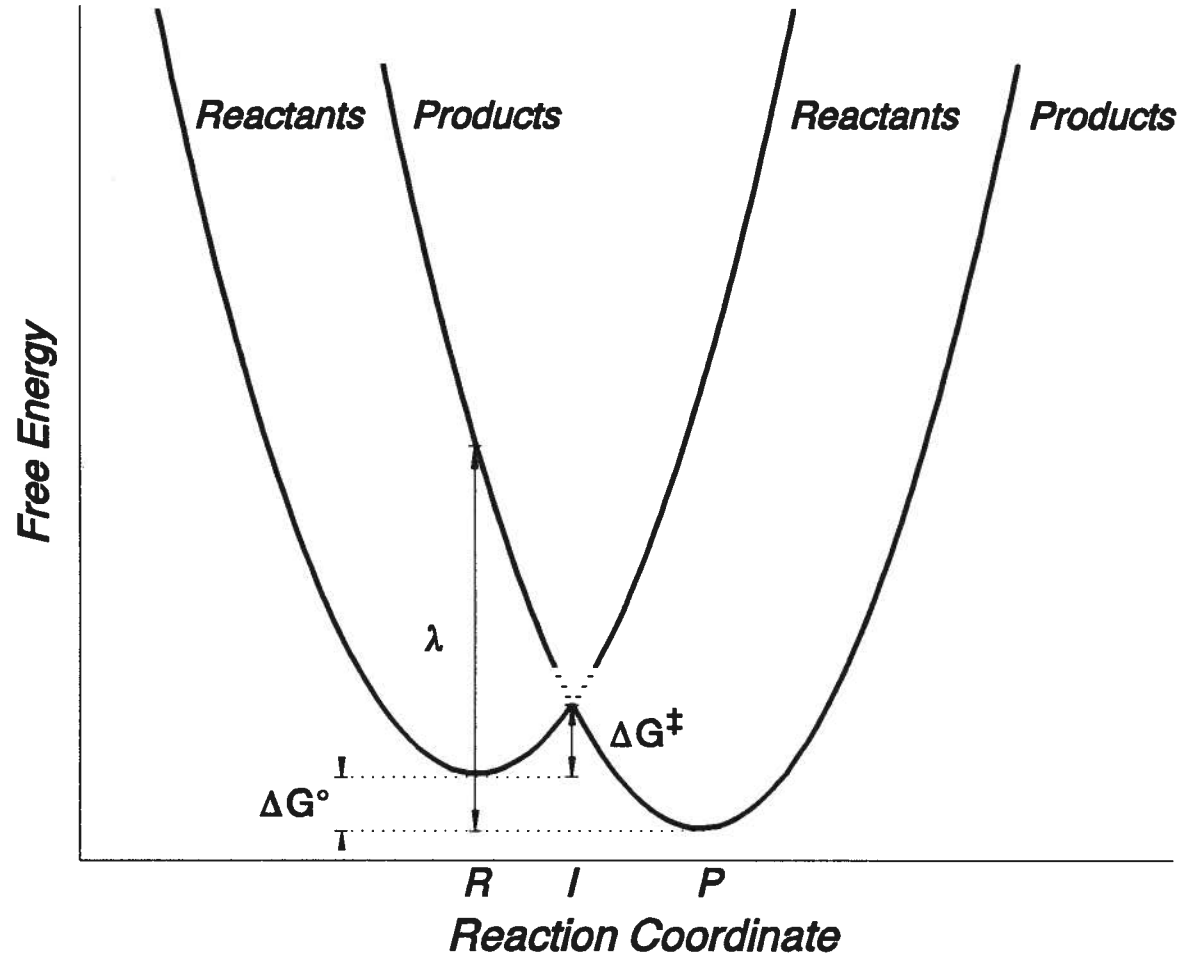

Figure 11 A diagram of the reaction coordinate for outer sphere electron transfer within the precursor complex (Devault, 1984). Symbols: ΔG^0, free energy of the reaction; $\Delta G^{\ddagger}$, free energy of activation; λ, reorganization energy; *R*, equilibrium nuclear coordinates of the precursor complex; *I*, nuclear coordinates of the transition state; *P*, equilibrium nuclear coordinates of the successor complex.

and the corresponding conformation of the reacting molecules is called the transition state. Nuclear reorganization from the equilibrium coordinates of the precursor complex to the coordinates of the transition state consists of changes in equilibrium bond lengths and bond angles (inner sphere reorganization) and reorientation of surrounding solvent molecules and their dipoles (outer sphere reorganization).

The activation free energy depends on the reaction free energy, ΔG^{o}, and the reorganization free energy λ. The reorganization free energy is the energy required to bring the precursor complex from its equilibrium nuclear coordinates to those of the successor complex without the actual transfer of an electron. The reorganization free energy can be considered as the sum of two contributions. The inner sphere reorganization energy, λ_i, is associated with changes in the equilibrium bond lengths and bond angles and is determined from the molecular vibrational coordinates. Outer sphere reorganization free energy, λ_o, is the contribution from the changes in the orientation of the surrounding solvent dipoles to adjust to the altered charges on the reaction centres. Its contribution is often calculated using dielectric continuum theory (Marcus, 1965). The activation free energy also has contributions from the work required to form the precursor complex, w^r, and the work required to dissociate the successor complex, $-w^p$. The term $\Delta G^{o'}$ is the free energy difference between the precursor and successor complexes, which may differ from ΔG^{o}, the free energy difference between the separated products and reactants:

$$\Delta G^{0'} = \Delta G^{0} + w^{p} - w^{r} \tag{6}$$

The work terms most often considered are those attributable to electrostatic interactions between the participants. The influence of these interactions can be estimated from the size and charge of the participants and the application of Coulomb's Law.

The relation between the aforementioned terms is given by the following equation (Marcus, 1964; see also Devault, 1984, for the derivation of this relationship):

$$\Delta G^{*} = w^{r} + \frac{1}{4\lambda}(\lambda + \Delta G^{0'})^{2} \tag{7}$$

The Marcus expression for activation energy (equation 7) can be substituted into equation 5 and the latter equation can be used to predict rate constants for electron transfer if the system under study is defined with respect to the structure and dynamics of the products and reactants. Rarely is a reaction so well characterized to allow the use of equations 5 and 7 directly. An experimentally more convenient relationship is the relative Marcus equation, which relates the rate constant of electron transfer between two species (the cross reaction rate constant, k_{12}) to those of the electron transfer self-exchange rate constants of the individual reactants (k_{11}, k_{22}) and the equilibrium constant for the reaction (K_{12}):

$$k_{12} = \sqrt{k_{11}\, k_{22}\, K_{12}\, f_{12}} \qquad (8)$$

Where f_{12} is equal to unity for adiabatic or uniformly nonadiabatic reactions. The key assumption of this useful relationship is that the reactants undergo the same activation processes in their cross reaction (k_{12}) as they do in their self-exchange reactions (k_{11}, k_{22}).

Relative Marcus theory has been accurate in predicting cross reaction rate constants from self-exchange rate constants of simple coordination complexes, in which the assumption regarding the similarity of the activation process is more valid for reactants of similar charge, size, and hydrophobicity. Experimental values for the self-exchange rates of such complexes are obtained from isotope exchange measurements (Baker *et al.*, 1959), NMR saturation transfer experiments (Shporer *et al.*, 1965), or approximated from cross reaction rates between reactants of similar structure (Wilkins & Yelin, 1968). Self exchange rates for several small electron transfer proteins have been measured by NMR saturation transfer experiments, including those of mitochondrial cytochromes *c* (Gupta, 1973; Concar *et al.*, 1991). Cross reaction rates of electron transfer proteins with small nonphysiological complexes are easily measured (reviewed by Wherland & Gray, 1976) and the relative Marcus equation is often rearranged to calculate the self exchange rate constant of the protein. Comparisons of the self exchange rate constants of a given protein

obtained with several different inorganic complexes is a useful way of studying the differences in the activation processes of these cross reactions (Wherland & Gray, 1976).

1.5.3.2 Electron Transfer Kinetics of Cytochrome c

Because of the solubility, stability and commercial availability of horse heart cytochrome *c*, the electron transfer kinetics of this protein with simple inorganic complexes was an early target of experimentalists using stopped flow spectrophotometry. Electron transfer rates have been measured with $(Fe(CN)_6^{3-}$, (Morton *et al.*, 1970), Cr^{2+} (Yandell *et al.*, 1973), $Ru(NH_3)_6^{2+}$ (Ewall & Bennett, 1974), $Fe(edta)^{2-}$ (Hodges *et al.*, 1974), $Co(phen)_3^{3+}$ (McArdle *et al.*, 1974) and $Co(ox)_3^{3-}$ (Holwerda *et al.*, 1980). These experiments demonstrated that in most cases cytochrome *c* participates in outer sphere electron transfer. The exception is the reduction of cytochrome *c* by Cr^{2+}, in which the presence of Cr^{3+} bound to the reduced protein suggests an inner sphere mechanism.

The self-exchange rate for horse heart cytochrome *c* has been determined directly using NMR spectroscopy by measuring the spin-lattice relaxation time of the Met80 methyl resonance of the reduced protein in the presence of variable amounts of oxidized protein (Gupta, 1973). The self exchange rate, uncorrected for the effect of electrostatic repulsion, is approximately 1000 $M^{-1}s^{-1}$ at 0.1 M ionic strength, 40 °C, pH 7. Self exchange rates for yeast iso-1-cytochrome *c* wild type and Phe82Gly variant are 200 and 350 $M^{-1}s^{-1}$ respectively (Concar *et al.*, 1991).

These experiments also demonstrated that the rates of electron transfer involving cytochrome *c* are comparable to those of inorganic complexes. This observation indicated that the limited exposure of the heme in cytochrome *c* does not greatly impede its reactivity. Consequently, attention was focussed on the conserved basic residues surrounding the exposed heme edge to determine their role in directing the formation of electron transfer active precursor complexes through favourable electrostatic interactions with electron transfer partners.

Chemical modification of amino acid side chains of cytochrome *c* has been used to assess the functional consequences of altered protein structure at specific locations (reviewed by Brautigan *et al.*, 1978a). In one particular study, Margoliash and coworkers prepared derivatives of horse heart cytochrome *c* with singly modified lysine residues at different positions (Brautigan *et al.*, 1978b,c). Lysine residues were modified by carboxydinitrophenylation, which gives these residues negative charges. Those derivatives with singly modified lysines nearest the exposed heme edge had the greatest influence on the rates of electron transfer of cytochrome *c* with inorganic complexes (Butler *et al.*, 1983; Armstrong *et al.*, 1986a) and the electron transfer proteins cytochrome *c* oxidase (Ferguson-Miller, 1978), azurin, stellacyanin and plastocyanin (Augustin *et al.*, 1983; Armstrong *et al.*, 1986b).

Chemical modification has been used in a different manner to further establish the role of surface charges at the exposed heme edge in cytochrome *c* electron transfer. In shielding experiments, the susceptibility of lysine residues of free cytochrome *c* to chemical modification is compared to their susceptibility when cytochrome *c* is in a complex with an electron transfer partner protein (Bosshard, 1979; Rieder & Bosshard, 1980). Those lysines present at the part of the surface of cytochrome *c* that interacts with its electron transfer partner are protected from chemical modification.

Both the shielding experiments and the kinetic experiments on chemically modified cytochrome *c* show that lysine residues around the exposed heme edge are involved in complexation with other electron transfer proteins (reviewed in Pettigrew & Moore, 1987). These are lysines 8, 13[3], 25, 27, 72, 73, 79, 86, and 87. Of these, positions 13, 72, 73, 79 and 87 are conserved in yeast iso-1-cytochrome *c*.

Computer graphics models for complexes formed by cytochrome *c* with bovine microsomal cytochrome b_5 (Salemme, 1976) and cytochrome *c* peroxidase (Poulos & Kraut, 1980) also indicate the involvement of the ring of basic residues about the exposed heme edge in complex stabilization. These models were constructed using the structures of the individual partners determined by X-ray diffraction analysis and minimizing the electrostatic energy between the two structures. The model complexes are

[3]Position 13 is an arginine residue in yeast-iso-1cytochrome *c*

stabilized by complementary electrostatic interactions between the charges surrounding the exposed heme edges of each protein. In addition, the hemes within the complexes are approximately coplanar, with heme edge to edge distances of 18 Å and 10 Å for the complexes with cytochrome *c* peroxidase and cytochrome b_5 respectively. While bovine microsomal cytochrome b_5 is not a natural electron transfer partner of cytochrome *c*, the complex of these two proteins is relevant because of the sequence homology cytochrome b_5 shares with the cytochrome *b* subunits of flavocytochrome b_2, sulphite oxidase and cytochrome b_5 of the mitochondrial outer membrane.

Because of the relatively long range over which electrostatic forces act, the arrangement of complementary charge arrays on electron transfer partners was proposed to be important in enhancing or promoting rapid reaction by steering the reactants to an optimal docking arrangement. A Brownian dynamics simulation of cytochrome *c* / cytochrome *c* peroxidase (Northrup *et al.*, 1988) complex formation suggests rather that the electrostatic interactions serve to bring the reactants together in a relatively nonspecific manner. Subsequently there is reorientation of the electron transfer partners within the complex to an electrostatically favoured geometry. Further evidence for alternative geometries in the precursor complexes involving cytochrome *c* was provided by electrostatics calculations on the interaction of cytochrome *c* with cytochrome b_5 by Mauk *et al.* (1986) which suggested the existence of two isoenergetic, electrostatic complexes at alkaline pH, one of which was the complex proposed by Salemme (1976).

1.5.4 The Alkaline Isomerization

UV-visible spectroscopy distinguishes five pH dependent forms of ferricytochrome *c*, and three such forms of ferrocytochrome *c* between pH 0 and 13 (Theorell & Åkesson, 1941). These spectral differences are attributed to differences in the nature of the axial ligands to the heme iron. A combination of structural analysis of the native protein and comparison of its pH dependent spectroscopic properties to those of model compounds has led to the assignment of the pH dependent transitions to the changes

in axial ligation shown in Figure 12. Transitions at the extremes of pH are accompanied by unfolding of the protein. However, the transition of ferricytochrome *c* from state III (native) to state IV occurs with the retention of a folded, globular conformation (Myer, 1968). The transition from state III to IV of ferricytochrome *c* is called the alkaline isomerization, with state IV known as the alkaline isomer. Evidence for an analogous transition in the reduced protein, with a pK_a of approximately 14.5, has been reported (Barker & Mauk, in press).

The alkaline isomer differs from the native form in several ways. Unlike the native protein, the alkaline isomer is not reducible by ascorbate (Greenwood & Palmer, 1965; Wilson & Greenwood, 1971), and its reduction potential is 450 mV lower than that of the native protein (Barker & Mauk, in press). The UV-visible spectrum of the alkaline isomer indicates that the heme iron remains low spin, but there are differences in the spectra, particularly the absence of the absorbance band at 695 nm. The 695nm band is associated with the presence of methionine as an axial ligand to ferriheme (Shechter & Saludjian, 1967; Schejter *et al.*, 1991) and has been used to monitor the transition from native to alkaline isomer. The native and alkaline isomers also differ in their NMR (Gupta & Koenig, 1971; Wooten *et al.*, 1981), EPR (Brautigan *et al.*, 1977) CD (Myer, 1968), and MCD (Vickery *et al.*, 1976; Gadsby *et al.*, 1987) spectra. There is no crystal structure currently available for the alkaline isomer.

The absence of the 695 nm band, the retention of the low spin state, and the lowered reduction potential of the alkaline isomer suggest that Met80 has been replaced by a strong field ligand at high pH. The ligand replacing methionine 80 is believed to be the deprotonated ϵ-amino group of a lysine residue, based on the similarity of the MCD and EPR spectra of the alkaline isomer to those of heme proteins with known histidyl/amino axial coordination (Gadsby *et al.*, 1987; Rigby *et al.*, 1988; Simpkin *et al.*, 1989). Additionally, trifluoroacetylation of all lysine residues in cytochrome *c* prevents the formation of a low spin alkaline species (Stellwagen *et al.*, 1975). However, which lysine replaces Met80 is unknown. It is likely that the alkaline isomer consists of several species with different lysines as potential ligands as is suggested from the results of NMR experiments which indicated the presence of at least two alkaline

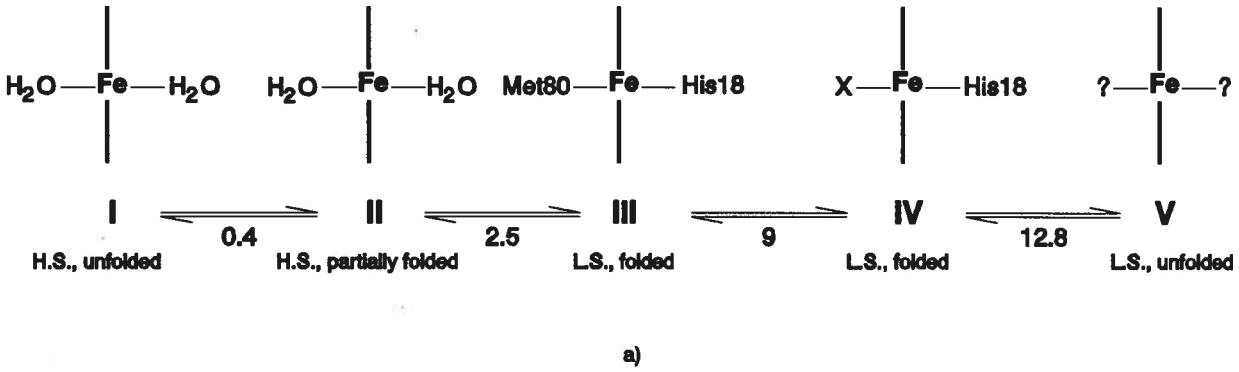

a)

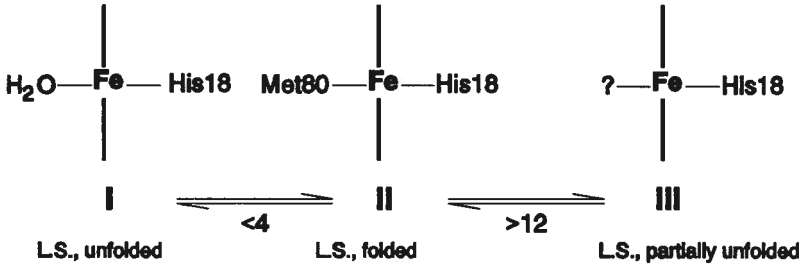

b)

Figure 12 The pH dependent ligation states of mitochondrial cytochrome *c*, with the pK_as of the associated transitions, spin states, and state of the protein fold. a) Ferricytochrome *c*; b) Ferrocytochrome *c*. Abbreviations: H.S., high spin; L.S., low spin. The ligand 'X' of state IV ferricytochrome *c* is likely a lysine residue, but its specific identity is unknown. (Data from Dickerson & Timkovich, 1975).

conformational states of ferricytochrome *c* in equilibrium with the native structure at alkaline pH (Hong & Dixon, 1989). Additional support for this proposal is provided by the behaviour of single site mutants of yeast iso-1-cytochrome *c* in which lysine residues were replaced by alanine residues. Such mutations at positions 72 and 79, proposed to be the most likely potential ligands in the alkaline isomer, did not alter the alkaline isomerization pK_a (Inglis *et al.*, unpublished results).

The transition from native to alkaline form involves the net release of one proton from cytochrome *c*, with a pK_a that is dependent on the species of cytochrome *c* (9.0 to 9.5 for horse heart and 8.5 for yeast cytochromes *c*). Davis and coworkers (1974) measured the pH dependence of the kinetics of the alkaline isomerization of horse heart cytochrome *c* and proposed a mechanism involving a deprotonation followed by a conformational change that results in the loss of Met80 as the axial ligand:

$$\textit{Native Ferricytochrome c (protonated)} \overset{K_H}{\rightleftharpoons} \textit{Native Ferricytochrome c (deprotonated)}$$

$$\textit{Native Ferricytochrome c (deprotonated)} \underset{k_b}{\overset{k_f}{\rightleftharpoons}} \textit{Alkaline Ferricytochrome c}$$

The measured values were pK_H = 11, k_f = 6 s^{-1} and k_b = 0.05 s^{-1}, which were consistent with the overall observed pK_a of 9.0. Above pH 10.5, a second, faster kinetic phase is observed (Kihara *et al.*, 1976).

The alkaline isomerization is sensitive to the environment about the heme. For example, the influence of position 82 mutants on this transition was examined by Pearce *et al.* (1989) who found that replacement of Phe82 by leucine, isoleucine, serine or glycine lowered the alkaline pK_a of yeast iso-1-cytochrome *c* by 0.8 to 1.3 pH units. Rate measurements from pH-jump experiments revealed that the lower pK_as of the Leu and Ile mutants were caused solely by decreases in the pK_H of the deprotonation, with no effect on the subsequent conformational equilibrium. The Ser and Gly variants showed similar decreases in their pK_Hs, but these were partially offset by changes in the conformational equilibrium which stabilized the native isomer.

1.5.5 Ligand Substitution

Mitochondrial ferricytochrome *c* binds added ligands such as imidazole (Schejter & Aviram, 1969; Sutin & Yandell, 1972), azide (Sutin & Yandell, 1972; Saigo, 1986), and cyanide (George & Tsou, 1952) with loss of the 695nm band, indicating displacement of Met80 as one of the axial ligands. At pH 7 and an ionic strength of 1 M, horse heart cytochrome *c* binds azide and imidazole with equilibrium constants of 4 M^{-1} and 15 M^{-1}, respectively (Sutin & Yandell, 1972; Schejter & Avriam, 1969). The ligand binding affinity of ferricytochrome *c* towards imidazole and azide is low when compared to heme proteins whose role is reversible ligand binding, but it is consistent with the role of cytochrome *c* as an electron carrier. However, cyanide binding to ferricytochrome *c* is an exception, with a binding constant of approximately 10^6 M^{-1} (George & Tsou, 1952).

The kinetics of ligand binding to ferricytochrome *c* were investigated by Sutin & Yandell (1972) using azide, imidazole and cyanide. In each case, ligand binding was reversible, and at high ligand concentrations rate saturation was observed. The maximum rate was independent of the identity of the added ligand, within experimental error. Based on these observations, the following mechanism was proposed to describe ligand binding to ferricytochrome *c* where 'opened' and 'closed' refer to the susceptibility of the heme to binding of the added ligand:

$$\begin{aligned} &\textit{Ferricytochrome c (closed)} \underset{k_{-1}}{\overset{k_1}{\rightleftharpoons}} \textit{Ferricytochrome c (open)} \\ &\textit{Ferricytochrome c (open)} + \textit{ligand} \underset{k_{-2}}{\overset{k_2}{\rightleftharpoons}} \textit{Ferricytochrome c–ligand} \end{aligned} \qquad (10)$$

The forward rate constant k_1 is rate limiting and has a value from 30 to 60 s^{-1}. This rate constant may be associated with the rate of disruption of the iron(III)-Met80 sulfur bond. Alternatively, it may reflect the rate at which the heme crevice opens sufficiently to allow access of competing ligands to the heme. The high affinity of ferricytochrome *c* for cyanide was attributed to a slow rate of dissociation of the cyanide-cytochrome *c* complex characterized by k_{-2} of less than 10^{-5} s^{-1}.

Both alkaline isomerization and addition of ligands displace Met80 as one of the axial ligands of ferricytochrome *c*. Saigo (1986) observed that low alkaline pK_a was correlated to high ligand affinity among several different species of ferricytochrome *c* and suggested that both properties were measures of the stability of the native ligation state of the heme crevice. In addition, Saigo observed a correlation between high ligand affinity and increased sensitivity of cytochrome *c* towards guanidine hydrochloride denaturation that indicated a link between local (around the heme) and global (protein unfolding) conformational changes of cytochrome *c*.

1.6 Methods of Structure-Function Analysis of Cytochrome c

1.6.1 Genetic Analysis

Saccharomyces cerevisiae possesses two forms of cytochrome *c* known as iso-1 and iso-2, that are encoded by genes CYC1 and CYC7 respectively. Iso-1-cytochrome *c* accounts for over 95 percent of the total mitochondrial protein (Sherman *et al.*, 1966). The expression of iso-1-cytochrome *c* is controlled mainly at the transcriptional level and is induced by the presence of heme, oxygen, and lactate as a non-fermentable carbon source. CYC1 is repressed under anaerobic conditions and in the presence of glucose as a fermentable carbon source.

Genetic studies on the CYC1 locus by Sherman and coworkers (summarized in Hampsey *et al.*, 1986) have been of great use in examining the influence of changes in the sequence of cytochrome *c* on its function. In these investigations, randomly mutated yeast strains are screened for their ability to grow in a medium containing a nonfermentable carbon source, which requires a functional cytochrome *c*. Mutation sites which abolish function are located by DNA sequencing of the mutant gene. With this method a large number of mutants can be examined rapidly, and critical residues can be identified by their tendency to have a high frequency of nonfunctional mutants. Among the positions most resistant to alteration are those hydrophobic residues are in contact with the heme, such as Trp59 (Schweingruber *et al.*, 1978). An added advantage of this technique is its potential to identify compensatory, second site

revertants, in which mutations at a different residue from the first give a functional gene product. In this manner the single site mutant Ile52 was prepared and found to exhibit enhanced thermal stability over the wild type protein (Das *et al.*, 1989; Berroteran & Hampsey, 1991).

1.6.2 Comparative Analyses

Four strategies are commonly used to investigate the influence of structure on the function of cytochrome *c*. Of these, comparison of the properties of cytochromes *c* from different species is the simplest method to perform, but the most ambiguous to interpret. It does not require modification of the proteins to be studied, as nature supplies the structural variants of the protein. However, it is unlikely that differences in the properties between proteins of different species can be assigned to particular structural features because proteins from different species generally differ in sequence at several positions. This method is best suited for comparison of the properties of cytochromes *c* from closely related species where there are fewer sequence differences and for determining the range of variation of a property among diverse species. One example of the latter is the comparison of the susceptibility of mitochondrial cytochromes *c* to tryptic digestion (Endo *et al.*, 1985).

The remaining techniques are suited to examining the functional consequences of specific structural changes to proteins. The use of chemically modified cytochrome *c* has been discussed previously. While the use of this technique has been beneficial in the study of the structure-function relationships in cytochrome *c*, its limitations include the difficulty of isolating singly modified proteins and the unreactive nature of some residues of interest towards modification.

When cytochrome *c* is cleaved by cyanogen bromide at Met 65, the cleavage products reassociate to give a folded conformation similar to the intact protein (Corradin & Harbury, 1971). Moreover, the two polypeptide fragments are able to reform the broken peptide bond spontaneously (Corradin & Harbury, 1974). This property is the basis of the preparation of semisynthetic cytochromes *c*, in which the N-terminal heme binding polypeptide derived from cyanogen bromide cleavage is combined with a C-

terminal polypeptide prepared by chemical synthesis (Nix *et al.*, 1979). The nature of the C-terminal polypeptide can thus be specifically altered and covalently reattached to the N-terminal polypeptide (Koul *et al.*, 1979; Wallace *et al.*, 1989). This method is not limited to the use of naturally occurring amino acids, and proteins that are physiologically nonfunctional can be investigated. However, only changes in the polypeptide fragment that is not covalently attached to the heme may be studied. Using semisynthetic methods, Wallace and coworkers prepared several cytochrome *c* variants to assess the roles of residues Tyr67, Thr78, and Gly83 in maintaining the function and stability of the protein (Wallace *et al.*, 1989). In addition, the axial ligand Met80 of cytochrome *c* has been altered by semisynthesis to give Leu, His, and Cys variants; these species have reduction potentials 220 to 650 mV lower than the wild type protein (Raphael & Gray, 1991). In the case of the position-80 variants, the contribution of axial ligand heterogeneity, as exemplified by the alkaline transition, to the reduction potentials of these proteins as measured by equilibrium methods has not been evaluated.

The most useful and generally applicable technique for investigation of structure-function relationships is to make the desired structural variations at the genetic level by site directed mutagenesis (Zoller & Smith, 1983, Kunkel, 1985). *Saccharomyces cerevisiae* iso-1-cytochrome *c* was among the first electron transfer proteins to be cloned, sequenced (Smith *et al.*, 1979), and modified by site directed mutagenesis (Pielak, *et al.*, 1985). Although a gene for any mutant can be prepared, not all such mutations may be expressed as the currently used expression system requires a functional cytochrome *c*. As with semisynthesis, site directed mutagenesis has the advantage of selectively altering the sequence of the protein. The two techniques are complementary, and mutagenesis can in principle extend the potential use of semisynthesis by introducing methionine residues along the protein sequence (Wallace *et al.*, 1991). Site directed mutagenesis has been used to generate cytochrome *c* variants at many positions, as exemplified by studies of the invariant residue Phe-82 (Pielak *et al.*, 1985); the structural (Louie & Brayer, 1988, 1989), functional (Pielak *et al.*, 1985; Michel *et al.*, 1989), and physicochemical (Pearce *et al.*, 1989; Concar *et al.*, 1991) properties of several position-82 variants have been investigated.

1.7 Thesis Objectives

Conserved residues in the heme environment of cytochrome *c* are proposed to have important roles in maintaining the heme in a functional state (Kassner, 1972, 1973) and in the oxidation state linked conformational changes of the protein (Takano & Dickerson, 1981b). To evaluate this proposal, site directed mutants of yeast iso-1-cytochrome *c* have been prepared at two regions within the heme crevice, and the physicochemical properties of these variants have been measured and compared to the wild type protein.

Phe82 is an invariant residue located at the exposed heme edge of cytochrome *c* where interaction with other electron transfer proteins takes place. The identity of the residue at position 82 has significant influence on the structure (Louie & Brayer, 1988, 1989), function (Michel *et al.*, 1989; and stability (Pearce *et al.*, 1989) of cytochrome *c*. Mutants of yeast iso-1-cytochrome *c* with Tyr, Leu, Ile, Ala, Ser, and Gly at position 82 have been supplied by Dr. J.G. Guillemette of the laboratory of Dr. M. Smith.

Residues Asn52, Tyr67, and Thr78 form a conserved hydrogen bond network with WAT166 that undergoes relatively large oxidation state linked conformational changes (Figure 4; Takano & Dickerson, 1981a,b; Bushnell *et al.*, 1990). The conserved residue Ile75 protects this region from exposure to solvent. The yeast iso-1-cytochrome *c* mutants Ala52, Phe67, Met75, and Gly78 have been supplied by Dr. J. G. Guillemette.

Experiments have been performed on these mutants that assess their influence on the function of yeast iso-1-cytochrome *c*. To determine their influence on the oxidation-reduction equilibrium of cytochrome *c*, the reduction potentials of the variants have been measured by cyclic voltammetry. The temperature dependence of reduction potential has been measured for each mutant to determine the thermodynamic parameters of reduction. For several mutants, the pH dependence of reduction potential has been measured. The electron transfer rates of these mutants with the reductant $Fe(edta)^{2-}$ and the oxidant $Co(phen)_3^{3+}$ have been measured. Using the results from the electrochemical and kinetic experiments,

relative Marcus theory has been applied to assess the influence of mutation in the heme crevice on electron transfer activity.

To determine the influence of heme crevice mutations on the stability of the native heme conformation, the equilibrium and kinetics of alkaline isomerization and ligand binding to cytochrome *c* mutants were examined. The alkaline isomerization of the position-82 variants studied here has been evaluated previously (Pearce *et al.*, 1989), thus the present work considers the alkaline isomerization of the mutants in the hydrogen bond network about WAT166 only. Equilibrium and kinetic measurements of azide binding to both sets of mutants were performed to determine the effects of these mutations on the dynamic properties of the active site of cytochrome *c*.

In all experiments the results were interpreted with respect to known or possible structural properties of the proteins. The likely roles of the conserved residues of the heme crevice are discussed in light of the results obtained in this work.

METHODS

2.1 Cytochrome c Preparation

2.1.1 Fermentation of Yeast

Mutagenesis of yeast iso-1-cytochrome *c* was performed in the laboratory of Professor Michael Smith by Dr. J.G. Guillemette as described previously (Pielak *et al.*, 1985; Inglis *et al.*, 1991). The host yeast strain, GM3C-2 has no CYC1 gene, and the CYC7 gene has been inactivated by a point mutation. In addition GM3C-2 is unable to synthesize leucine due to a point mutation in the leu2 locus. The plasmid that bears the mutant CYC1 gene also possesses a functional leu2 gene, thus transformed GM3C-2 can be selected for either on the basis of growth on a nonfermentable carbon source or in the absence of leucine.

Transformed yeast cultures bearing the mutant CYC1 genes were supplied on agar plates in SC leu$^-$ medium, consisting of yeast nitrogen base, uracil and adenine supplements, amino acids (without leucine), and dextrose as a carbon source. For each mutant cytochrome *c*, a single isolated colony was used to inoculate three tubes, each containing 5 mL of liquid SC leu$^-$ medium. The cultures were grown for 24 hours at 30 °C in a shaker bath and used to inoculate three flasks each containing 1.5 L of SC leu$^-$ medium. The large cultures were grown for 48 hours at 30 °C in a shaker bath and were used to inoculate a sterilized 50 L fermenter.

The fermenter medium consisted of bactopeptone (2% w/v), yeast extract (1% w/v), and glycerol as a carbon source (3% v/v). Tetracycline (0.5 g) and streptomycin (2 g) were added to inhibit microbial growth, and antifoaming agent (15 mL) was also added. After inoculation the culture was grown aerobically for 48 hours at 30 °C. At this point, neutralized lactic acid was added to a final concentration of 1% v/v. Fresh antibiotics and antifoaming agent were also added. Growth was continued for another 48 hours. A sample of the culture was examined with a microscope to check for microbial contamination and to calculate the yeast cell density. The culture was harvested using a continuous flow centrifuge (CEPA Model Z41, New Brunswick Scientific) .

2.1.2 Cytochrome c Purification

All of the following steps were performed at 4 °C, except as indicated. Buffer A refers to sodium phosphate buffer, pH 7, μ = 0.1 M, containing 5 mM mercaptoethanol or 0.5 mM dithiothreitol. The purification of cytochrome *c* described here is based on a method described previously (Cutler *et al.*, 1987), with the addition of a final cation exchange chromatography step using Mono S resin (*vide infra*).

To each kilogram of yeast was added 250 mL of ethyl acetate and 500 mL of 1 M NaCl. The mixture was combined to a smooth consistency and stirred overnight with a magnetic stirrer. The mixture was poured into 400 mL polypropylene centrifuge bottles and centrifuged at 7500 rpm in a GSA rotor for 35 minutes. The orange-red supernatant fluid bearing the cytochrome *c* was filtered through cheese cloth. The yeast pellet was resuspended in 1 M NaCl and centrifuged as before. The supernatant fluids were pooled and diluted with distilled water to give a conductivity less than 8000 Ω^{-1}. Dithiothreitol (2g) was added to the solution to reduce the cytochrome *c*.

Cation exchange cellulose resin (Whatman CM-52, 300 mL, equilibrated in buffer A) was added to the protein solution, and the solution was stirred for 10 minutes by hand using a glass rod. The solution was left for 1 hour to let the resin settle. After 1 hour, the solution was decanted, leaving the cytochrome *c* bound to the settled resin. The resin was transferred to a sintered glass funnel and washed with several volumes of buffer A, 0.05 M in NaCl. The cytochrome was eluted from the resin with buffer A that was made 1.0 M in NaCl. The cytochrome *c* solution was dialysed against 16 L of buffer A using dialysis tubing with an exclusion cutoff of 8000 daltons.

The dialysed cytochrome solution was loaded onto a column of cation exchange resin (Pharmacia CM-Sepharose, 2.5 x 6 cm) and eluted from the column by a salt gradient developed with 400 mL each of buffer A, 0.075 M in NaCl and buffer A, 0.25 M in NaCl. The eluent solution was collected in 8 mL fractions with a Gilson fraction collector. Two cytochrome *c* bands were usually seen. The minor,early eluting band was discarded; fractions from the major, later eluting band with absorbance ratios A_{416} /A_{280} greater than 5 were pooled. The pooled fractions were concentrated by ultrafiltration using progressively

smaller ultrafiltration units: an Amicon stirred cell with a YM-5 membrane (exclusion cutoff 5000 daltons) was used to concentrate solutions from volumes greater than 100 mL to less than 20 mL; further concentration steps employed Centriprep and Centricon units (Amicon; both with an exclusion cutoff of 10 000 daltons).

A solution of concentrated, reduced protein (1 mL, 20-30 mg/mL) was equilibrated with 20 mM MES (pK_a 6.1, Perrin & Dempsey, 1974) buffer, pH 6, by passage through a column of gel filtration resin (Bio-Rad P6-DG, 1 x 20 cm). Cytochrome *c* was simultaneously oxidized on this column with excess $NH_4[Co(dipicolinato)_2]$ (Mauk *et al.*, 1979) which was applied to the column prior to the protein.

Final purification was achieved by ion exchange chromatography at room temperature with an FPLC system fitted with a Mono-S HR 10/10 cation exchange column (Pharmacia). A solution of cytochrome *c* (1 mL, 15-20 mg/mL) was loaded onto the column and eluted with 20 mM MES, pH 6, 1 M in NaCl, using a linear salt gradient from 0.25 to 0.45 M NaCl. The eluate solution was monitored at 280 nm, and chromatograms were acquired with a chart recorder. The eluate fluid was collected in 2 mL fractions, which were placed on ice. Fractions from the main eluting fraction with the highest $A_{409.5}/A_{280}$ ratios were pooled, concentrated, and the spectrum recorded from 700 to 250 nm. The yield of cytochrome *c* was determined spectroscopically using the extinction coefficient $\epsilon_{409.5}$ = 106.1 mM^{-1} cm^{-1} for the Soret band maximum of the oxidized protein (Margoliash & Frohwirt, 1959). Samples were placed in cryovials, flash frozen, and stored in liquid nitrogen.

2.2 Electrochemical Experiments

The three electrode cell used for cyclic voltammetry is shown in Figure 13. A schematic diagram of this cell is shown in Figure 14. The auxiliary electrode is made of platinum mesh, and the reference is a saturated calomel electrode (Radiometer K401) maintained at 25 °C with a water bath. The sample

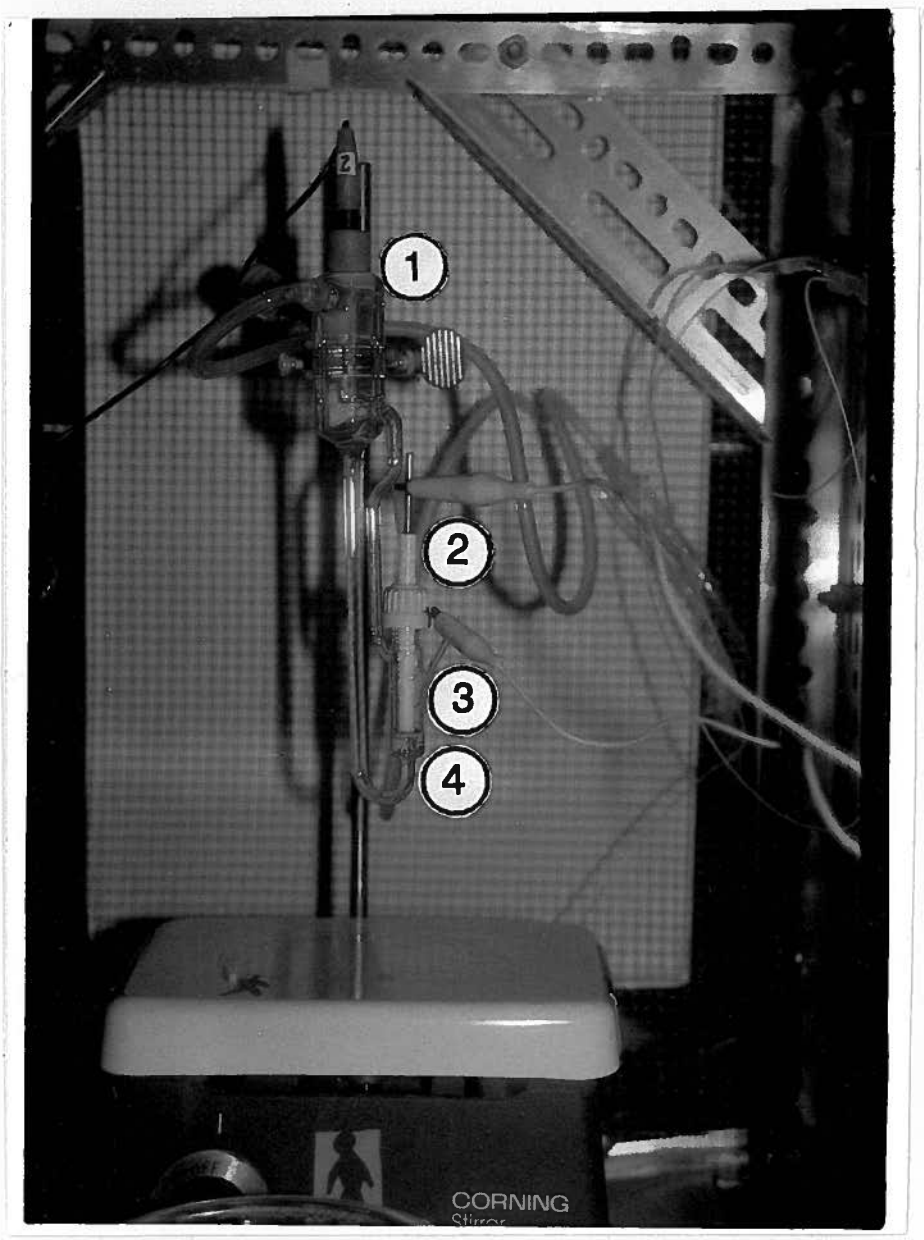

Figure 13 A photograph of the cyclic voltammetry cell used for reduction potential measurements. Legend: 1, reference electrode; 2, working electrode; 3, auxiliary electrode; 4, sample compartment.

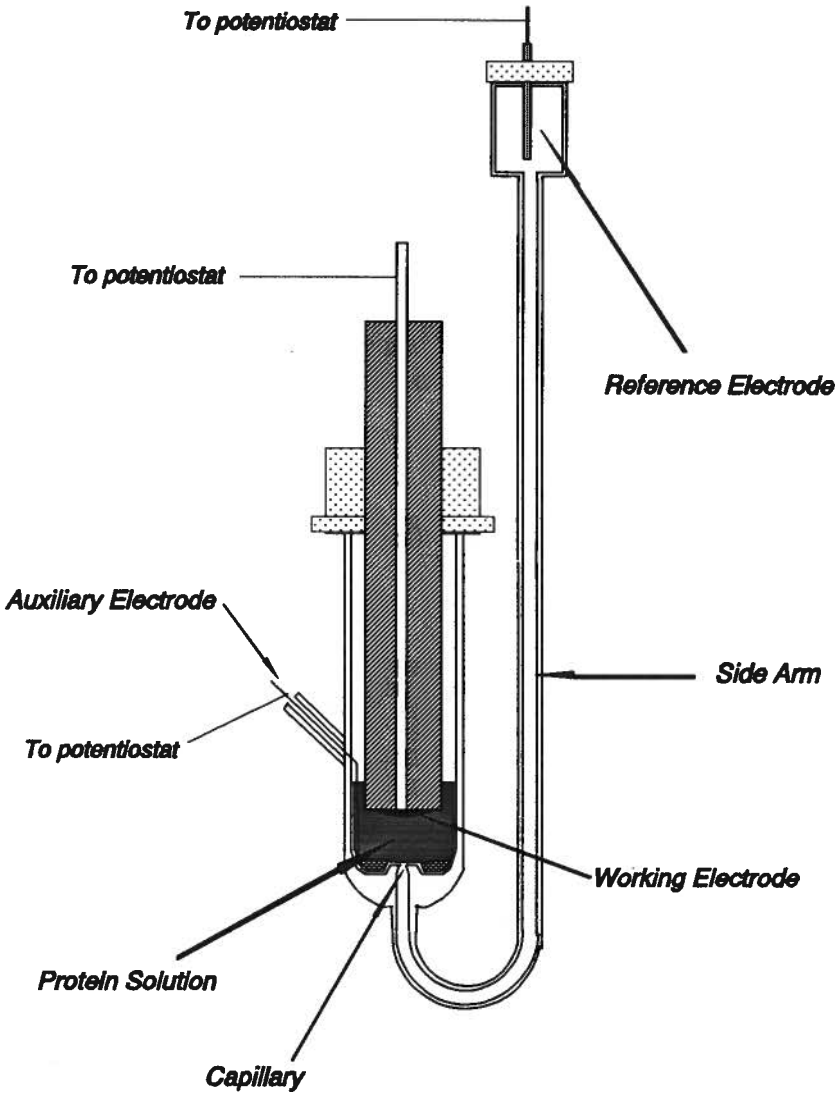

Figure 14 A schematic diagram of the cyclic voltammetry cell. The working electrode is a polished gold surface, treated with 4,4'-dithiodipyridine to promote rapid electron transfer between the electrode and the protein in solution. The auxiliary electrode is a platinum wire connected to platinum mesh at the bottom of the protein solution. The side arm is filled with buffer and provides contact between the reference electrode and the protein solution by means of a capillary located at the bottom of the protein solution. The electrodes are connected to the potentiostat by alligator clips at the indicated positions.

compartment was immersed in a jacketed beaker containing water, and the temperature was regulated with a second water bath.

The gold disc electrode (surface area 0.16 cm^2) was prepared by polishing with increasingly fine grades of alumina (Beuhler: 1.0, 0.3 and 0.05 μm) / water slurry on a polishing cloth (Mastertex). After freeing the polished electrode of alumina by sonication in a water bath and rinsing with deionized, distilled water, the electrode was immersed in a saturated solution of the surface modifier 4,4'-dithiodipyridine (Aldrithiol-4, Aldrich) for several minutes prior to being used.

Protein solution (0.5 mL, 0.4 mM) was placed in the sample compartment and deaerated by passage of a stream of water saturated, purified argon over the surface of the solution. The surface modified gold working electrode was immersed in the sample solution, and the leads from the electrodes were connected to the potentiostat used to control the cell potential (Ursar Electronics, Oxford U.K.). A potential range of -10 to 530 mV *vs* SHE was scanned at a rate of 5 to 200 mV/s. Cyclic voltammograms were obtained with an x-y recorder (Kipp & Zonen Model BD 90). Reduction potentials were measured from voltammograms acquired at a sweep rate of 20 mV/s. All experiments were carried out using μ = 0.1 M buffer (50 mM in KCl with the balance of the ionic strength provided by sodium phosphate). The temperature dependence of reduction potentials was measured between 10 and 40 °C at pH 6.0, with the reference electrode maintained at 25 °C. The pH dependence of reduction potential was measured in the pH interval 5.5 to 8.5 at 25 °C.

2.3 Electron Transfer Kinetics

All of the kinetic experiments were performed with a Durrum Model D-130 stopped flow spectrophotometer, modified as described previously to improve the anaerobicity of the apparatus (Reid & Mauk, 1982; Reid, 1984). The optical system used was a Durrum Model 120 Rapid Kinetics Monochromator with a tungsten source. Data acquisition was controlled by OLIS 4120AT software running on a Zenith Z-100 microcomputer (On-Line Instrument Systems, Jefferson, Ga.). The reaction

temperature was regulated by a water bath to within 0.2 °C of the desired value. At least four kinetic traces were averaged for each measurement at a given reagent concentration or temperature.

2.3.1 $Fe(edta)^{2-}$ Reduction Kinetics

Reactant solutions were prepared on the day of use and were kept under an argon atmosphere. $Fe(edta)^{2-}$ solutions were prepared in phosphate buffer as described by Wherland *et al.* (1975). Buffered ferricytochrome *c* (5 μM) solutions were deaerated by a stream of water saturated, purified argon. The reduction of cytochrome *c* by $Fe(edta)^{2-}$ was monitored at 412.5 nm under pseudo-first order conditions with reductant concentration in at least 20 fold excess (μ = 0.1 M, sodium phosphate buffer, pH 6.0, 25.0 °C). The temperature dependence of the reaction was measured between 10 and 40 °C.

2.3.2 $Co(phen)_3^{3+}$ Oxidation Kinetics

2.3.2.1 Synthesis of $[Co(phen)_3]Cl_3$

o-Phenanthroline monohydrate (BDH, 4.0 g, 0.02 moles) and 60 mL water were placed in a modified three necked 300 mL round bottom flask. $CoCl_2.6H_2O$ (MCB, 1.6 g, 0.0067 moles) was dissolved in 60 mL water; this solution was added in small increments by Pasteur pipette to the phenanthroline suspension with swirling of the flask. During the addition of the $CoCl_2$, the contents of the flask turned brown, and the phenanthroline dissolved completely. The flask contents were heated briefly on a steam bath and cooled to room temperature. The Co(II) complex was oxidized by chlorine gas generated by potassium permanganate oxidation of hydrochloric acid as described by Vogel (1978). The solution containing the oxidized product was heated, with stirring, on a hot plate until the volume had been reduced to about 20 mL. The product solution was made up to 60 mL with water, and the volume reduced as before; this was repeated twice. The precipitated product was recrystallized from 95% ethanol, washed with diethylether, and air dried.

2.3.2.2 Ferrocytochrome c Oxidation by $Co(phen)_3Cl_3$

Buffered $Co(phen)_3Cl_3$ solutions [μ = 0.1 M (2 mM MES, balance NaCl), pH 6.0] were prepared by weighing and were stored in modified, three necked 100 mL round bottom flasks equipped with Leuer fittings. Buffered ferrocytochrome *c* solutions were prepared on the day of use by reduction with dithionite followed immediately by passage through a column of gel filtration resin (Bio-Rad P6-DG, 1 x 10 cm) equilibrated with deaerated buffer. The eluting ferrocytochrome *c* was collected in a serum bottle, diluted with deaerated buffer to a concentration of 10-20 μM, and kept under a water-saturated argon atmosphere. Oxidation of cytochrome *c* by $Co(phen)_3Cl_3$ was monitored at 550 nm under pseudo-first order conditions, with oxidant in at least 20-fold excess. The temperature dependence of the reaction was examined between 10 and 40 °C.

2.4 Alkaline Isomerization

2.4.1 Spectrophotometric pH Titrations

Ferricytochrome *c* was exchanged into 0.1 M NaCl by ultrafiltration and diluted to a concentration of 0.15 to 0.2 mM. The cytochrome *c* solution was placed in a 3 mL quartz cuvette modified to hold a pH electrode, a microburette and a magnetic stir bar, as described previously (Pearce *et al.*, 1989). The initial pH of the solution was adjusted with 0.1 M HCl to pH 5.5. The titrant, 0.1 M NaOH, was added in microliter amounts by microburette (Manostat) to the stirred solution. The absorbance change at 695 nm was monitored after each addition of base. These steps were repeated with increasing pH values until no further significant absorbance change occurred.

2.4.2 pH Jump Kinetics

Ferricytochrome *c* solutions (40 μM) were prepared in unbuffered 0.1 M NaCl. For experiments involving jumps from low to high pH, the initial pH of the cytochrome *c* solution was adjusted to pH 6

using 0.1 M HCl. Stopped flow experiments were performed as described by Pearce *et al.* (1989). The unbuffered ferricytochrome *c* solution and a buffered solution of known pH were rapidly mixed in the stopped flow spectrophotometer, and absorbance changes were monitored at 695 nm. The final pH of the solutions after mixing was recorded. All experiments were done at 25 °C and μ = 0.1 M. Several buffers were used to span the pH region of interest: sodium phosphate, sodium borate, CHES, and CAPS, with pK_a's of 6.8, 9.1, 9.3, and 10.4, respectively (Perrin & Dempsey, 1974). For rapid jumps from high to low pH, the initial pH of the cytochrome *c* solution was adjusted with 0.1 M NaOH to 1.5 - 2 pH units above the expected alkaline pK_a. For this experiment the final pH was 6 in MES buffer.

2.5 Ligand Substitution

2.5.1 Azide Titrations

Two methods were used to measure the stability constants for azide binding to cytochromes *c*. In the first method, ferricytochrome *c* was exchanged into buffer [pH 6, μ = 1.0 M (20 mM MES, balance NaCl)] and concentrated by ultrafiltration. The concentrated protein solution (200 μL) was placed into each of two 5 mL volumetric flasks. One flask was diluted to volume with buffer, while the other was diluted to volume in 1.0 M NaN_3, pH 6. The concentration of azide in the latter solution was corrected for the volume of the protein solution added. The absorbance at 695 nm and spectrum (750-680 nm) of both solutions were recorded. Samples of the two solutions were mixed to produce a series of solutions that were equimolar in ferricytochrome *c* but possessing different azide concentrations. The azide concentration of each solution was calculated, and the absorbance at 695 nm measured. The spectrum of each solution in the range 750-680 nm was also recorded.

The second method used involved titration of a ferricytochrome *c* solution with a 2.5 M solution of sodium azide. Using the same buffer as above, a solution of ferricytochrome *c* was prepared in a quartz cuvette to a volume of 2.50 mL and a concentration of 40 to 120 μM. The absorbance at 695 nm and spectrum (750-680 nm) of the cytochrome *c* solution were recorded. A magnetic stir bar was placed in

the cuvette to allow efficient mixing. The absorbance at 695 nm was recorded after each incremental addition of azide. Absorbance changes at 695 nm were corrected for dilution resulting from the small volumes of titrant solution added.

2.5.2 Azide Binding Kinetics

Ferricytochrome *c* solutions (40 to 120 μM) were prepared in μ = 1.0 M buffer, pH 6.0 (20 mM MES, balance NaCl). Azide solutions (0.2 to 1.0 M in ligand) were of the same pH and ionic strength. The ligand exchange was monitored at 695 nm under pseudo-first order conditions, with azide in at least 1600 fold excess at 25 °C.

RESULTS

3.1 Protein Preparation

The yield of yeast from each 50 L fermentation was 0.8 to 1.4 kg. Protein yields were normally around 100 mg, but yields from 10 to 200 mg were obtained. While high yields of proteins are associated with high yields of yeast, the converse is not true, as the lowest yields of cytochrome *c* also gave good yields of yeast. Although cytochrome *c* is required for growth on a non-fermentable carbon source, only a relatively small amount of cytochrome *c* is required. Yeast will grow normally even if cytochrome *c* is expressed at only 10 percent of its usual level (Sherman *et al.*, 1974). Although the plasmid bearing the mutant cytochrome *c* gene is initially present in multiple copies and is expressed at high levels, with time the copy number may be lowered as the plasmid is lost from the yeast. Selection on a non-fermentable carbon source will ensure that only those yeast still bearing the plasmid will grow, but the plasmid copy number may be too low to be useful for large scale cytochrome *c* isolation. This explanation is consistent with the observation that low levels of expression are associated with mutant bearing yeast cultures prepared over six years ago, while more recently prepared cultures express cytochrome *c* at high levels.

Fermentations of yeast transformed with plasmids bearing genes encoding the variants Thr78Val and Thr78Gln both gave high yields of yeast and cytochrome *c*, although the protein was not stable *in vitro*. In both cases, the freshly isolated protein rapidly changed colour from orange to brown as the purification proceeded. Cation exchange chromatography revealed a mixture of coloured species, which eluted predominantly at ionic strengths above those normally required for native cytochrome *c* and most mutants. As both had sufficient function *in vivo* to support growth of yeast, their behaviour when isolated suggests a conformational change to a nonfunctional state with altered surface properties, and thus an inherent instability in the folded structures of their functional states.

A key step in the purification scheme is the ethyl acetate / salt extraction of the yeast cells. The ethyl acetate makes the organelle membranes leaky, and the salt solution dissociates the cytochrome *c* from the mitochondria. As ethyl acetate does not rupture the yeast (extracted yeast appear intact under a microscope) most of the cellular components remain within the cell, and the supernatant fluid containing the cytochrome *c* is relatively free of impurities. The two remaining cation exchange chromatography steps are greatly simplified by the relative purity of the cytochrome *c* obtained from the CM-cellulose batch extraction. The importance of the ethyl acetate / salt extraction cannot be fully appreciated until one compares it to alternate extraction procedures such as cell disruption using a ball mill. In this method the total cell contents are released, which lowers the efficiency of the binding of cytochrome *c* to the CM cellulose resin and increases the number of impurities that need to be removed.

Previously, the final purification step was cation exchange chromatography on CM-Sepharose. The further use of the FPLC Mono S column offers several advantages. The higher resolution of the Mono S column allows one to obtain purer protein through removal of minor components which coelute with cytochrome *c* on the CM-Sepharose column. In addition, more efficient use is made of the protein, as impure and used cytochrome *c* can easily be recycled by passage through the column.

Two bands of cytochrome *c* were often present on the CM-Sepharose ion exchange column. The minor, rapidly eluting band has been attributed to deamidated cytochrome *c* (Brautigan *et al.*, 1978a), or cytochrome *c* that has not undergone trimethylation of Lys73. However, the relatively low yield this band precluded confirmation of these suggestions. The rapidly eluting fraction accounted for about 10 percent of the total cytochrome *c*.

3.2 Electrochemical Experiments

The electrochemistry of the cytochrome *c* mutants was quasi-reversible as indicated by the peak to peak separations of 54 to 63 mV (25 °C, 20 mV s^{-1} scan rate) obtained from the majority of the voltammograms. In addition, the dependence of the faradaic current on the square root of the scan rate was measured for several proteins and was found to be linear up to 50 mV s^{-1}. A representative plot is shown in Figure 15.

The reduction potential of horse cytochrome *c* was 270 mV ± 2 mV (pH 7, 25 °C, μ = 0.1 M, scan rate 20 mV/s), in reasonable agreement with the value of 262 mV obtained by spectroelectrochemistry (Taniguchi *et al.*, 1982b) and the value of 274 mV obtained by cyclic voltammetry (Bond *et al.*, 1990) under similar conditions. For native yeast iso-1-cytochrome *c*, the reduction potential was 290 mV (pH 6, 25 °C, μ = 0.1 M, scan rate 20 mV s^{-1}). Under these same conditions of temperature, pH and ionic strength, the reduction potentials of the mutants range from 245 to 286 mV vs SHE (Table 1).

The thermodynamic parameters were determined from the temperature dependence of the reduction potentials by combining the two equations for free energy (Taniguchi *et al.*, 1982b):

$$\Delta G^\circ = -nFE_m \tag{11}$$

$$\Delta G^\circ = \Delta H^\circ - T\Delta S^\circ \tag{12}$$

Where the standard conditions are μ = 0.1 M, pH 6. As the reduction potentials are measured relative to the standard hydrogen electrode, the thermodynamic parameters of this reference must be taken into account.

$$Fe(III)Cyt\ c + 1/2\ H_2 \rightleftharpoons Fe(II)Cyt\ c + H^+ \tag{13}$$

$$\Delta H^\circ = \Sigma H_f\ (products) - \Sigma H_f\ (reactants) \tag{14}$$

By definition, the heats of formation of H^+ and H_2 are zero, thus the measured ΔH° is that of the cytochrome *c* Fe(III) / Fe(II) couple alone.

The entropy change in the cell is treated in a similar manner:

$$\Delta S^{\circ}_{cell} = \Delta S^{\circ}_{rc} - \Delta S^{\circ}_{SHE} \quad (15)$$

Where the subscript 'rc' (reaction centre) refers to the cytochrome *c* half cell and the subscript SHE refers to the reference electrode. The expression for the standard free energy of the cell can be rewritten as

$$\Delta G^{\circ} = \Delta H^{\circ} - (T\Delta S^{\circ})_{rc} + (T\Delta S^{\circ})_{SHE} \quad (16)$$

The partial molar entropies of the proton and of hydrogen gas are 0 and 31.2 entropy units, respectively (Latimer *et al.*, 1938; Latimer, 1952). This gives 15.6 entropy units for the change in entropy of the SHE reference. The reference electrode is maintained at 298 K, while the sample temperature is varied, thus the term $(T\Delta S^{\circ})_{SHE}$ remains constant. Equation 16 can be rewritten to take this into account:

$$\Delta G^{\circ} \ (calories/mol) = \Delta H^{\circ} - T\Delta S^{\circ}_{rc} + 4649 \quad (17)$$

Finally,

$$E_m \ (millivolts) = \frac{\Delta S^{\circ}_{rc}}{F} T - \frac{(\Delta H^{\circ} + 4649)}{F} \quad (18)$$

From a plot of E_m *vs* T, ΔS_{rc}° can be determined from the slope of the curve, and ΔH° is obtained from the intercept on the ordinate.

For horse heart cytochrome *c*, the reaction centre entropy, ΔS_{rc}°, determined by cyclic voltammetry was -9.7 $\pm$0.4 eu and the enthalpy of reduction, ΔH°, was -13.8 $\pm$0.1 kcal/mol (μ = 0.1 M, sodium phosphate, pH 7, gold electrode modified with 4,4'-dithiodipyridine). These results are comparable to ΔS_{rc}° = -12.9 $\pm$ 1.2 eu and ΔH° = -14.5 $\pm$ 0.4 kcal/mol obtained by spectroelectrochemistry [gold minigrid electrode, $[Ru(NH_3)_5py](ClO_4)_3$ mediator, nonisothermal cell, μ = 0.1 M sodium phosphate, pH 7.0 (Taniguchi *et al.*, 1982b)].

The plots of reduction potential against temperature for each variant of cytochrome *c* are shown in Figures 16 and 17, and the calculated thermodynamic parameters are presented in Table 1. All plots are

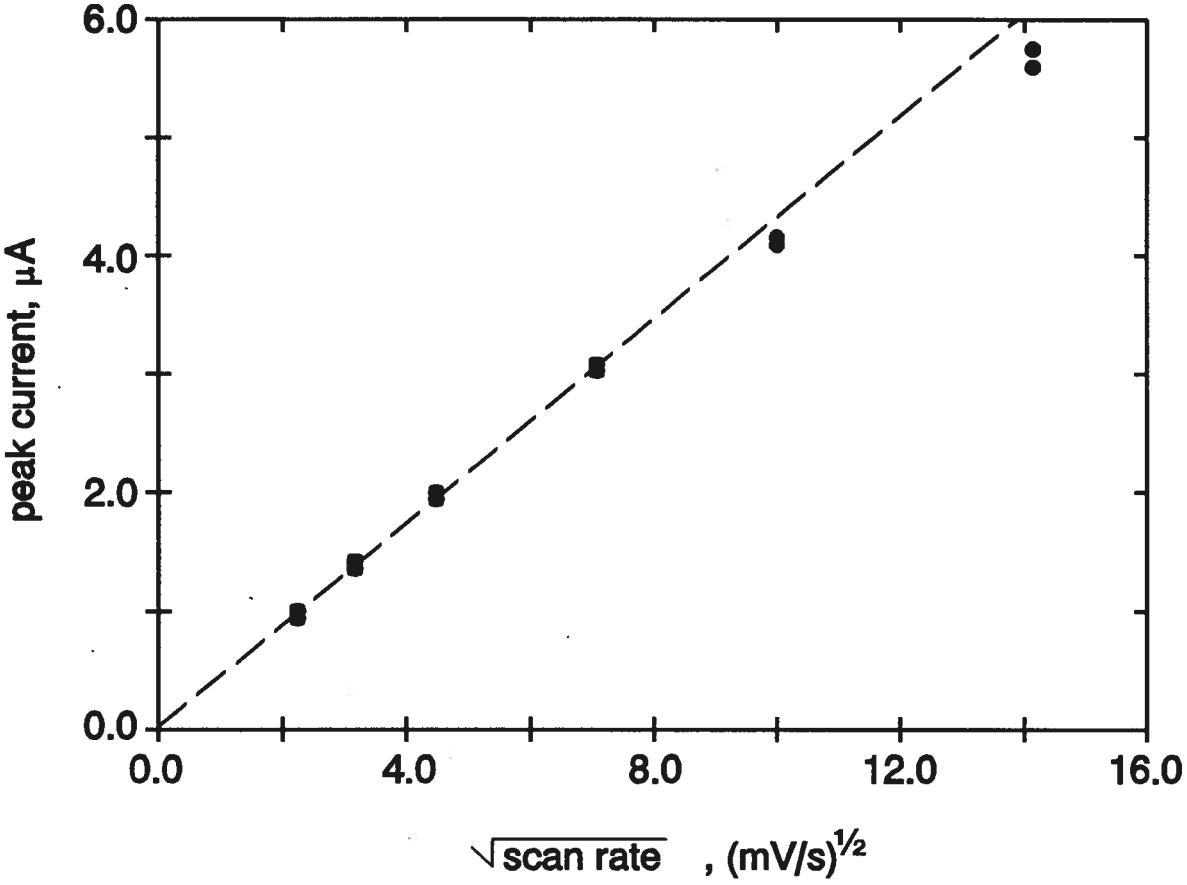

Figure 15 The dependence of faradaic peak current on the applied potential sweep rate for cytochrome *c* [pH 6.0, μ = 0.1 M, 25 °C, 20 mV/s].

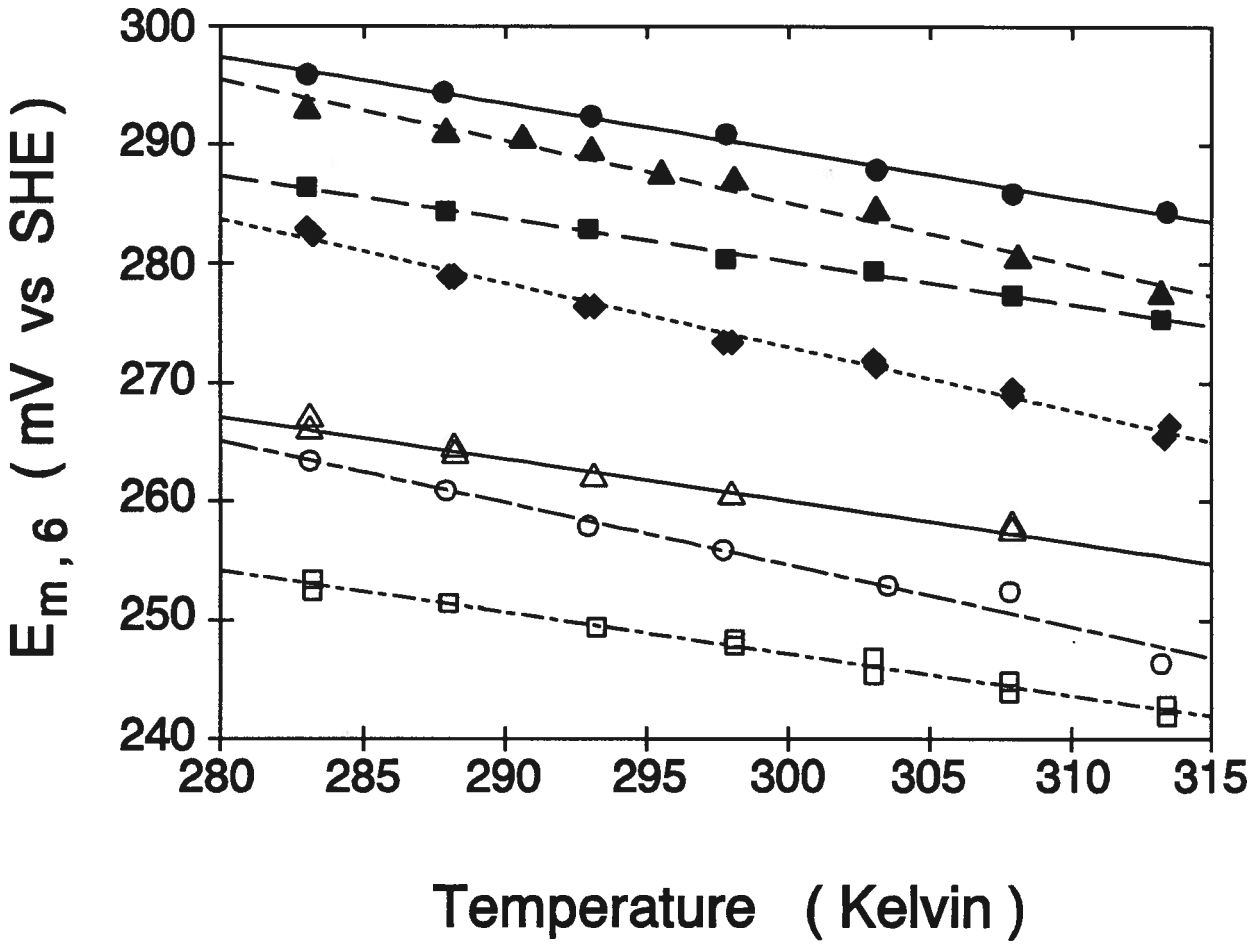

Figure 16 The temperature dependence of reduction potential for cytochrome *c* position-82 variants measured by cyclic voltammetry [pH 6.0, μ = 0.1 M sodium phosphate]. Legend: ●, Wild type; ▲, Phe82Leu; ■, Phe82Tyr; ◆, Phe82Ile; △, Phe82Ala; ○, Phe82Ser; □, Phe82Gly. For figures 16, 17, and 18, the error in the measured value of each point (±2 mV) is about twice the size of the symbols. $E_{m,6}$ is the midpoint reduction potential of the protein measured at pH 6.0 and the specified temperature. Numerical values of the data points in Figures 16 to 18 are tabulated in Appendix A.

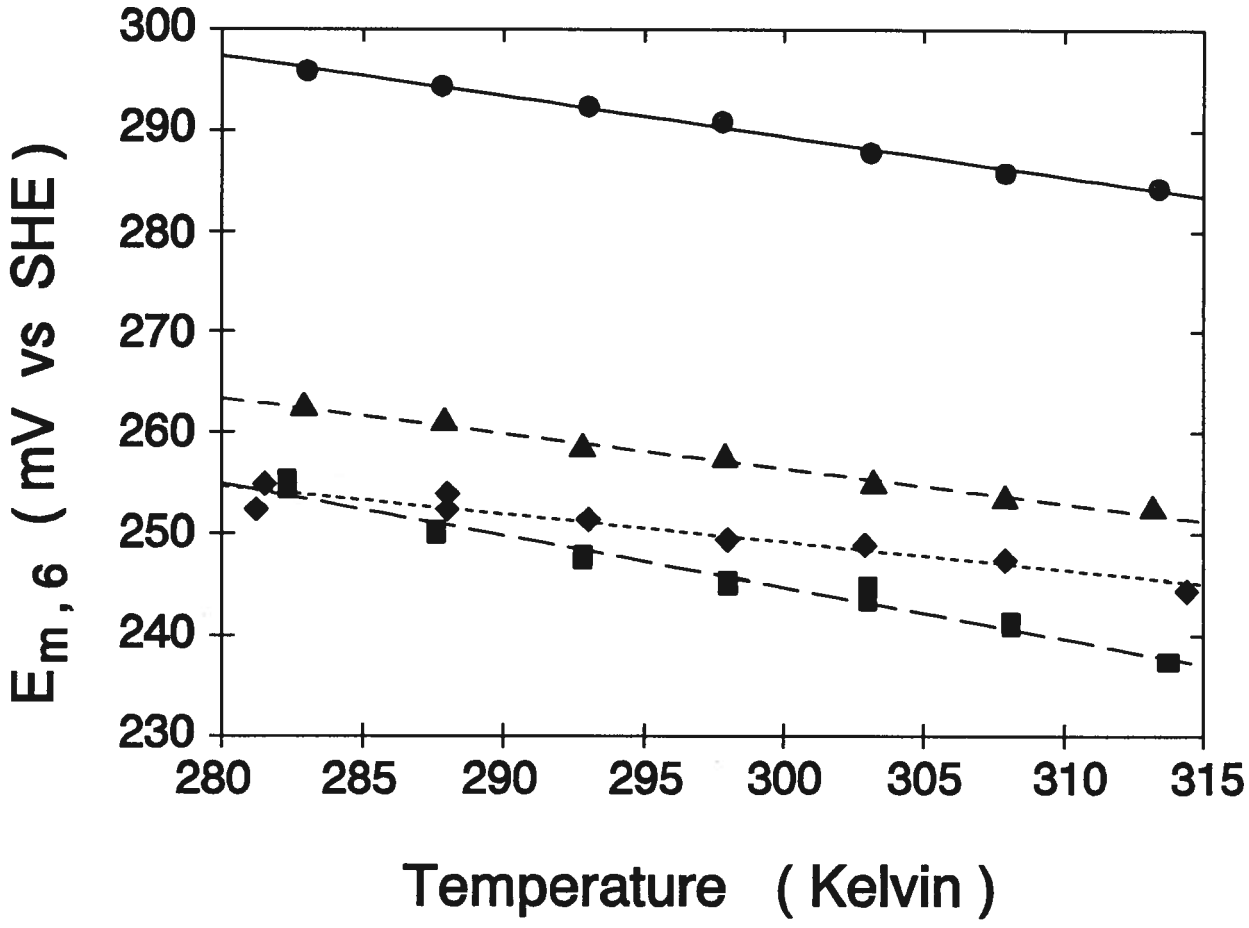

Figure 17 The temperature dependence of reduction potential for cytochrome *c* water switch variants measured by cyclic voltammetry [pH 6.0, μ = 0.1 M sodium phosphate]. Legend: ●, Wild type; ▲, Asn52Ala; ◆, Thr78Gly; ■, Ile75Met.

Protein	$E_{m,6}$ (mV)	$\Delta G°$ (kcal/mol)	$\Delta S_{rc}°$ (eu)	$\Delta H°$ (kcal/mol)
Wild Type	290 ± 2	-6.7 ± 0.2	-9.1 ± 0.3	-14.1 ± 0.1
Phe82Tyr	280 ± 2	-6.5 ± 0.2	-8.3 ± 0.3	-13.6 ± 0.1
Phe82Leu	286 ± 2	-6.5 ± 0.2	-12.0 ± 0.7	-14.8 ± 0.2
Phe82Ile	273 ± 2	-6.3 ± 0.2	-12.3 ± 0.3	-14.6 ± 0.1
Phe82Ala	260 ± 2	-6.0 ± 0.2	-8.1 ± 0.5	-13.1 ± 0.1
Phe82Ser	255 ± 2	-5.9 ± 0.2	-12 ± 0.9	-14.1 ± 0.3
Phe82Gly	247 ± 2	-5.7 ± 0.2	-8.0 ± 0.3	-12.8 ± 0.1

a)

Protein	$E_{m,6}$ (mV)	$\Delta G°$ (kcal/mol)	$\Delta S_{rc}°$ (eu)	$\Delta H°$ (kcal/mol)
Wild Type	290 ± 2	-6.7 ± 0.2	-9.1 ± 0.3	-14.1 ± 0.1
Thr78Gly	249 ± 2	-5.7 ± 0.2	-6.3 ± 0.7	-12.3 ± 0.2
Ile75Met	245 ± 2	-5.7 ± 0.2	-11.7 ± 0.3	-13.8 ± 0.2
Asn52Ala	257 ± 2	-5.9 ± 0.2	-8.0 ± 0.3	-12.9 ± 0.1
Tyr67Phe [1]	236 ± 2	-5.4 ± 0.2	-	-

b)

[1] Guillemette *et al.*, in preparation

Table 1 Thermodynamic parameters associated with the reduction of cytochrome *c* variants, measured by cyclic voltammetry [25 °C, μ = 0.1 M sodium phosphate]. a) position 82 variants; b) water switch variants. The uncertainties in $\Delta S°_{rc}$ and $\Delta H°$ were calculated by linear least squares fits of the data sets to equation 18 and are best regarded as a lower limit of the error. More realistic uncertainties in these fitted parameters are ± 1 eu in $\Delta S°_{rc}$, and ± 0.5 kcal/mol in $\Delta H°$.

linear with negative slopes, resulting in small negative entropies of reduction ranging from -7 to -13 entropy units. The enthalpies of reduction are negative and of similar magnitude for all of the cytochromes studied, ranging from -12.5 to -14.6 kcal mol^{-1}. The differences between $\Delta G°$ of wild type and any mutant of cytochrome *c* are less than 1 kcal mol^{-1}.

The pH dependence of reduction potential was used to determine the dissociation constants of titratable groups whose ionization state is sensitive to the oxidation state of the protein. Previous measurements using equilibrium techniques have shown that the pH dependence for yeast iso-1-cytochrome *c* can be described by three dissociation constants, two (K_{O1}, K_{O2}) in the oxidized state and one (K_r) in the reduced state (Moore *et al.*, 1984; Cutler *et al.*, 1989). The second dissociation constant in the oxidized protein is generally attributed to the alkaline isomerization (Moore *et al.*, 1984). Using cyclic voltammetry, the electrochemical properties of the alkaline isomer do not interfere with observation of the electrochemical behaviour of the native conformation, so the pH dependence of reduction potentials determined in this manner is described by a single oxidation state-linked pK_a:

$$E_{m,pH} = E_{m,0} + \frac{RT}{nF} \ln \frac{K_r+[H^+]}{K_o+[H^+]} \qquad (19)$$

By fitting the measured values to this equation, the oxidation state dependent dissociation constants are obtained, as well as the reduction potential extrapolated to pH 0, ($E_{m,0}$). Figure 18 shows the plots of reduction potential *vs* pH for the variants examined. The calculated parameters derived from a nonlinear least squares fit of the data to equation 19 are presented in Table 2. The values of pK_o and pK_r for wild type cytochrome *c* are in good agreement with previous measurements (pK_o = 6.6, pK_r = 7.2; Cutler *et al.*, 1989). The data for all mutants studied are consistent with the simple model involving a single ionizing group with a pK_a near neutrality that shifts by 0.3 to 0.4 pH units upon a change in oxidation state.

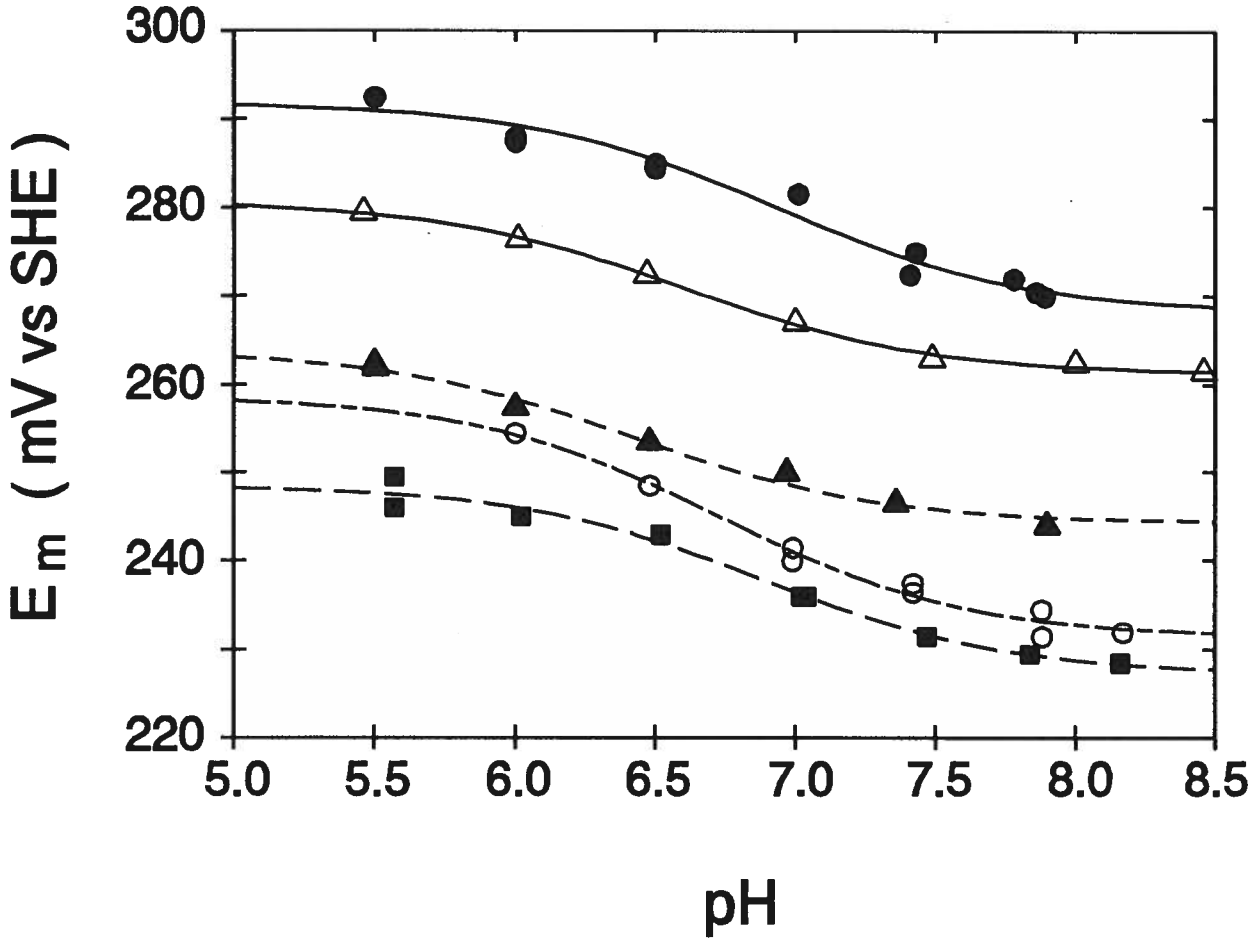

Figure 18 The pH dependence of reduction potential for several variants of cytochrome *c*, measured by cyclic voltammetry [25 °C, μ = 0.1 M sodium phosphate]. Legend: ●, Wild type; ▵, Gln42Lys / Ala43His; ▲, Asn52Ala; ○, Phe82Ser; ■, Ile75Met. The interpolated curves were calculated by least squares fitting of the data to equation 19.

Protein	$E_{m,0}$ (mV)	pK_r	pK_o
Wild Type	292 ± 2	7.1 ± 0.1	6.7 ± 0.1
Phe82Ser	259 ± 2	7.0 ± 0.1	6.5 ± 0.1
Ile75Met	248 ± 2	7.1 ± 0.1	6.7 ± 0.1
Asn52Ala	264 ± 2	6.6 ± 0.1	6.2 ± 0.1
Gln42Lys/ Ala43His	281 ± 2	6.8 ± 0.1	6.4 ± 0.1

Table 2 Parameters derived from the pH dependence of reduction potential for several variants of cytochrome *c* as measured by cyclic voltammetry [25 °C, μ = 0.1 M sodium phosphate].

3.3 Electron Transfer Kinetics

3.3.1 $Fe(edta)^{2-}$ Reduction Kinetics

For each cytochrome *c* variant, the dependence of the observed reaction rate on reductant concentration was linear. The intercept of each plot was within experimental error of zero. The second order reduction rate constant (k_{12}) for each cytochrome *c* variant could be calculated from the equation

$$k_{obs} = k_{12}[Fe(edta)^{2-}] \qquad (20)$$

Plots of k_{obs} against reductant concentration are presented in Figures 19 and 20, and second order rate constants calculated are presented in Table 3. For horse heart cytochrome *c*, k_{12} =2.86 x 10^4 $M^{-1}s^{-1}$, in good agreement with a previously measured value of 2.72 x 10^4 $M^{-1}s^{-1}$ (Hodges *et al.*, 1974) under identical conditions. The second order rate constants obtained for the yeast cytochromes *c* variants are all within a two-fold range of the rate constant obtained for the wild type protein [low =4.18 x 10^4 $M^{-1}s^{-1}$ (Ile75Met), high = 1.5 x 10^5 $M^{-1}s^{-1}$ (Phe82Ser)].

Those mutant proteins with an alkaline pK_a below 8 (position-82 mutants Leu, Ile, Ala, Ser, & Gly, and water switch mutant Thr78Gly) exhibited biphasic kinetics even at pH 6. In these cases, the reduction of the oxidized protein is the principal rate process at this pH and was several orders of magnitude faster than the rate of the slower phase. Consequently, the second order rate constants for reduction of the native proteins were readily determined. The slower phase exhibits a similar rate constant to that observed for the conversion of the alkaline form of these proteins to the native conformation in pH-jump experiments (Pearce *et al.*, 1989) and is thus ascribed to this conformational change.

To account for differences in thermodynamic driving force on the observed reaction rates, apparent self-exchange rate constants calculated for these reactions, k_{11}^{corr}, were determined as described by Wherland & Gray (1976). These values are also presented in Table 3. The value of k_{11}^{corr} for yeast wild type cytochrome *c* in this reaction is similar to that of horse heart cytochrome *c*

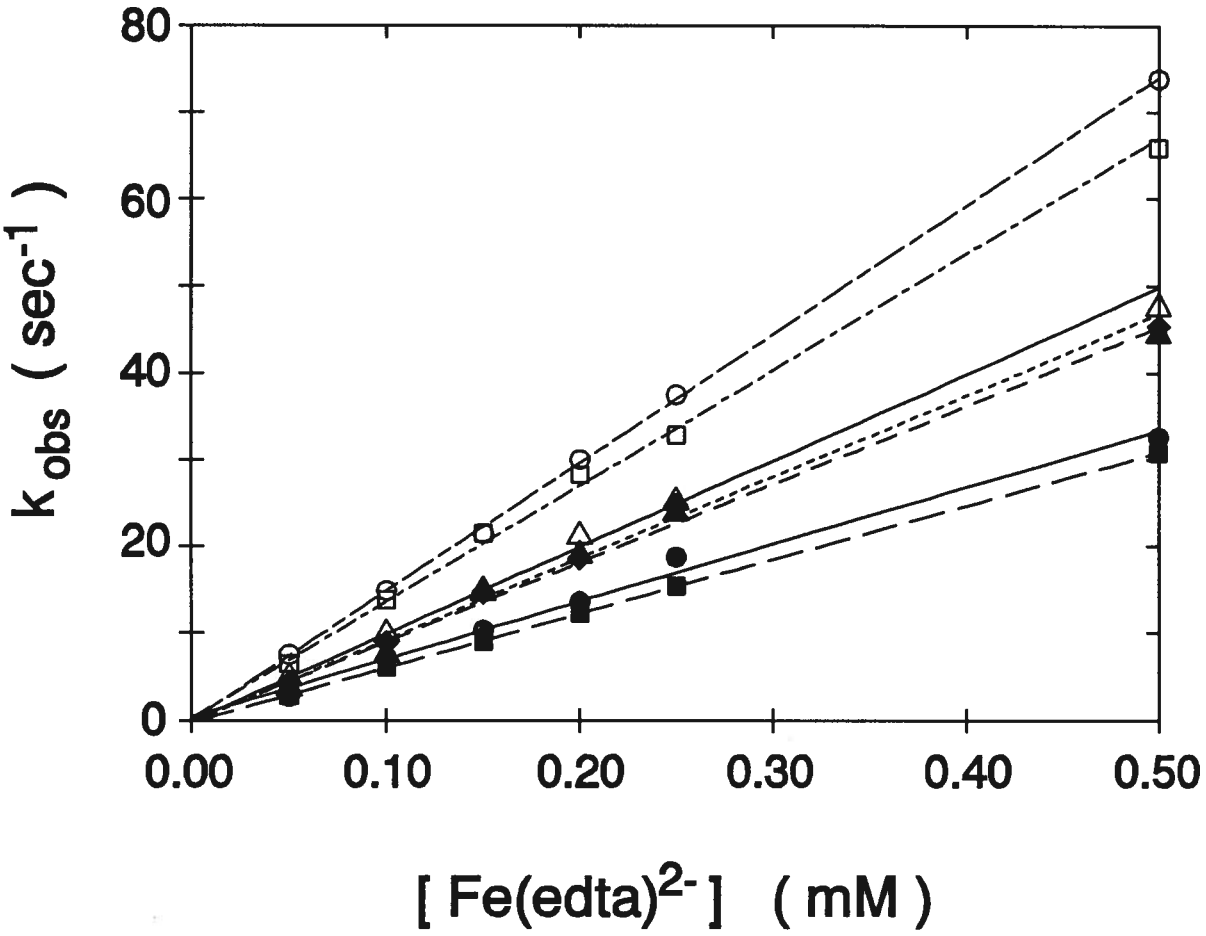

Figure 19 The dependence of pseudo-first-order rate constants for ferricytochrome *c* reduction on $Fe(edta)^{2-}$ concentration for position-82 variants. [25 °C, pH 6.0, μ = 0.1 M sodium phosphate]. Legend: ●, Wild type; ▲, Phe82Leu; ■, Phe82Tyr; ◆, Phe82Ile; △, Phe82Ala; ○, Phe82Ser; □, Phe82Gly. For this and subsequent kinetics figures, the error in each point is estimated to be ± 5%. Numerical values of the data points for Figures 19 to 22 are tabulated in Appendix B.

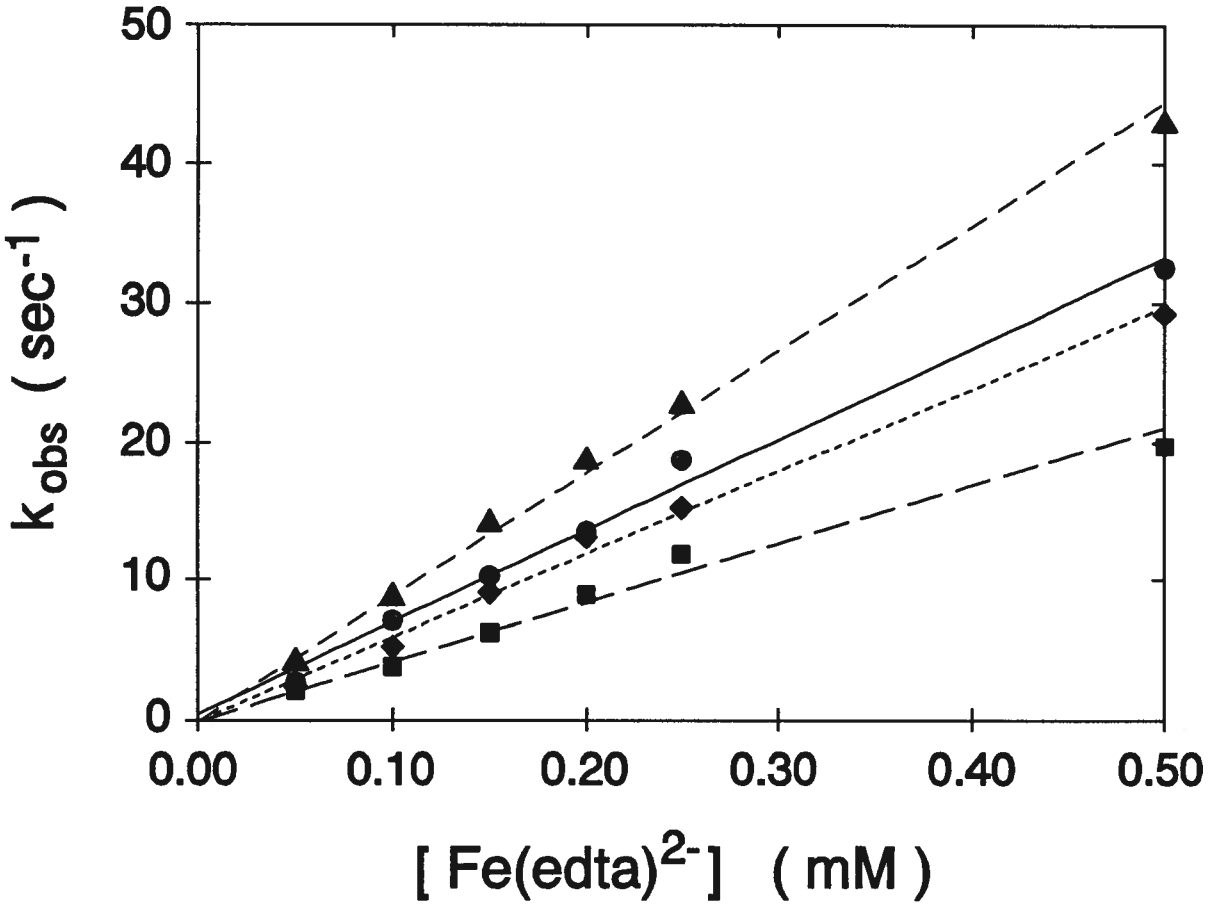

Figure 20 The dependence of pseudo-first-order rate constants for ferricytochrome *c* reduction on $Fe(edta)^{2-}$ concentration for water switch variants. [25 °C, pH 6.0, μ = 0.1 M sodium phosphate]. Legend: ●, Wild type; ▲, Asn52Ala; ■, Ile75Met; ◆, Thr78Gly.

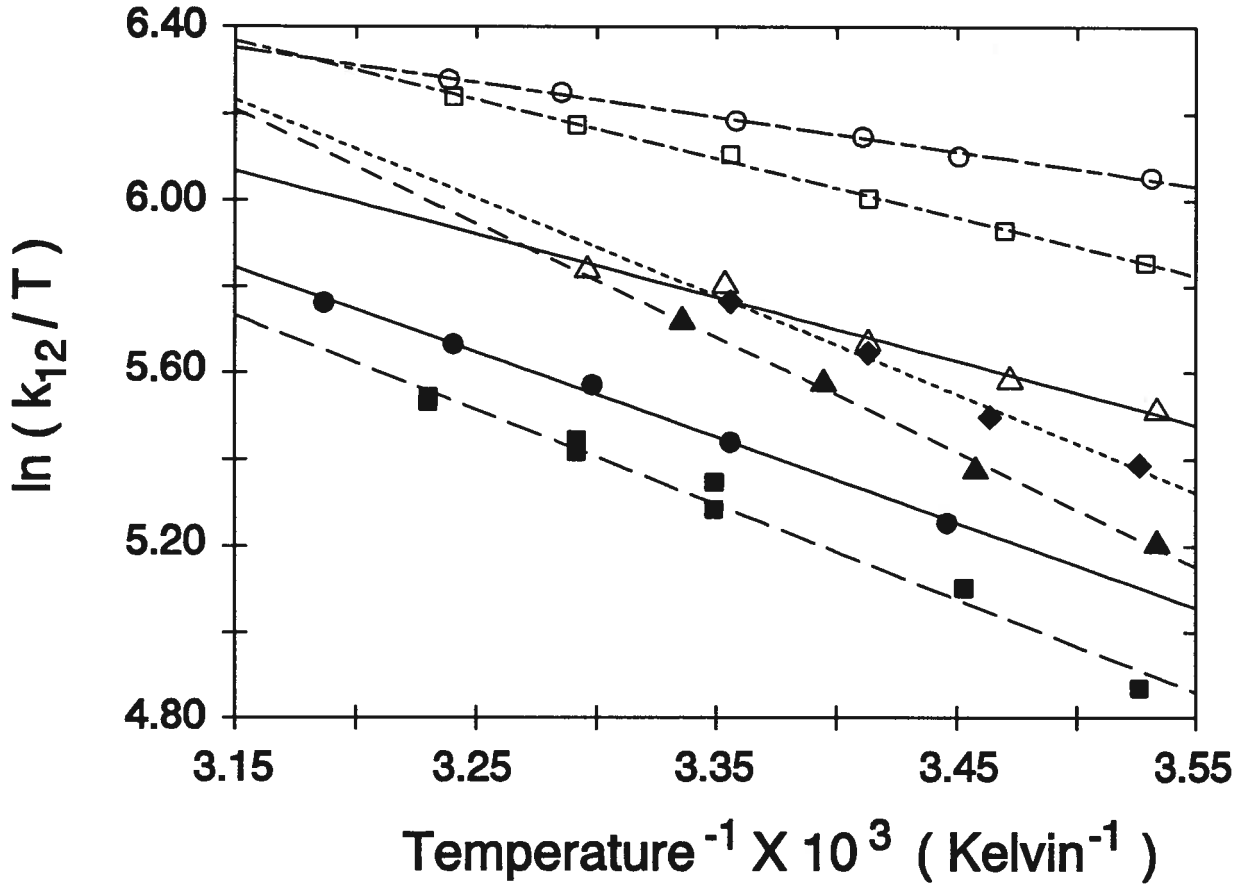

Figure 21 Eyring plots for the $Fe(edta)^{2-}$ reduction of position-82 variants of ferricytochrome *c*. [pH 6.0, μ = 0.1 M sodium phosphate]. Legend: ●, Wild type; ▲, Phe82Leu; ■, Phe82Tyr; ◆, Phe82Ile; △, Phe82Ala; ○, Phe82Ser; □, Phe82Gly.

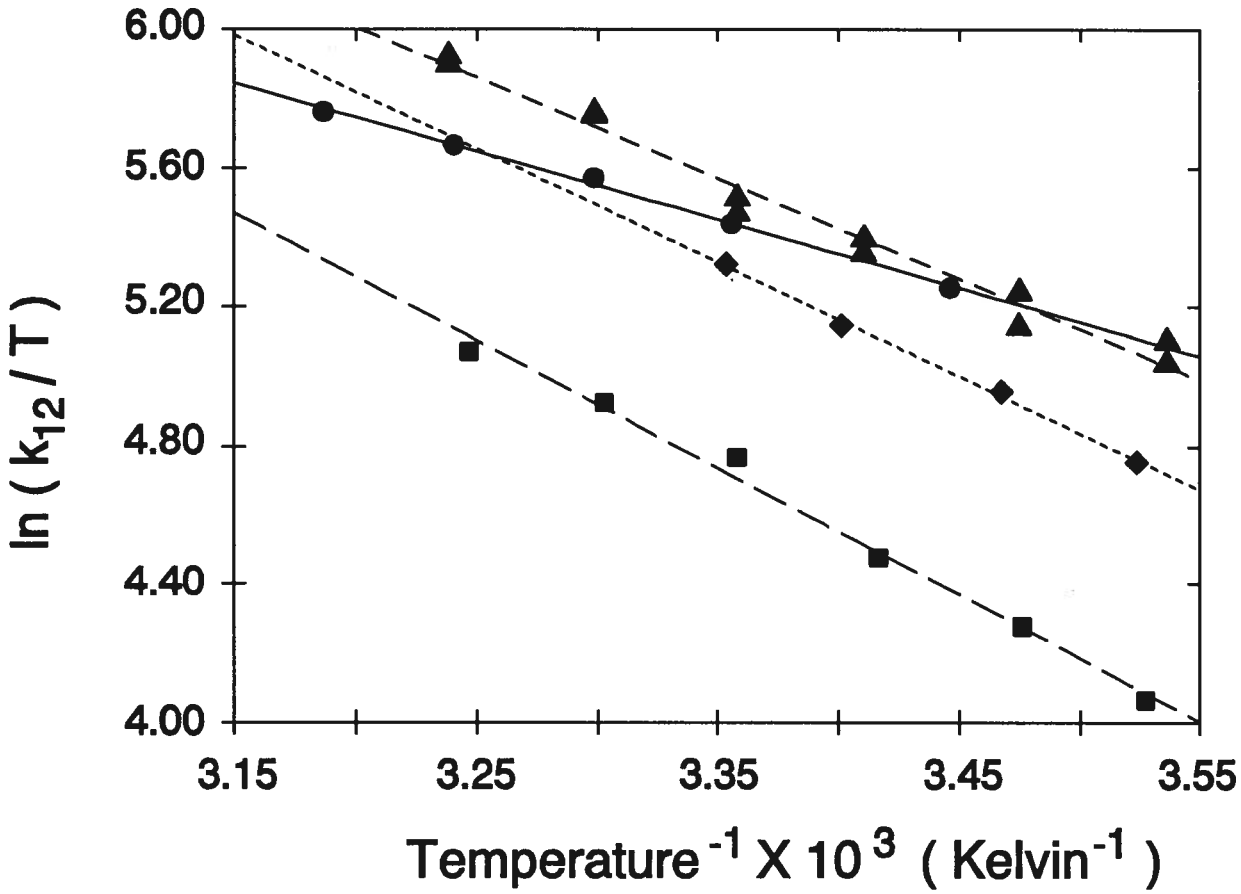

Figure 22 Eyring plots for the $Fe(edta)^{2-}$ reduction of water-switch variants of ferricytochrome *c*. [pH 6.0, μ = 0.1 M sodium phosphate]. Legend: ●, Wild type; ▲, Asn52Ala; ■, Ile75Met; ◆, Thr78Gly.

Protein	Rate Constant ($M^{-1}s^{-1}$) (25°C)	k_{11}^{corr} ($M^{-1}s^{-1}$) (25°C)	Activation Entropy (eu)	Activation Enthalpy (kcal/mol)
Wild Type	7.2×10^4	10.9	-24.7 ± 0.8	3.5 ± 0.2
Phe82Tyr	6.2×10^4	11.8	-22.2 ± 0.8	4.3 ± 0.2
Phe82Leu	8.8×10^4	19	-18.3 ± 0.9	5.3 ± 0.3
Phe82Ile	9.4×10^4	35	-21 ± 1	4.5 ± 0.3
Phe82Ala	9.9×10^4	62	-25 ± 1	3.2 ± 0.3
Phe82Ser	1.48×10^5	165	-29.6 ± 0.2	1.6 ± 0.1
Phe82Gly	1.37×10^5	190	-26.1 ± 0.3	2.7 ± 0.1

a)

Protein	Rate Constant ($M^{-1}s^{-1}$) (25°C)	k_{11}^{corr} ($M^{-1}s^{-1}$) (25°C)	Activation Entropy (eu)	Activation Enthalpy (kcal/mol)
Wild Type	7.2×10^4	10.9	-24.7 ± 0.8	3.5 ± 0.2
Thr78Gly	5.9×10^4	33.5	-14.8 ± 0.8	6.5 ± 0.2
Ile75Met	4.2×10^4	19	-13 ± 1	7.3 ± 0.3
Asn52Ala	8.9×10^4	56	-16.8 ± 0.9	5.8 ± 0.3
Tyr67Phe [1]	8.8×10^4	119	-	-

[1] Guillemette *et al.*, in preparation.

b)

Table 3 Rate parameters for the reduction of variants of ferricytochrome *c* [iron(II)edta reductant, pH 6.0, μ = 0.1 M sodium phosphate]. a) position 82 variants; b) water switch variants. The errors in the cross reaction rate constants are approximately 5 %. Errors in the activation entropies presented here and in Table 4 are those obtained from least squares fitting of the data points to equation 21 and are best regarded as a lower limit to the actual error. To calculate k_{11}^{corr}, the following values were used. $Fe(edta)^{2-}$: $E_{m,6}$ = 104 mV (Reid, 1984), k_{22} = 30 000 M^{-1} s^{-1} (Wilkins & Yelin, 1968), radius = 4 Å (Wherland & Gray, 1976), charge = -1 (oxidized), -2 (reduced). Cytochrome *c*: radius = 16.7 Å, charge = +7 (oxidized), +6 (reduced).

(Wherland & Gray, 1976), with values of 10.9 and 6 $M^{-1}s^{-1}$ respectively. The Phe82Gly and Phe82Ser variants possess the highest reactivity, with k_{11}^{corr} values of 165 and 190 $M^{-1}s^{-1}$ respectively.

The temperature dependences of the reduction rates were measured to determine the activation parameters of the reactions using the Eyring equation:

$$\ln\frac{k_{12}}{T} = \ln\frac{k_B}{h} + \frac{\Delta S^*}{R} - \frac{\Delta H^*}{RT} \qquad (21)$$

The activation enthalpies and entropies (Table 3) were calculated from the Eyring plots shown in Figures 21 and 22. For most variants, the plots were linear in the interval from 10 to 40 °C. Eyring plots of variants with alkaline pK_a values near 7 were linear over the abbreviated range of 10 to 25 °C. These mutants also had a larger contribution of the second, slower kinetic phase as the temperature increased. Activation entropies and enthalpies for all variants studied are similar to those found with horse heart cytochrome *c* ($\Delta H^{\ddagger}$ = 6.0 ± 0.3 kcal/mole, $\Delta S^{\ddagger}$ = -18 ± 1 entropy units; Hodges *et al.*, 1974).

3.3.2 $Co(phen)_3Cl_3$ Oxidation Kinetics

The reduction potential of $Co(phen)_3^{3+/2+}$ determined by cyclic voltammetry was 370 mV, (gold electrode, pH 6, μ = 0.1 M, 25 °C.), in good agreement with previous spectroelectrochemical measurements under similar conditions [377 mV, (Taniguchi *et al.*, 1982b)]. The extinction coefficients of $Co(phen)_3Cl_3$ at 330 and 350 nm were 4700 M^{-1} cm^{-1} and 3730 M^{-1} cm^{-1} respectively, compared to the values of 4680 $M^{-1}cm^{-1}$ and 3700 M^{-1} cm^{-1} found by Przystas & Sutin (1973).

Figures 23 and 24 show the dependence on $Co(phen)_3Cl_3$ concentration of the pseudo-first-order rate constants for ferrocytochrome *c* oxidation. Oxidation of each cytochrome *c* conformed to the rate equation of the type shown above (Equation 20). The second-order rate constant for each cytochrome *c* variant was calculated from the slope of its curve (Figures 23 and 24), and the results are presented in Table 4. For horse heart cytochrome *c*, this rate constant was 1.5 x 10^3 $M^{-1}s^{-1}$ (μ = 0.1 M, pH 6, 25

°C). This value differs from 1.0×10^3 $M^{-1}s^{-1}$ found by McArdle et al. (1974) under the same conditions. The rate constant was determined several times with different buffer compositions and protein purity, but consistently gave the higher value.

The electrostatics corrected self exchange rates were calculated from the second order rate constants of the cross reaction (Table 4). For most position 82 mutants, the differences in k_{11}^{corr} span only a three-fold range and show a dependence on the size of the side chain at this position, as was noted in the reduction kinetics measurements previously described. One exception to this general relationship is the Phe82Ile variant, with a k_{11}^{corr} almost seven fold greater than wild type. The water switch mutants span the same range as they do in the reduction kinetics experiments.

The oxidation rate dependence on temperature was treated as described for the reduction kinetics. Eyring plots (Figures 25 and 26) were linear over 10 to 40 °C for all variants. Activation parameters determined from these plots are shown in Table 4; they are similar to those previously determined for horse heart cytochrome *c* ($\Delta H^{\ddagger}$ = 11.3 kcal/mol, $\Delta S^{\ddagger}$ = -6 entropy units, pH 7; McArdle *et al.*, 1974).

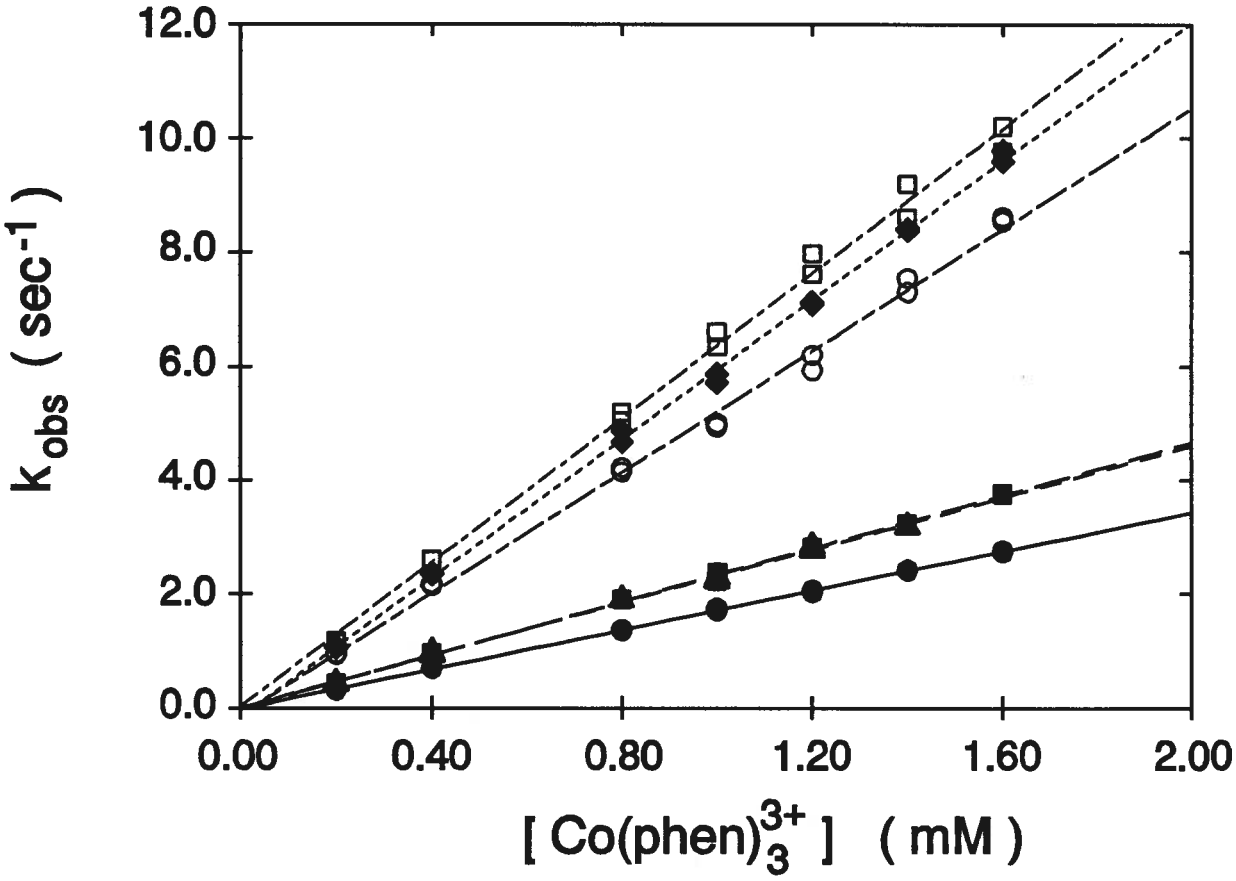

Figure 23 The dependence of pseudo-first-order rate constants for oxidation of position-82 variants of ferrocytochrome *c* on $Co(phen)_3^{3+}$ concentration [25 °C, pH 6.0, μ = 0.1 M (2 mM MES, 98 mM NaCl)]. Legend: ●, Wild type; ▲, Phe82Leu; ■, Phe82Tyr; ◆, Phe82Ile; ○, Phe82Ser; □, Phe82Gly. Numerical values of the data points for Figures 23 to 26 are tabulated in Appendix C.

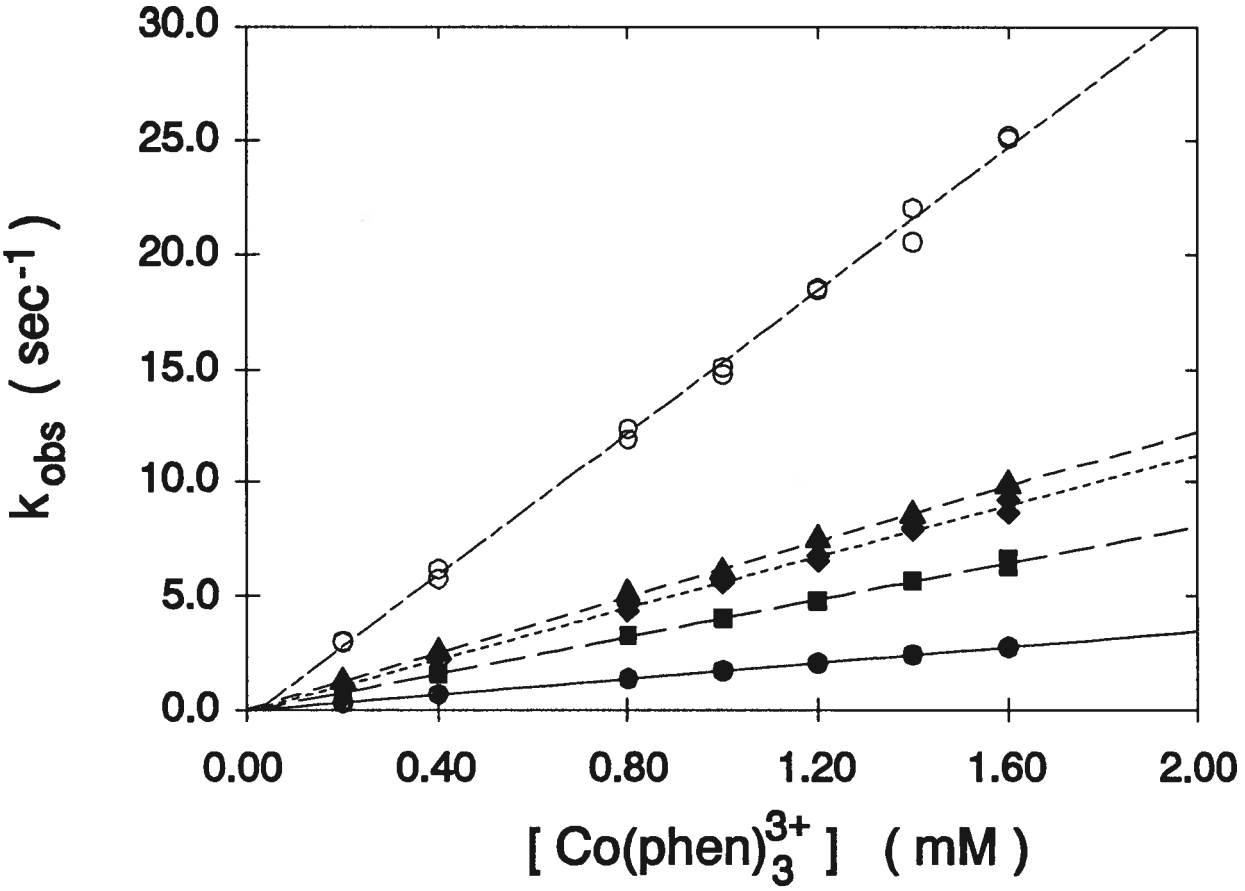

Figure 24 The dependence of pseudo-first-order rate constants for oxidation of water switch variants of ferrocytochrome *c* on $Co(phen)_3^{3+}$ concentration [25 °C, pH 6.0, μ = 0.1 M (2 mM MES, 98 mM NaCl)]. Legend: ●, Wild type; ▲, Asn52Ala; ■, Ile75Met; ◆, Thr78Gly; ○, Tyr67Phe.

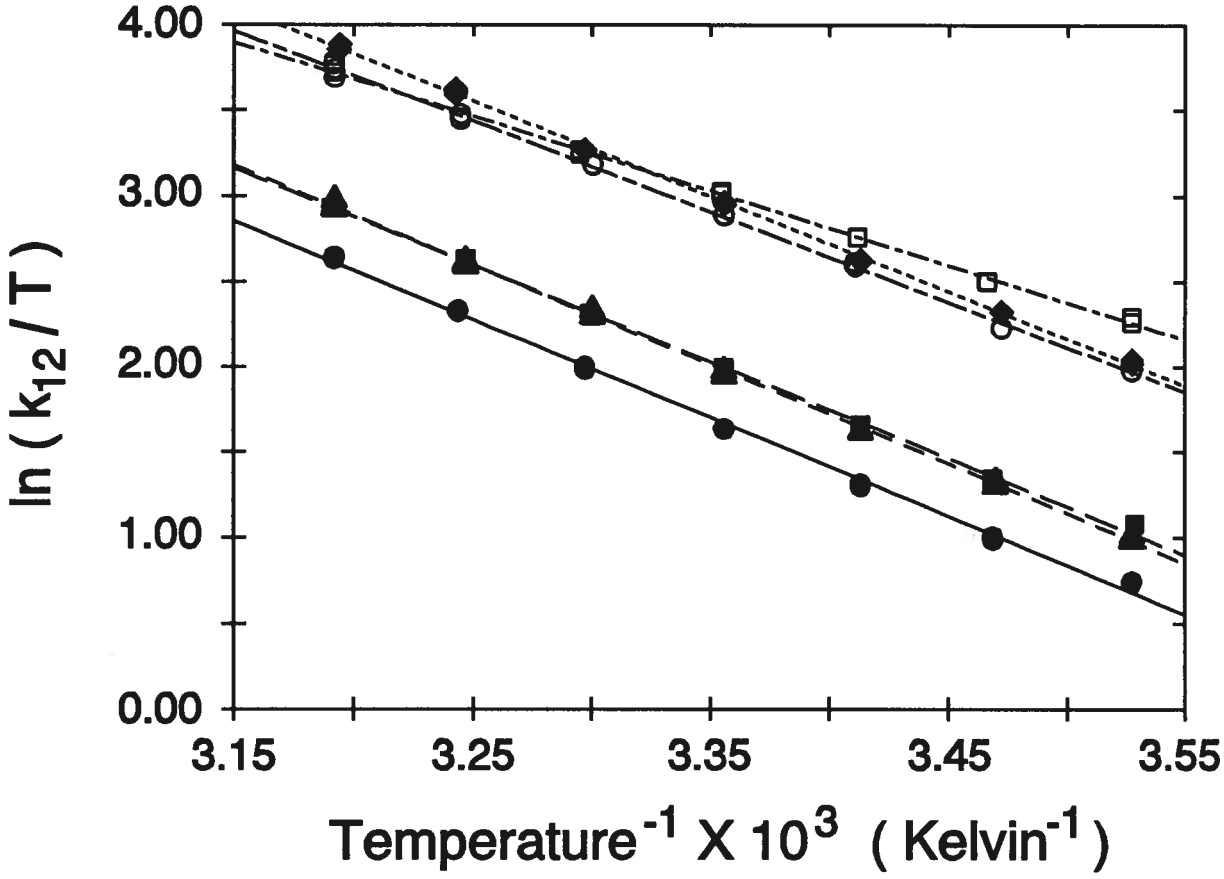

Figure 25 Eyring plots for the oxidation of position-82 variants of ferrocytochrome *c* by $Co(phen)_3^{3+}$ [pH 6.0, μ = 0.1 M (2 mM MES, 98 mM NaCl)]. Legend: ●, Wild type; ▲, Phe82Leu; ■, Phe82Tyr; ◆, Phe82Ile; ○, Phe82Ser; □, Phe82Gly.

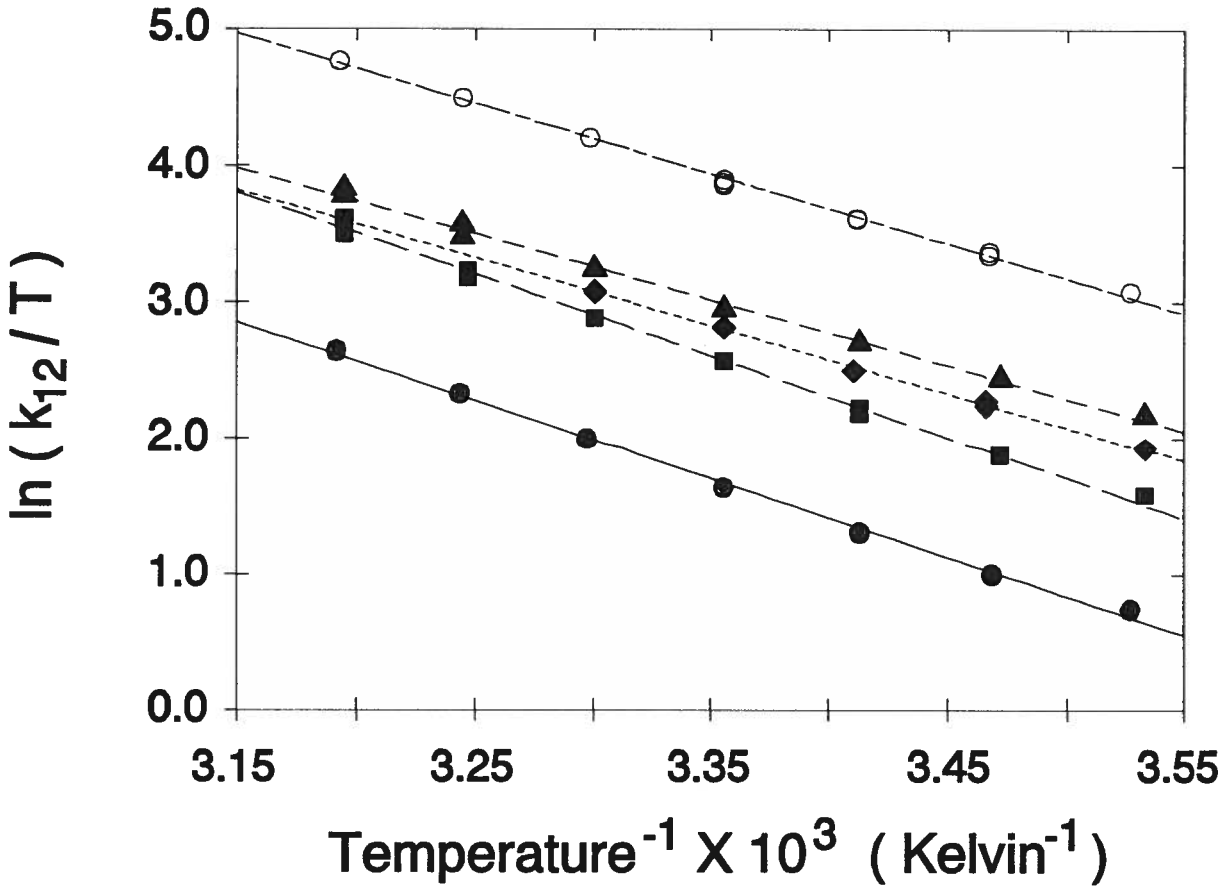

Figure 26 Eyring plots for the oxidation of water switch variants of ferrocytochrome *c* by $Co(phen)_3^{3+}$ [pH 6.0, μ = 0.1 M (2 mM MES, 98 mM NaCl)]. Legend: ●, Wild type; ▲, Asn52Ala; ■, Ile75Met; ◆, Thr78Gly; ○, Tyr67Phe.

Protein	Rate Constant ($M^{-1}s^{-1}$) (25°C)	k_{11}^{corr} ($M^{-1}s^{-1}$) (25°C)	Activation Entropy (eu)	Activation Enthalpy (kcal/mol)
Wild Type	1.7×10^3	3.1×10^3	-5.5 ± 0.6	11.4 ± 0.2
Phe82Tyr	2.4×10^3	4.1×10^3	-5.5 ± 0.5	11.3 ± 0.1
Phe82Leu	2.4×10^3	5.0×10^3	-4.4 ± 0.3	11.6 ± 0.1
Phe82Ile	6.1×10^3	2.1×10^4	-4.4 ± 0.3	11.0 ± 0.1
Phe82Ser	5.4×10^3	8.1×10^3	-6.3 ± 0.4	10.5 ± 0.1
Phe82Gly	6.6×10^3	9.2×10^3	-12.2 ± 0.4	8.6 ± 0.1

a)

Protein	Rate Constant ($M^{-1}s^{-1}$) (25°C)	k_{11}^{corr} ($M^{-1}s^{-1}$) (25°C)	Activation Entropy (eu)	Activation Enthalpy (kcal/mol)
Wild Type	1.7×10^3	3.1×10^3	-5.5 ± 0.6	11.4 ± 0.2
Thr78Gly	5.6×10^3	7.0×10^3	-8.7 ± 0.7	9.9 ± 0.2
Ile75Met	4.1×10^3	3.2×10^3	-2.1 ± 0.7	11.9 ± 0.2
Asn52Ala	6.2×10^3	1.1×10^4	-9.0 ± 0.7	9.6 ± 0.2
Tyr67Phe	1.5×10^4	3.3×10^4	-5.3 ± 0.5	10.2 ± 0.2

b)

Table 4 Rate parameters for oxidation of variants of ferrocytochrome *c* [$Co(phen)_3^{3+}$ oxidant, pH 6.0, μ = 0.1 M (2 mM MES, 98 mM NaCl)]. a) position 82 variants; b) water switch variants. The errors in the cross reaction rate constants are approximately 5 %. To calculate k_{11}^{corr}, the following values were used. $Co(phen)_3^{3+}$: $E_{m,6}$ = 370 mV, k_{22} = 41.7 M^{-1} s^{-1} (Baker *et al.*, 1959), radius = 7 Å (Wherland & Gray, 1976), charge = +3 (oxidized), +2 (reduced). Cytochrome *c*: refer to Table 3, page 69.

3.4 Alkaline Isomerization

3.4.1 pH Titrations

The pH dependent absorbance changes observed at 695 nm were used to calculate the ratio of alkaline to native isomer according to the relation:

$$\frac{[alkaline]}{[native]} = \frac{A_{695}^{native} - A_{695}^{i}}{A_{695}^{i} - A_{695}^{alkaline}} \qquad (22)$$

Where A_{695}^{native}, $A_{695}^{alkaline}$, and A_{695}^{i} are respectively the absorbances at 695 nm of the native isomer, the alkaline isomer, and of a mixture of the two at the intermediate pH.

The alkaline isomerization pK_a is calculated from the Henderson-Hasselbach equation:

$$pH = pK_a + n \log\frac{[alkaline]}{[native]} \qquad (23)$$

Data from the titration of horse heart cytochrome *c* plotted in this fashion gave a straight line with slope n = 1, consistent with obedience to the Henderson-Hasselbach equation with a stoichiometry of one proton. The calculated pK_a was 9.1, in excellent agreement with the results of other workers (Davis *et al.*, 1974; Pearce *et al.*, 1989). Titration of the yeast variant Thr78Gly was also consistent with the model, with a measured pK_a of 7.0; this value is compared to 8.5 obtained for the wild type protein (Pearce *et al.*, 1989). The pK_a values for these proteins are presented in Table 5.

3.4.2 pH Jump Kinetics

For the five proteins examined (horse heart cytochrome *c*, and yeast wild type, Thr78Gly, Ile75Met, and Asn52Ala), the observed rate constants for the loss of absorbance monitored at 695 nm (k_{obs}) were first order over the range of pH examined. The model of Davis *et al.* (1974) and the accompanying equation were used to determine the pK_H of the ionization and the rate constants of the subsequent conformational change:

$$Cyt\text{-}H \overset{K_H}{\rightleftharpoons} Cyt \underset{k_b}{\overset{k_f}{\rightleftharpoons}} Cyt^* \qquad (24)$$

Cyt-H and ***Cyt*** are the protonated and deprotonated forms, respectively, of native ferricytochrome *c*, and ***Cyt**** is the alkaline isomer.

The pH dependences of the first order rate constants were fitted to the following equation, derived from the above mechanism (Davis *et al.* 1974):

$$k_{obs} = k_b + \frac{k_f K_H}{K_H + [H^+]} \qquad (25)$$

The reverse rate constant k_b was estimated from the observed rate constant of the process at pH 6.

The results of the kinetic experiments and their analysis in terms of the model presented above are shown in Figure 27. The rate data for all of the proteins except Asn52Ala could be fitted to Equation 25. The parameters k_f, k_b, and pK_H calculated for each variant are presented in Table 5. There is good agreement between these results and those of previous investigators for the horse heart and yeast wild type cytochromes (Davis *et al.*, 1974; Pearce *et al.*, 1989). The parameters derived for horse heart cytochrome *c*, yeast wild type, and yeast variant Thr78Gly also give an estimate of the alkaline isomerization pK_a (pK_H + pK_c) that is in agreement with the value determined from the titration. The lowered alkaline pK_a for Thr78Gly is due to a pK_H that is 2 units below that of the wild type protein, partially compensated by a conformational equilibrium that is relatively more favourable to the native

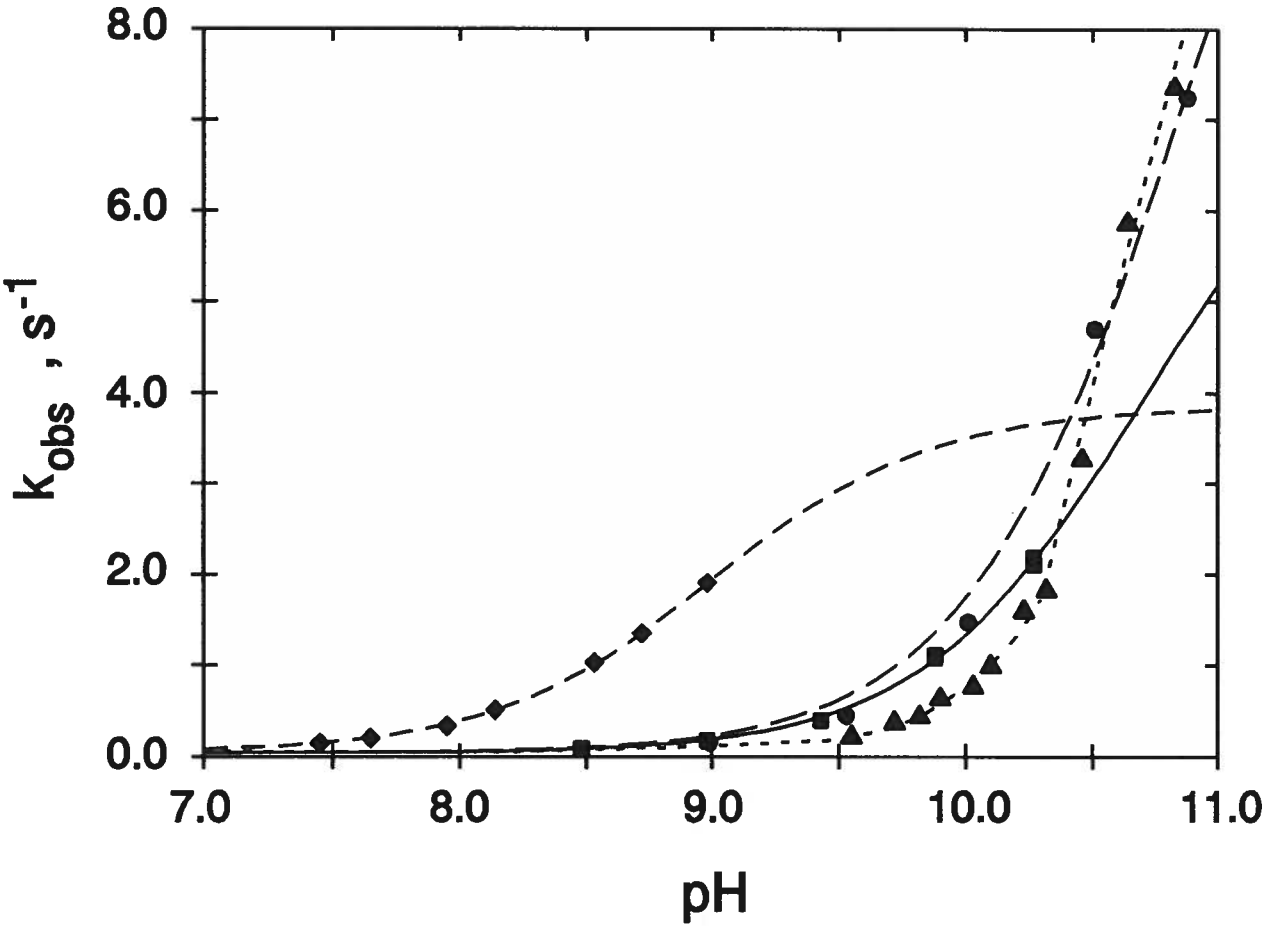

Figure 27 pH dependence of the rate of alkaline isomerization from stopped-flow pH jump experiments [25 °C, μ = 0.1 M]. Legend: ●, Wild type; ▲, Asn52Ala; ■, Ile75Met; ◆, Thr78Gly. The interpolated curves were calculated from least squares fitting of the data to equation 25. The data for the Asn52Ala variant could not be fitted to equation 25, thus the line through this data set is presented only as a visual aid. Numerical values of the data points are tabulated in Appendix D.

Protein	pK_a	pK_H	k_f (sec^{-1})	k_b (sec^{-1})	K_c	$pK_H + pK_c$
Horse *c* [1]	9.0	11.0 ± 0.1	6 ± 2	0.049 ± 0.003	120 ± 40	8.9
Horse *c*	9.1	11.24 ± 0.05	5.5 ± 0.4	0.035 ± 0.002	160 ± 20	9.0
Wild Type	8.5[2]	10.9 ± 0.1	16 ± 2	0.043 ± 0.001	370 ± 60	8.4
Ile75Met	-	10.7 ± 0.1	7.7 ± 0.9	0.041 ± 0.004	180 ± 30	8.4
Thr78Gly	7.0	9.0 ± 0.03	3.8 ± 0.1	0.047 ± 0.004	80 ± 9	7.1
Asn52Ala	8.3 [3]	-	-	0.007 ± 0.001	-	-

[1] Davis *et al.*, 1974.
[2] Pearce *et al.*, 1989.
[3] Guillemette *et al.*, in preparation.

Table 5 Alkaline isomerization parameters for variants of ferricytochrome *c* [25 °C, μ = 0.1 M].

conformation. The kinetic parameters of Ile75Met are similar to those found for yeast wild type. The sum $pK_H + pK_c$ for this variant gives a pK_a identical to that of the wild type cytochrome.

The data for the yeast Asn52Ala variant could not be fitted to the above equation. As shown in Figure 27, the observed rate constant increases more sharply with pH than observed for the other proteins. Similar behaviour has been seen in the Tyr67Phe variant (Guillemette, in preparation) and in *Euglena* cytochrome *c*, which also has a phenylalanine residue at position 67 (Pettigrew *et al.*, 1975).

Above pH 10.5 a second, faster, first-order phase was detected for both yeast wild type and the Asn52Ala variant. This phase accounted for an increasing amount of the total absorbance change at 695 nm as the pH was increased. The presence of this phase was more readily detected by monitoring the absorbance change at 529 nm (Figure 28). The rate constant for the faster phase was $45 \pm 1\ s^{-1}$ and was not dependent on wavelength.

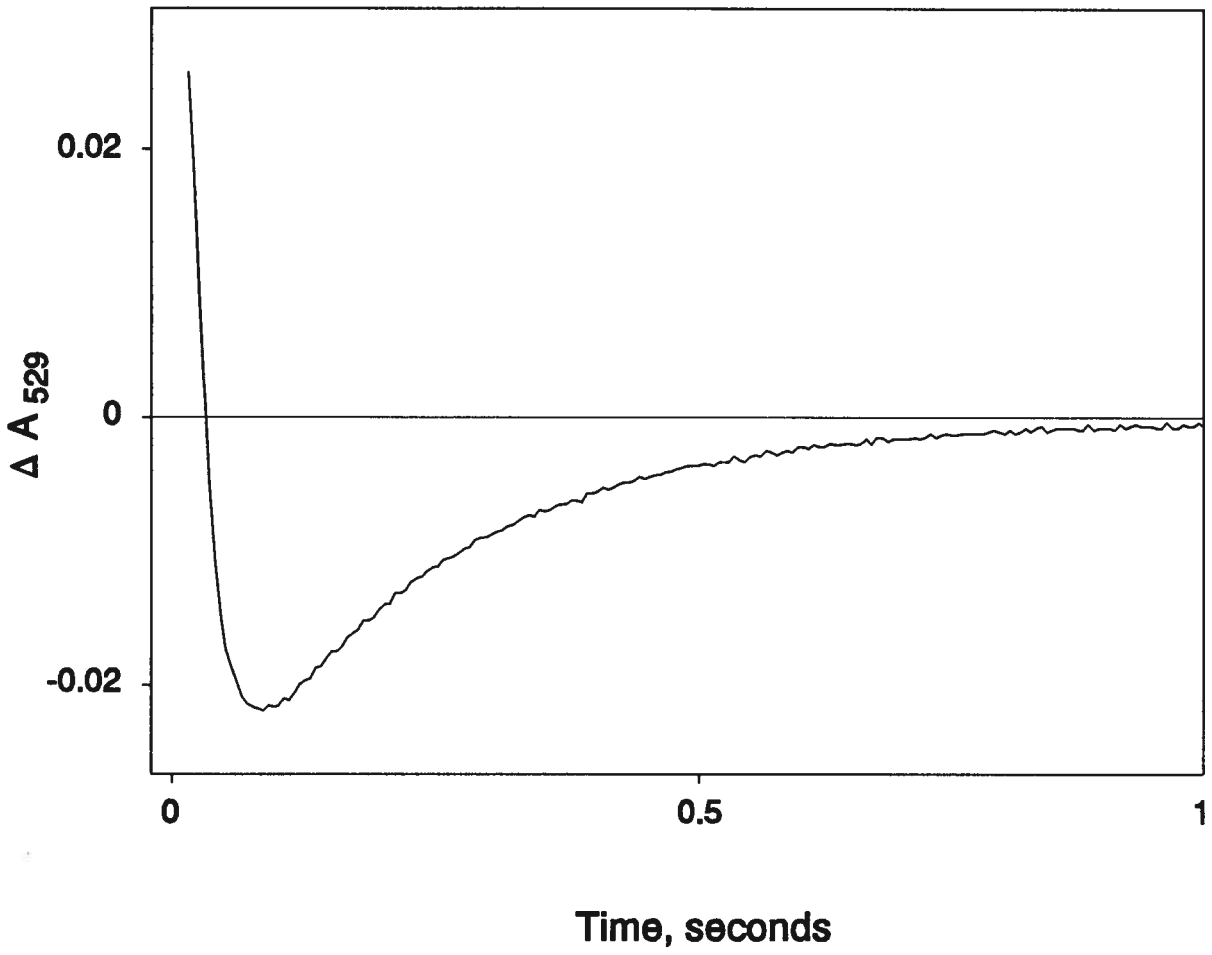

Figure 28 Kinetic trace of the alkaline isomerization of yeast-iso-1-ferricytochrome *c* at pH 10.5 monitored at 529 nm. The rate constant of the initial phase is 44 $\pm$ 2 s^{-1} while that of the second phase is 4.7 $\pm$ 0.4 s^{-1}

3.5 Ligand Substitution

3.5.1 Azide Binding Titrations

Azide binding to ferricytochrome *c* causes several changes to the visible spectrum, most notably a shift in the position of the Soret maximum from 409.5 nm to 412 nm and a 20 percent increase in the intensity of the Soret absorbance (Figure 29). There is also a shift in the position of the β-band from 530 to 539 nm, and a loss of the band at 695 nm (700 nm for Tyr67Phe). In contrast, there were no detectable differences between the visible spectra of reduced cytochrome *c* in the presence and absence of azide.

The absorbance changes at 695 nm that were observed upon addition of azide to ferricytochrome *c* were fitted to an equation of a binding isotherm for a 1:1 ligand-receptor complex (Connors, 1987):

$$\Delta A_{695} = \frac{\Delta A_{max}\,[azide]}{1/K_{azide} + [azide]} \qquad (26)$$

In this relationship, ΔA_{695} is the difference in the absorbance at 695 nm between native ferricytochrome *c* and ferricytochrome *c* at a known azide concentration, and ΔA_{max} is the difference in absorbance at 695 nm between native and azido-ferricytochromes *c*. Figures 30 and 31 show for each cytochrome *c* the fit of the experimental data to the binding isotherm with ΔA_{max} normalized to 0.1. The calculated binding constants, K_{azide}, are presented in Table 6 along with the results of the azide binding kinetics experiments. Measurements for all of the variants studied were consistent with 1:1 binding of azide. K_{azide} for horse heart cytochrome *c* was 4.5 $\pm$ 0.1 M^{-1}, comparable to 4 M^{-1} found by Sutin & Yandell (1972). K_{azide} for the wild type yeast protein was 16.7 $\pm$ 0.6 M^{-1} compared to 15 M^{-1} found by Saigo (1986).

The affinity of yeast cytochrome *c* for azide is strongly dependent on the identity of the residue at position 82. All of the variants at this site possessed greater azide affinities than that of the wild type protein. The azide binding constants for the Leu, Ile, Gly and Ser variants were three to five-fold greater than that for azide binding to wild type cytochrome *c*. The azide binding affinity of Phe82Tyr was the most similar to that of the wild type protein but was still two-fold greater.

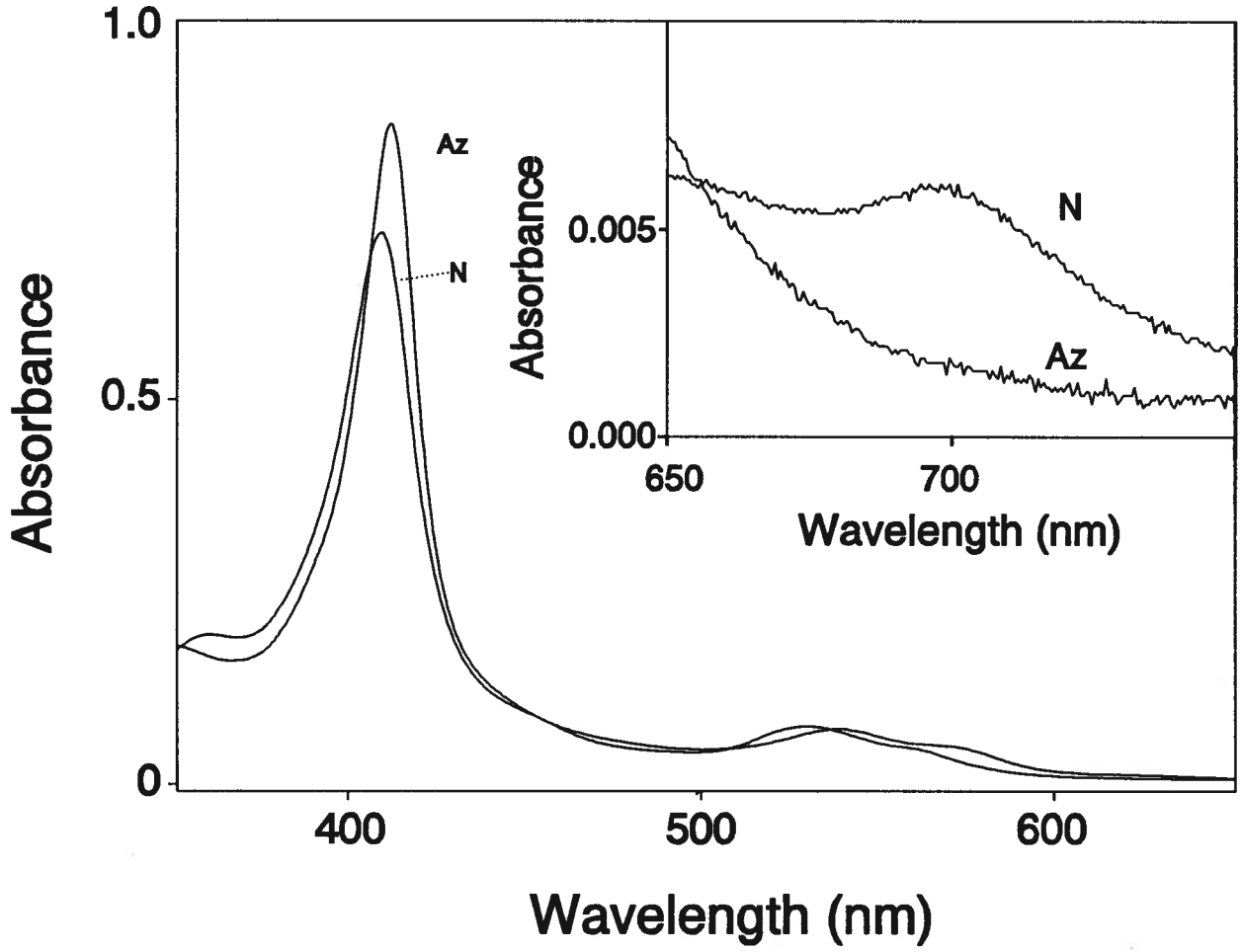

Figure 29 The visible spectra of yeast iso-1-ferricytochrome *c* in the presence (Az) and absence (N) of 2.5 M azide, 25 °C, pH 6.0.

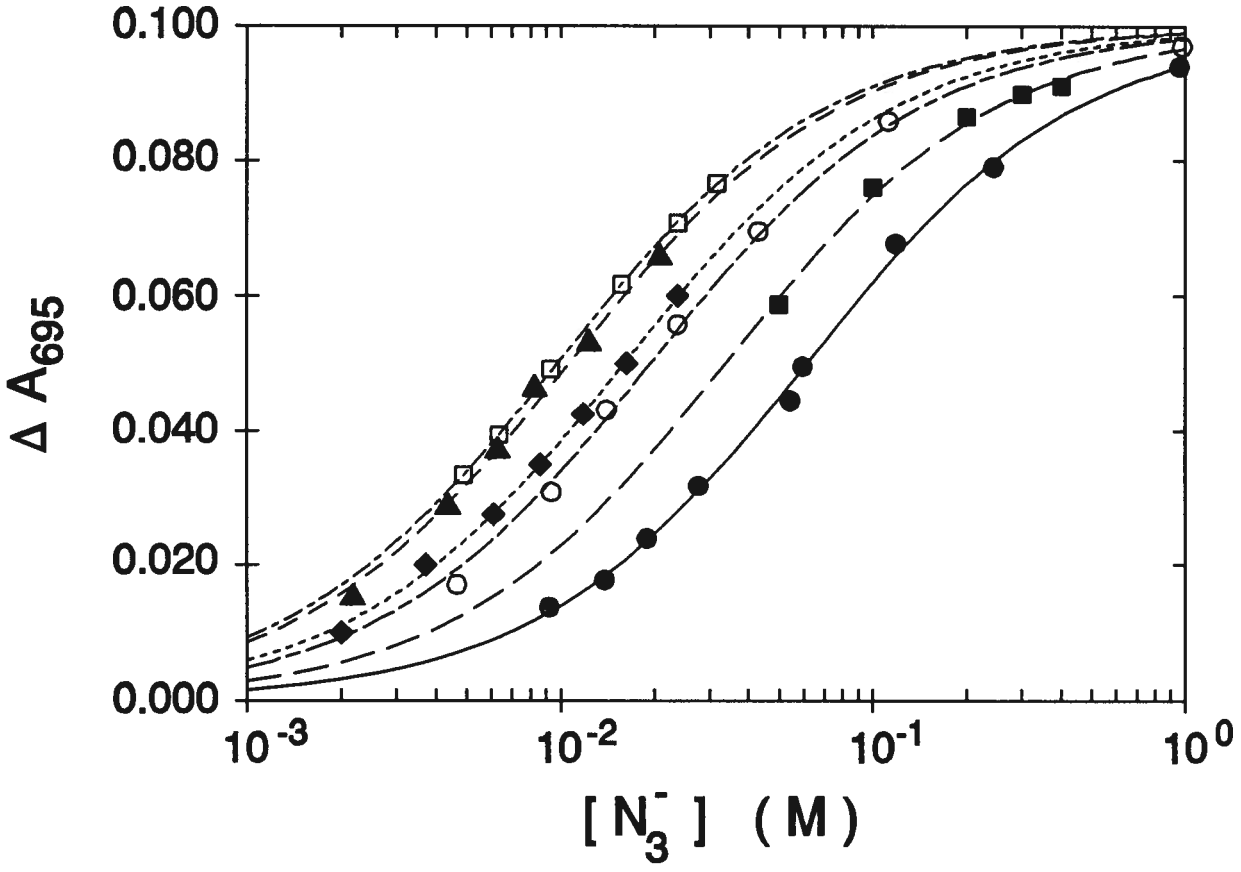

Figure 30 Azide binding isotherms for position-82 variants of ferricytochrome *c* [25 °C, pH 6.0, μ = 1.0 M]. Legend: ●, Wild type; ▲, Phe82Leu; ■, Phe82Tyr; ◆, Phe82Ile; ○, Phe82Ser; □, Phe82Gly.

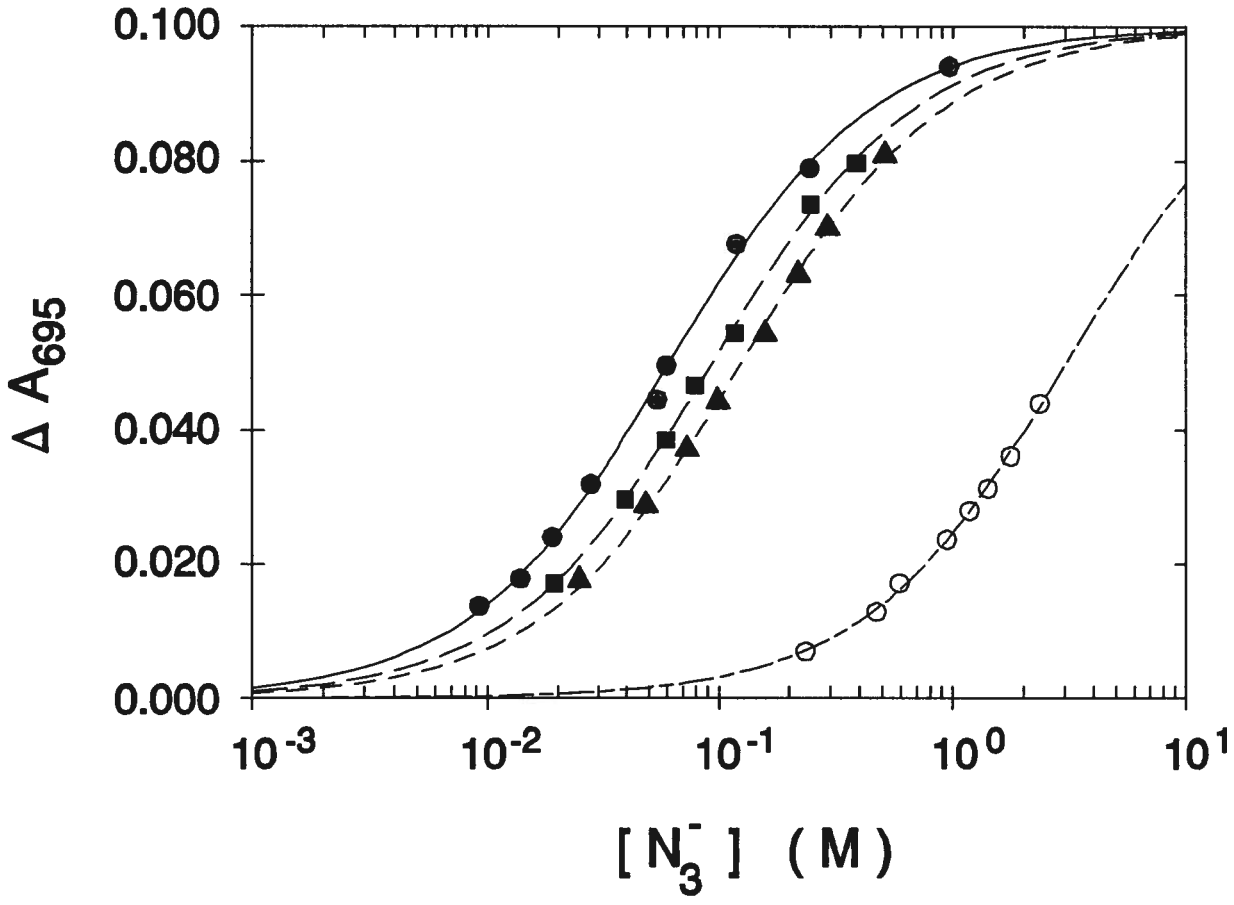

Figure 31 Azide binding isotherms for water switch variants of ferricytochrome *c* [25 °C, pH 6.0, μ = 1.0 M]. Legend: ●, Wild type; ▲, Asn52Ala; ■, Ile75Met; ◆, Thr78Gly; ○, Tyr67Phe.

In contrast, the variants at the water switch positions possessed azide affinities similar to or lower than that of wild type cytochrome *c*. This observation was most evident with the Tyr67Phe variant, with a K_{azide} estimated to be lower than 1 M^{-1}. Even in the presence of 2 M azide, this variant could not be saturated with azide, as shown by its incomplete titration curve. The binding constants for the Ile75Met and Asn52Ala variants were closer to that of the wild type protein but both exhibited a lower affinity for azide.

3.5.2 Azide Binding Kinetics

For all proteins studied, the loss of absorbance at 695 nm followed monophasic, first order kinetics. The relation of observed rate constant to [azide] was fitted to the following equation, which is derived from the mechanism shown in equation 10 on page 37 (Sutin & Yandell, 1972):

$$k_{obs} = \frac{k_1 k_{-2}(1 + K_{azide}[N_3^-])}{k_1 + k_{-2} K_{azide}[N_3^-]} \qquad (27)$$

Here k_{obs} is the observed first-order rate constant for the change in absorbance at 695 nm. This mechanism assumes a steady state concentration of the active intermediate ***Cyt-c****. The variation in observed rate constants with the azide concentration is shown in Figures 32 and 33, along with the calculated fits to equation 27. The resulting rate parameters are presented in Table 6. Equation 27 predicts rate saturation at increasing azide concentrations, but this is not always apparent from inspection of the experimental data. Nevertheless, the data for all variants except Tyr67Phe and Ile75Met are consistent with this mechanism as judged by their fits to the equation. There is fair agreement between the results for horse heart cytochrome *c* of this work ($k_1 = 65 \pm 9\ s^{-1}$) and those of Sutin & Yandell (1972), who estimate a forward rate constant k_1 of 30 to 60 s^{-1} under similar conditions.

Curvature of the plots is detectable in the Ile, Leu, Ser and Gly variants at position 82. These four variants are far more reactive than the wild type protein, with calculated forward rate constants k_1

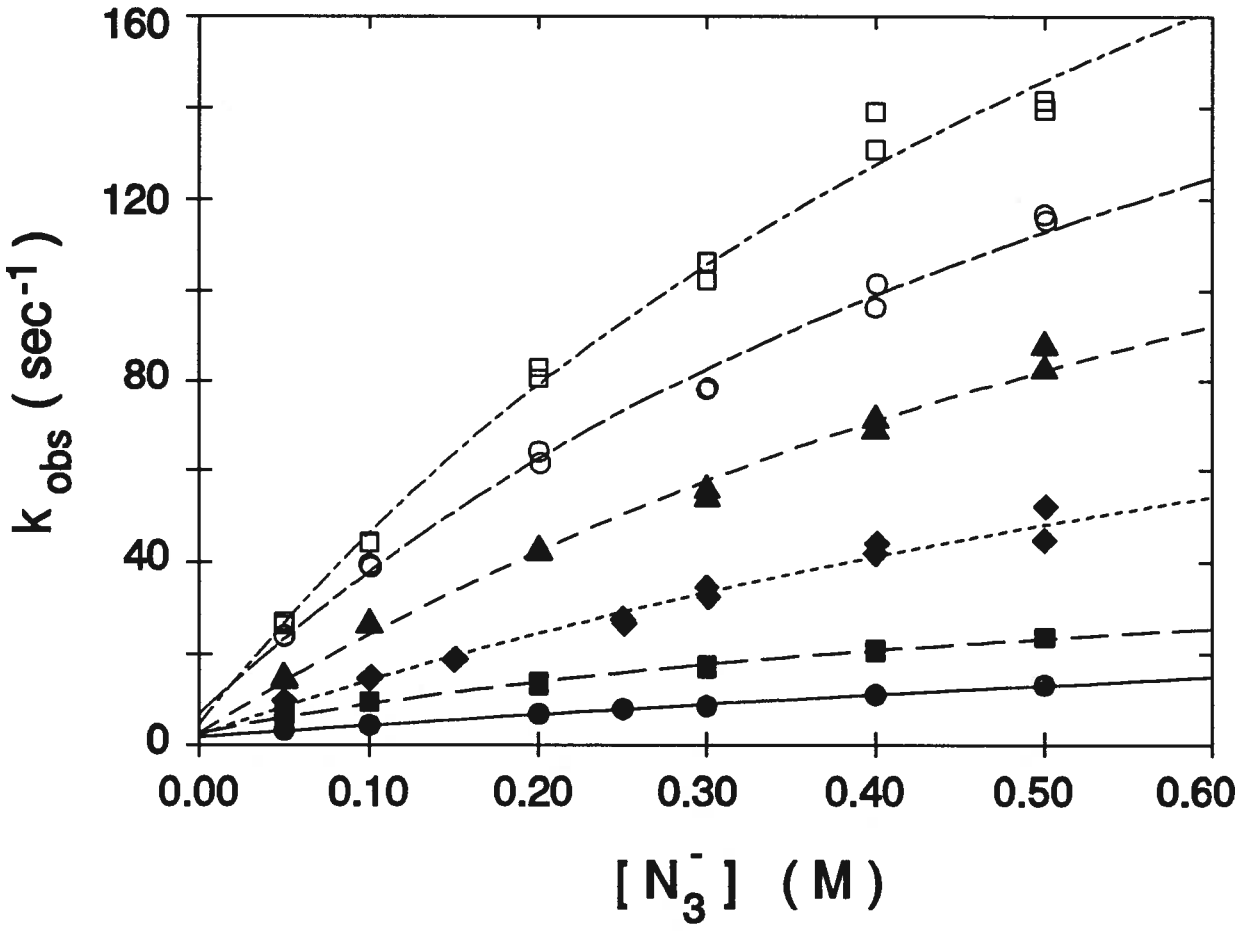

Figure 32 The dependence of observed rate constant of azide binding to position-82 variants of ferricytochrome *c* on azide concentration [25 °C, pH 6.0, μ = 1.0 M]. Legend: ●, Wild type; ▲, Phe82Leu; ■, Phe82Tyr; ◆, Phe82Ile; ○, Phe82Ser; □, Phe82Gly. Numerical values of the data points for Figures 32 and 33 are tabulated in Appendix E.

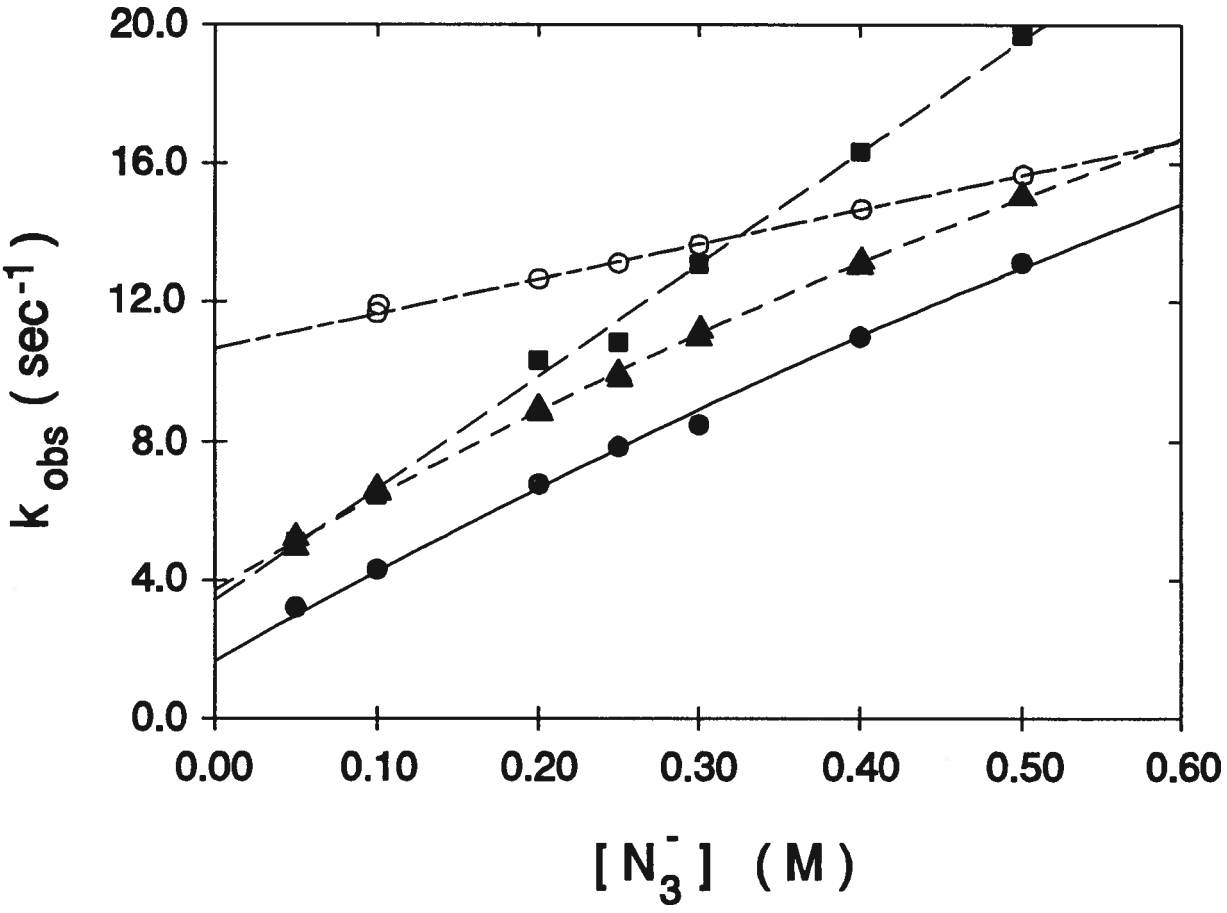

Figure 33 The dependence of observed rate constant of azide binding to water switch variants of ferricytochrome *c* on azide concentration [25 °C, pH 6.0, μ = 1.0 M]. Legend: ●, Wild type; ▲, Asn52Ala; ■, Ile75Met; ○, Tyr67Phe.

Protein	K_{eq} (M^{-1})	k_1 (s^{-1})	k_{-2} (s^{-1})	k_2/k_{-1}
Wild Type	16.7 ± 0.6	74 ± 20	1.65 ± 0.06	0.4 ± 0.1
Phe82Tyr	31 ± 2	49 ± 3	2.5 ± 0.1	1.6 ± 0.3
Phe82Leu	96 ± 11	240 ± 30	2.5 ± 0.1	1.0 ± 0.3
Phe82Ile	64 ± 4	160 ± 30	2.1 ± 0.1	1.0 ± 0.3
Phe82Ser	53 ± 2	270 ± 20	6.8 ± 0.2	1.3 ± 0.2
Phe82Gly	105 ± 1	360 ± 30	4.6 ± 0.2	1.3 ± 0.2

a)

Protein	K_{eq} (M^{-1})	k_1 (s^{-1})	k_{-2} (s^{-1})	k_2/k_{-1}
Wild Type	16.7 ± 0.6	74 ± 20	1.65 ± 0.06	0.4 ± 0.1
Asn52Ala	8.2 ± 0.3	58 ± 3	3.71 ± 0.04	0.5 ± 0.1

	K_{eq} (M^{-1})	k_f (M^{-1} s^{-1})	k_b (s^{-1})	k_f/k_b (M^{-1})
Ile75Met	10.9 ± 0.4	32.4 ± 0.9	3.4 ± 0.3	9.5 ± 1
Tyr67Phe	0.34 ± 0.03	9.7 ± 0.3	10.8 ± 0.3	0.9 ± 0.1

b)

Table 6 Azide binding parameters for variants of cytochrome *c* [25 °C, pH 6.0, μ = 1.0 M]. a) position 82 variants; b) water switch variants.

exceeding 160 s^{-1}. For the Gly and Ser variants, the reverse rate constant k_{-2} is also increased three to four fold over the corresponding value observed for the wild type cytochrome.

The rate constants that characterize the reaction of the active intermediate, k_{-1} and k_2, cannot be measured directly; the steady state assumption implies that these steps are not rate limiting. Consequently, only the ratio of these constants can be estimated from the relation

$$K_{azide} = \frac{k_1 k_2}{k_{-1} k_{-2}} \tag{28}$$

The ratios for horse heart cytochrome *c* and yeast wild type are similar, at 0.4 M^{-1}; the other position 82 variants have ratios of 1 to 1.6 M^{-1}, indicating an increased preference to form the azide bound species upon reaching the intermediate complex.

The azide binding behaviour of the water switch mutants is variable. The Asn52Ala variant is similar in most respects to the wild type cytochrome, and the observed decrease in K_{azide} is caused solely by an increase in the reverse rate constant k_{-2}. The inertness of Tyr67Phe to azide substitution, previously revealed from the titration experiment, was further exemplified by the small net absorbance changes during the kinetic experiments and the relatively small dependence of the observed rate constant on azide concentration. The dependence of observed rate constant on azide concentration obtained from the Tyr67Phe variant was fitted to a linear equation. Ile75Met was the most unusual variant, possessing a linear dependence of observed rate constant on azide concentration which suggests a simple two state equilibrium. The data for the Ile75Met variant was fitted to a linear equation; from the slope and intercept of the line, the forward and reverse rate constants respectively were calculated. The ratio of the forward to the reverse rate constant was in good agreement with the value of K_{azide} determined by titration.

DISCUSSION

4.1 Overview of the Structural Features of the Cytochrome c Variants

In this work, the influence of amino acid changes at several positions within the heme environment of cytochrome *c* on the electrochemical, kinetic, and ligand binding properties of this protein has been determined. Before discussing the results of these experiments, it is appropriate to review briefly the known structural features of the cytochrome *c* variants that have been the subject of this work.

The three-dimensional structures of several position 82 and water switch variants are available (Table 7). This information has been extremely useful, not only for revealing the basis for differences in the properties of variants of known structure, but also as a departure point for discussion of factors likely to contribute to the measured properties of variants for which no structural information is available. Figures 34 and 35 present the known structures of the position-82 and water switch variants respectively within the vicinity of the mutation site.

The structural features of yeast iso-1-cytochrome *c* wild type protein that are relevant to this work have been addressed previously in the Introduction. The structure of the Phe82Tyr variant has been solved to 1.97 Å resolution by Louie (1990). The conformation of the polypeptide backbone is essentially the same as that of the wild type structure. The side chain of Tyr82 projects 0.7 Å further out of the heme crevice than does the wild type Phe82 side chain. Small alterations in the backbone conformation of residues 81 to 85 compensate for the slightly different position of the tyrosine side chain. The exposure of the heme to solvent is unchanged from that of the wild type protein. Louie (1990) has proposed that the hydroxyl oxygen of Tyr82 forms a hydrogen bond with the guanidinium group of the nearby Arg13 side chain.

The Phe82Ser mutant possesses a solvent channel at the mutation site extending from the surface of the protein to Met80, thus increasing the solvent accessibility of the heme (Louie & Brayer, 1988).

Protein	Oxidation State	Resolution	Reference
Wild Type	reduced	1.23 Å	Louie & Brayer, 1990
	oxidized	1.9 Å	Berghuis & Brayer, submitted
Phe82Tyr	reduced	1.97 Å	Louie, 1990
Phe82Ile	reduced	2.3 Å	Louie, 1990
Phe82Ser	reduced	2.80 Å	Louie & Brayer, 1988
Phe82Gly	reduced	2.60 Å	Louie & Brayer, 1989
	oxidized	1.76 Å	Louie, 1990
Tyr67Phe	reduced	1.95 Å	Guillemette *et al.*, in preparation
	oxidized	2.2 Å	Guillemette *et al.*, in preparation
Asn52Ala	reduced	2.0 Å	Berghuis & Brayer, unpublished

Table 7 Current status of the structure determinations for those *Saccharomyces cerevisiae* iso-1-cytochrome *c* variants examined in this work. At present there is no information for the Phe82Leu, Phe82Ala, Ile75Met, and Thr78Gly variants of this protein.

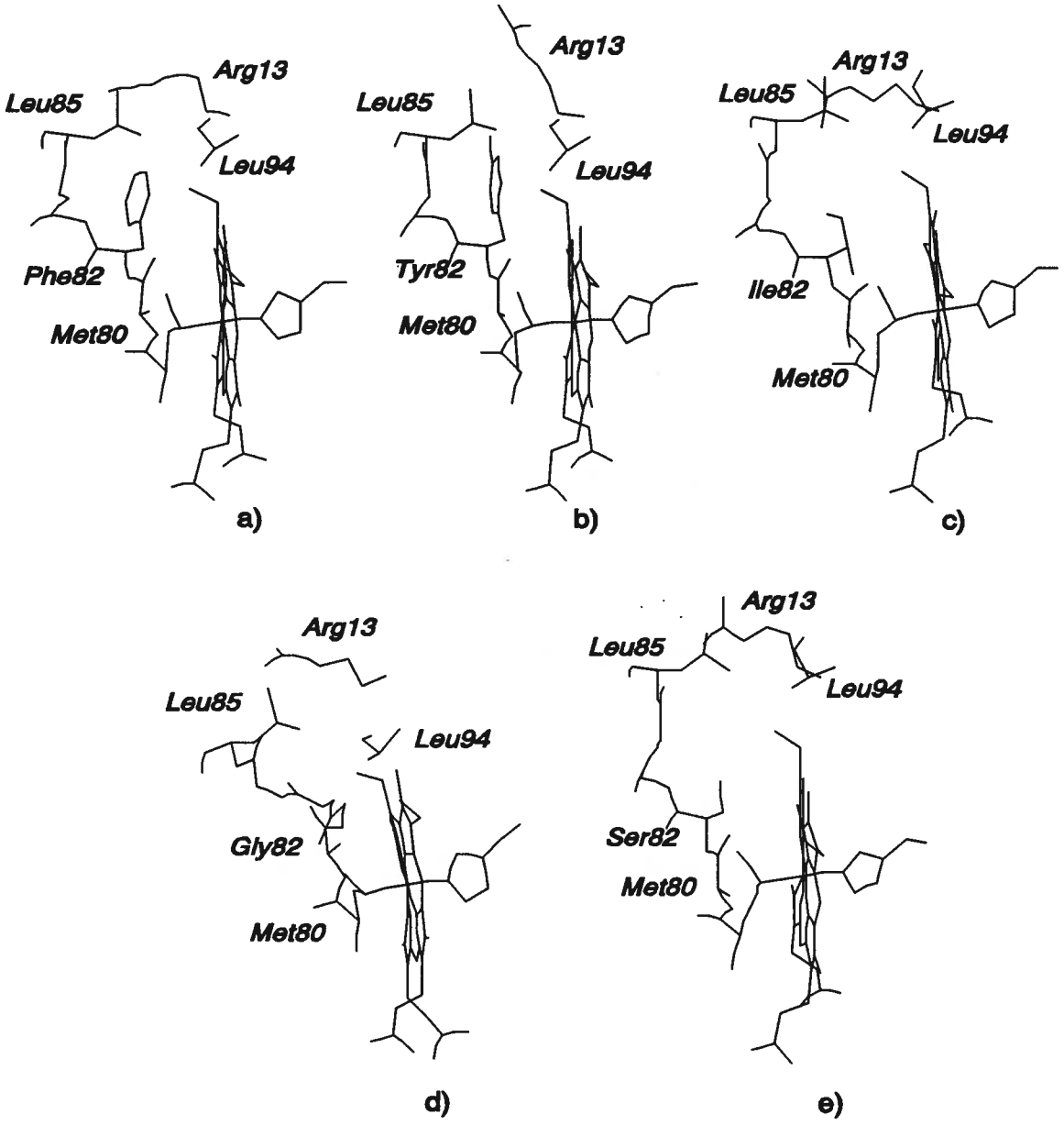

Figure 34 The structures of the position-82 variants of reduced iso-1-cytochrome *c* in the vicinity of the mutation site (Louie & Brayer, 1988, 1989, 1990; Louie, 1990). a) Wild Type Protein b) Phe82Tyr c) Phe82Ile d) Phe82Gly e) Phe82Ser.

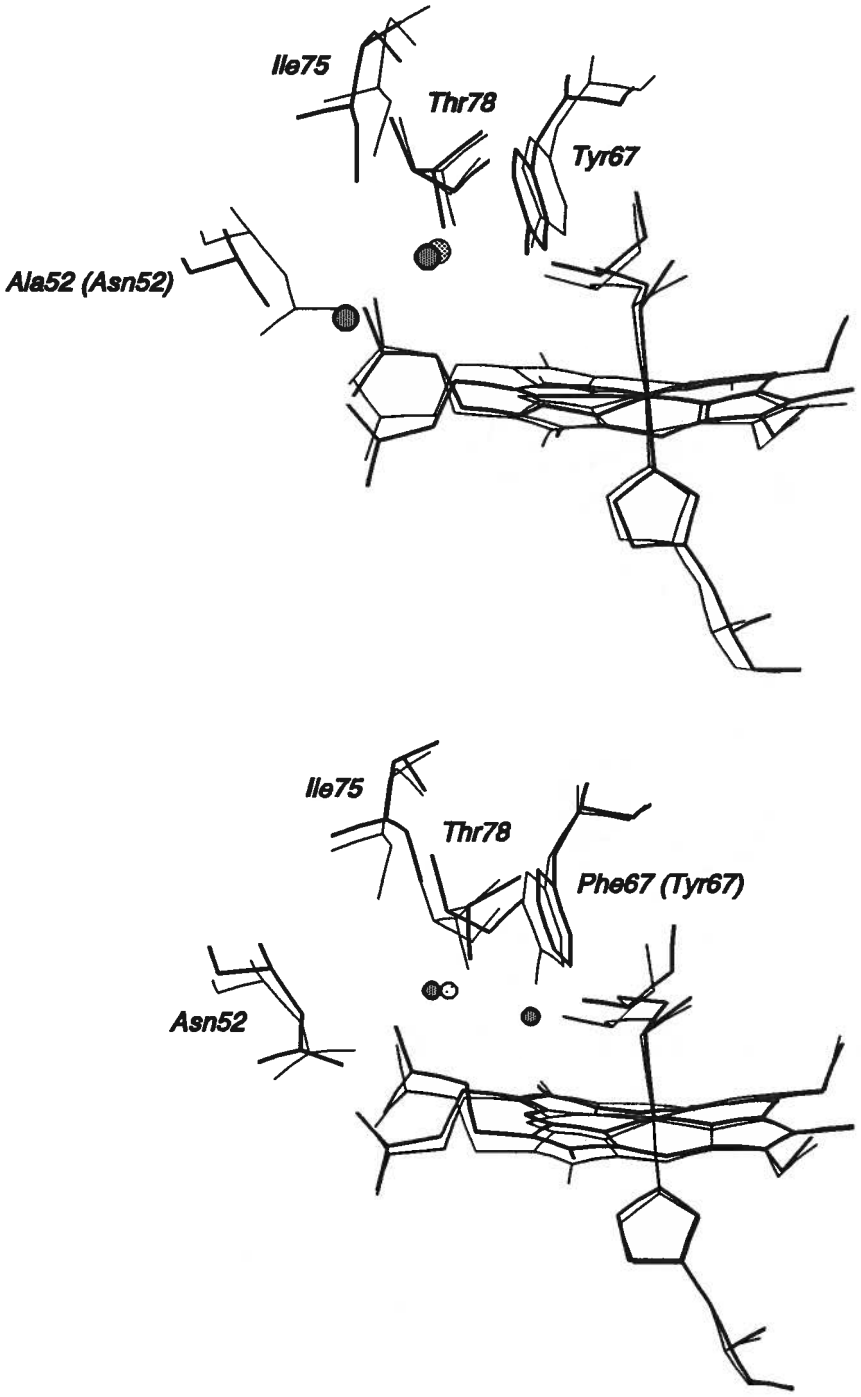

Figure 35 The structure of a) Asn52Ala (Berghuis *et al.*, in preparation) and b) Tyr67Phe (Guillemette *et al.*, in preparation) variants of reduced cytochrome *c* about WAT166. Thin lines, native; thick lines, mutants. The heavily shaded circles represent the location of the internal water molecules in the variant structures; the lightly shaded circles correspond to the position of WAT166 in the wild type cytochrome.

In addition, WAT166 is 1 Å closer to the heme in the reduced structure of this mutant than in the wild type structure. The presence of a buried water molecule closer to the heme will also contribute to an increase in the polarity of the heme environment. There is no structure currently available for the Phe82Ala variant. Because of the similar size of a serine and alanine side chain, Phe82Ala might also possess a solvent channel, which would account for the similar reduction potentials of the two proteins. The position of WAT166 would also be similar to that of Phe82Ser.

In the 2.6 Å structure of the reduced Phe82Gly mutant, the polypeptide backbone in the mutation site folds to occupy the same space as the phenylalanine side chain in the wild type protein. This is the only cytochrome *c* mutant investigated to date with a significantly altered folding of the polypeptide backbone (Louie & Brayer, 1989). This change appears be caused by the flexibility of the sequence of three consecutive glycine residues in positions 81 to 83 that is present in this variant. This flexibility is demonstrated by the observation that the orientations of two peptide bonds (between residues 81 and 82, and 83 and 84) in the oxidized structure of this variant are opposite to those observed in the structure of the ferrocytochrome (Louie, 1990). Because of this unique folding of the main chain in the mutation site, the solvent accessibility of the heme in the Phe82Gly variant does not differ significantly from that found for the wild type protein. However, the negative ends of several peptide bonds dipoles are directed towards the heme, which increases the polarity of the heme environment. As seen in the structure of the Phe82Ser variant, the position of WAT166 in reduced Phe82Gly is also 1 Å closer to the heme than in the wild type protein.

The structure of Phe82Ile has been solved to 2.3 Å resolution (Louie, 1990) and found to exhibit a backbone folding pattern similar to that of the wild type protein. The β-branching of the Ile side chain causes unfavourable steric interactions with neighbouring groups, and the β-methyl group is in van der Waals contact with the methyl and γ-methylene groups of the Met80 side chain. The conformational strain within this region may cause flexibility of the side chain, allowing a transient increase in the solvent exposure of the heme. Beyond the side chain of the Phe82Ile residue is a void space resembling the

solvent channel of Phe82Ser, which could serve as a transiently exposed solvent channel. The position of WAT166 in Phe82Ile is approximately 0.5 Å closer to the heme than in wild type structure, which would also contribute to the lowered reduction potential. There is no three-dimensional structure available for the Phe82Leu variant. The γ-branch position for leucine is in the same relative position as the γ atom of phenylalanine, thus the leucine side chain should be more easily accommodated at position 82 without as much unfavourable steric interactions with neighbouring atoms as are observed with isoleucine at this position.

In both the Tyr67Phe and Asn52Ala variants, the polypeptide backbone configuration is similar to that of the native protein (Guillemette *et al.*, in preparation; Berghuis *et al.*, unpublished) The replacement of the native side chain with smaller, non-hydrogen bonding residues leads to the formation of an internal cavity that is occupied by two water molecules (Figure 35). One of the water molecules corresponds to the position of WAT166 in wild type, while the other water molecule occupies the position of the tyrosine hydroxyl (Tyr67Phe) or the asparagine amide (Asn52Ala) in the wild type structure. In the case of Thr78Gly, for which no structure is available, the lack of a hydrogen bonding side chain could be filled by a second internal water molecule, as in the Asn52Ala and Tyr67Phe variants. However, one must also consider that in this variant the entire branched side chain of threonine residue would not be present. It is possible that the polypeptide backbone in the region of the mutation folds in a manner different from that of the wild type protein to avoid the formation of a large cavity.

Structural information regarding the Ile75Met variant is currently unavailable. If the main chain conformations of the variant and wild type proteins are the same, as appears to be the rule with the cytochrome *c* variants studied in this work, there are two likely positions that the Met75 side chain could occupy with minimal alteration to the protein structure. These positions would place the methionine side chain on the direction of the longer or shorter β-branches of the wild type isoleucine. In both cases, unfavourable steric interactions with nearby atoms would be avoided, as the noncovalently bonded atoms nearest to the methionine sulphur atom and methyl group are 3.5 Å away. Another possibility, although

one that would cause significant structural changes, is that the methionine side chain is directed inward and occupies the space of WAT166 to completely alter the nature of the hydrogen bonded network in this region of the protein. The results of the electron transfer kinetics experiments and the alkaline isomerization experiments argue against such a drastic alteration to this region of the protein (*vide infra*).

4.2 Cytochrome c Oxidation-Reduction Equilibrium

At pH 6 and 25 °C, all variants investigated had reduction potentials within 45 mV of the value observed for the wild type protein. This range corresponds to a difference in the free energy between the two oxidation states of 1 kcal/mol or less. The wild type protein possesses the highest reduction potential, while position 82 mutants have progressively lower potentials in the order leucine > tyrosine > isoleucine > alanine > serine > glycine (Table 1a, page 60). Qualitatively, smaller residues at position 82 result in lower potentials, although the presence of a hydroxyl group on the mutant residue will also contribute to a lower potential. Thus the reduction potential of Phe82Ser is lower than that of Phe82Ala, and the potential of Phe82Tyr is lower than that of wild type. The contribution of a hydroxyl group in these variants is to lower the potential by 5 to 10 millivolts. The difference between the reduction potentials of the Phe82Leu (290 mV) and Phe82Ile (273 mV) variants reflects the large effects that can result from seemingly small structural differences. In the case of these variants, the difference is in the position of the branch point of the aliphatic side chain. The reduction potential of the variant Phe82Leu is similar to that of the wild type protein, suggesting that this residue maintains the normal dielectric for the heme environment. The Phe82Gly variant possesses the lowest reduction potential in spite of having a solvent accessibility similar to that of wild type. The lower reduction potential of Phe82Gly could be caused by transient solvent exposure at the mutation site. Alternatively, the peptide bond dipoles within the mutation site are considerably closer to the heme in this variant, and are oriented in a manner that would be consistent with stabilization of a positive charge on the heme.

Unlike the position 82 mutants, which have reduction potentials distributed evenly across the range between 290 and 245 mV, the water switch mutants all have potentials that are at least 30 mV lower than that of the wild type protein (Table 1b, page 60). This result cannot be attributed to increased solvent exposure of the heme in the case of the two water switch variants whose structures have been solved (Tyr67Phe and Asn52Ala). A possible reason for the lowered potentials of these two mutants is that the water molecule that replaces the hydrogen bonding residue of wild type has greater mobility and is better able to stabilize the oxidized state either by reorientation of its dipole or by moving closer to the heme upon oxidation. Such a mechanism is consistent with the lower reduction potential of Tyr67Phe (236 mV) relative to Asn52Ala (257 mV), as the second water molecule of Tyr67Phe is closer to the heme than is the second water molecule of Asn52Ala. New water molecules closer to the heme would be expected to have a greater influence on the reduction potential than water molecules that are more remote. This proposal would also be consistent with the finding that the reduction potential of Thr78Gly (247 mV) is halfway between those of Tyr67Phe and Asn52Ala; a proposed second solvent molecule replacing the hydrogen bonding hydroxyl group of the wild type Thr78 residue would be midway between the locations of the second solvent molecules in these variants.

The 45 mV drop in the reduction potential of Ile75Met relative to the wild type protein is likely caused by increased solvent accessibility of the heme as the straight chain methionine side chain would not be as effective as the branched isoleucine at shielding this region from the bulk solvent. After isoleucine, the most commonly occurring residue at position 75 is valine, which also possesses a β-branched side chain. Met75 occurs naturally in only two species of cytochrome *c* whose sequences are known, those of *Crithidia oncopelti* (Pettigrew, 1972) and *Crithidia fasciculata* (Hill & Pettigrew, 1975). However, the reduction potential of *Crithidia oncopelti* cytochrome *c* as determined by an equilibrium method is 270 mV (pH 6, Moore *et al.*, 1984). The reduction potential of *Crithidia oncopelti* cytochrome *c* may also be influenced by other unusual amino acid residues in the heme crevice, the most notable difference

being the lack of one of the thioether bonds from the heme to the protein caused by the occurrence of an alanine residue instead of cysteine at position 14.

None of the mutations studied here altered the net protein charge, nor changed the axial ligands of the heme iron. Potentially the mutations could alter the distribution of the charged residues about the heme and in this manner alter the electrostatic interactions of these residues with the heme but, with the possible exception of Phe82Tyr, this seems unlikely. The available crystallographic evidence indicates that in most cases the difference in the position of main chain atoms between wild type and mutant are small. In the case of Phe82Gly, where a refolding of the main chain occurs, this effect is limited to the mutation site and adjacent residues and leaves the rest of the main chain in a conformation similar to wild type.

In the absence of changes in axial ligation and ionic interactions, the source of the differences in the reduction potentials must arise from mutation-induced changes in the dielectric of the heme environment. This environment includes the polypeptide backbone, amino acid side chains, and buried and bulk solvent water molecules. The lower reduction potentials of most of the cytochrome *c* variants studied indicates that the variants are more effective than the wild type protein at stabilizing the oxidized state, or, alternatively, at destabilizing the reduced state.

The entropy and enthalpy of reduction for each variant were calculated from the temperature dependences of the reduction potentials (Table 1, page 60). Small differences in the thermodynamic parameters can have large effects on reduction potentials. For example, the mutants Phe82Leu, Phe82Ile, Phe82Ser and Ile75Met have reduction entropies only 2 to 3 eu more negative than that of the wild type protein, but at room temperature this difference contributes to a lowering of the reduction potential by 25 to 40 mV. In the cases of Phe82Leu and Phe82Ile, the reduction enthalpy compensates for this entropy change, and the reduction potentials at room temperature are only 4 to 17 mV lower than that observed for the wild type protein, respectively. Phe82Ser and Ile75Met exhibit no enthalpic compensation. Their lower reduction potentials are due almost entirely to entropic effects that stabilize

the oxidized protein. In the case of these four variants, the relatively larger standard free entropies suggest slightly larger conformational and/or solvational differences between the ferri- and ferrocytochromes.

In contrast, the mutants Phe82Gly, Phe82Ala, Thr78Gly and Asn52Ala exhibit standard free entropy changes that are similar to or more positive than that of the wild type cytochrome, which indicates conformational differences between oxidation states may be smaller in these variants than for the wild type protein. The lowered reduction potentials of these mutants are caused by more positive standard free enthalpy changes.

Despite the differences in thermodynamic parameters, all of the variants investigated exhibited behaviour typical of mitochondrial cytochromes *c* that have been studied previously. The reaction centre entropy changes of -6 to -12.3 eu are small in magnitude and negative, while the standard free enthalpy changes are between -12.8 and -14.8 kcal/mol. In all variants, the entropy change favours the oxidized state while the enthalpy change favours the reduced state. Such behaviour data suggest a more ordered and thermodynamically more stable reduced structure for the cytochrome compared to the oxidized structure. It seems likely that all of the variants undergo oxidation-state linked conformational changes similar in magnitude to those observed for tuna and yeast wild type cytochromes *c*.

The small reaction centre entropy of cytochrome *c* may have a role in promoting rapid electron transfer. Yee and coworkers (1979) measured the influence of ligands on the reaction entropies of transition metal complexes. These authors found that ΔS_{rc}° for aquo complexes of $M^{3+/2+}$ (M = Fe, Cr, Ru, Os, V, Eu) were between 36 and 49 eu, while for ammine complexes of $M^{3+/2+}$ (M = Os, Ru) ΔS_{rc}° was 18 eu, and for $Fe^{3+/2+}$ complexes with the chelating ligands bipyridine and phenanthroline ΔS_{rc}° was 2 and 3 eu, respectively. Yee *et al.* proposed that this relationship between ΔS_{rc}° and ligand environment is due in part to differences in the ability of the ligands to order solvent molecules surrounding the inner coordination shell. Water as a ligand is able to hydrogen bond surrounding water molecules more effectively than is ammonia. Large, bulky chelating ligands are effective at shielding the charge of the

metal centre from the surrounding solvent, thus solvent reorientation upon a change in oxidation state is minimized. The authors suggested that the value of $\Delta S_{rc}°$ is an indicator of the contribution of solvent reorganization to the Franck-Condon barrier to electron transfer because those complexes with reaction centre entropies closer to zero tend to have higher self exchange rates.

In cytochrome *c*, the polypeptide and buried water molecules surrounding the inner coordination shell of the heme iron shield the metal centre from bulk solvent. In addition, the mobility of this environment in response to a change in oxidation state is limited, as demonstrated by the relatively small oxidation state linked conformational change. The low reaction centre entropy for cytochrome *c* presumably facilitates rapid electron transfer by minimizing the extent of solvent reorganization, where 'solvent' includes everything except the heme and the axial ligands. As the observed reaction centre entropies are not zero, a compromise with other biologically essential requirements, such as the maintenance of a biologically relevant reduction potential, may be a more important evolutionary constraint in the development of cytochrome *c* function.

The pH dependences of reduction potential for several cytochrome *c* variants are all consistent with the presence of a single titratable group, the pK_a of which is sensitive to the oxidation state of the protein (Table 2, page 63). NMR spectroscopy has been used to identify His39 as the residue whose pK_a is dependent on the oxidation state (Robinson *et al.*, 1983). This assignment is consistent with the observation that horse heart cytochrome *c*, which has a lysine residue at position 39, has a reduction potential that is independent of pH between pH 4 and 9, while *Candida krusei* and *Rhodopseudomonas viridis* cytochromes *c*, which possess His39, have oxidation-state dependent pK_as similar to that exhibited by iso-1-cytochrome *c*.

The oxidation-state linked change in the pK_a of His39 is small (0.4 pH units), suggesting a weak interaction between the heme charge and this residue. This finding is consistent with the 14 Å distance between the α-carbon of this residue and the heme iron. In comparison, the pK_a of heme propionate-7 of bacterial cytochrome c_{551} decreases a full pH unit upon oxidation of the heme iron. Moore and

coworkers have proposed that the change in pK_a of His39 of iso-1-cytochrome *c* is transmitted from the heme via the small conformational changes that occur in the environment of this residue upon a change in oxidation state (Robinson *et al.*, 1983). His39 is located in a flexible region of cytochrome *c* that includes the residues in contact with the heme propionates.

For the wild type cytochrome and the Phe82Ser and Ile75Met variants, the plots of reduction potential *vs* pH give similar curves that differ in their vertical displacement by an amount determined by their value of $E_{m,0}$, the reduction potential extrapolated to pH 0. The calculated pK_as for these proteins were thus identical to each other, within experimental error. This finding suggests that the two mutations do not affect the oxidation state-linked conformational changes in the environment of His39. The mutation sites in Ile75Met and Phe82Ser are remote from His39, so they are not expected to exert an influence on the ionization of this residue.

The difference in pK_o and pK_r for the Asn52Ala variant is 0.4 as for the other yeast cytochromes studied, but both values are 0.5 pH units lower than those determined for the wild type protein. In contrast to the Ile75Met and Phe82Ser variants, residue 52 is located near the heme, between the heme propionates and His39. The lower values for pK_o and pK_r of this mutant suggest a more hydrophobic environment for His39. Such a change could be caused by closer contact with neighbouring residue Leu58.

The double mutant Asn42Lys / Ala43His was constructed to increase the pH dependence of the reduction potential in the physiological range. In certain bacterial cytochromes *c*, an oxidation-state dependent ΔpK_a of 1 pH unit is attributed to the ionization of a heme propionate in the physiological range between pH 5 and 8. The presence of additional, positively charged side chains near the heme propionates is expected to lower the pK_a of these groups. As one of the heme propionates is believed to ionize above pH 9 in the wild type protein (*vide supra*), the double mutation Asn42Lys / Ala43His would be expected to lower the pK_a of this heme propionate into the physiological range. This was not observed. Although the reduction potential of this mutant was lowered by 10 mV, the pH dependence

of the reduction potential was not altered. Examination of the structure of the protein suggests that the altered residues would be directed towards the solvent, thus having minimal influence on the pH dependence of the oxidation-reduction potential. The lower reduction potential of this mutant is interesting, as the addition of positively charged residues to cytochrome *c* would be expected to destabilize the oxidized state. This result illustrates the complexity of determining the influence a mutation can have on reduction potential, as a single mutation can have several and often opposing effects on the observed property. While the electrostatic interaction between the mutated residues and the heme may favour a higher reduction potential, the influence of these residues on the local polypeptide structure and other structural characteristics may have a stronger tendency to lower the reduction potential.

4.3 Electron Transfer Kinetics

4.3.1 General Comments

Previous workers (Augustin *et al.*, 1983; Armstrong *et al.*, 1986a) have investigated the influence of modifying the charge properties of cytochrome *c* on its reactivity toward small inorganic electron transfer agents and other electron transfer proteins. The present work demonstrates that the electron transfer reactivity of cytochrome *c* is equally sensitive to mutations that do not alter its electrostatic properties.

Rather than comparing directly the cross reaction rates of the cytochrome *c* variants with the inorganic complexes used in this study, each experimentally determined cross reaction rate constant is used with the known self exchange rate constant of the inorganic complex and the driving force of the reaction to calculate the self exchange rate constant exhibited for the protein in each reaction according to the relative Marcus equation. These calculated protein self-exchange rate constants are the basis for comparison of the influence of mutation on electron transfer reactivity. Thermodynamic driving forces are calculated from the measured reduction potentials of the cytochrome *c* variants and their electron transfer partners. The calculated protein self exchange rates, k_{11}^{corr}, have also been corrected for the influence that

electrostatic interactions between the reactants has on the reaction rate by the inclusion of appropriate work terms for precursor complex formation and successor complex dissociation.

There is an apparent contradiction if the value of the self exchange rate constant of cytochrome *c* depends on the inorganic complex used. Thus the self exchange rate for wild type iso-1-cytochrome *c* is 11 and 3100 $M^{-1}s^{-1}$ when calculated with cross reaction measurements using $Fe(edta)^{2-}$ and $Co(phen)_3^{3+}$ respectively. This apparent fault in the relative Marcus equation is resolved by examining the assumption that the activation free energy of the cross reaction is the average of the activation free energies of each reactant in its self exchange. Except for electrostatic work terms, no provisions are made for specific interactions between the two reagents in the cross reaction that do not occur in the component self exchange reactions. The dependence of the calculated self exchange rate constant of cytochrome *c* on the electron transfer partner employed in the cross reaction is not a drawback, as disparity in self exchange rate constants demonstrates differences in reaction mechanisms. This reasoning has been utilized by Wherland and Gray (1976) who considered the five orders of magnitude difference in self exchange rate constants of horse heart cytochrome *c* with various electron transfer partners. Differences in the hydrophobicity of the electron transfer partners of cytochrome *c* and differences in the nature of the molecular orbital types employed by these partners in electron transfer with the protein were proposed to explain the observed variation in the calculated self exchange rate of cytochrome *c* .

More important than the absolute value of k_{11}^{corr} for a mutant protein is this value relative to that of the wild type species. Describing the electron transfer reactivity of each variant in terms of its relative k_{11}^{corr} simplifies discussion of the results and facilitates comparisons between the results obtained using different electron transfer partners. In the following discussion the terms 'reactivity' and 'reactive' will refer to relative values of the calculated self exchange rates.

4.3.2 Position-82 Variants

The results obtained with the position 82 mutants show that while electron transfer occurs via the exposed heme edge, Phe82 itself is not essential for electron transfer with inorganic complexes. This has also been shown to be true for the reaction of position 82 variants with cytochrome b_5 (Barker *et al.*, unpublished), cytochrome c peroxidase (Pielak *et al.*, 1985), and cytochrome *c* oxidase (Michel *et al.*, 1989).

The main influence of mutations at position 82 on the reactivity of cytochrome *c* is on the nature of the precursor complex formed between cytochrome *c* and its electron transfer partners. As the size of the residue at position 82 decreases, reactivity increases. This affect is probably attributable to shorter distances between electron transfer centres, with position 82 mutants having small side chains allowing the electron transfer partner to approach the heme more closely. This trend is seen clearly with the results of kinetics experiments using $Fe(edta)^{2-}$, where k_{11}^{corr} varies over a seventeen-fold range (Table 3a, page 69). With $Co(phen)_3^{3+}$ oxidation of ferrocytochrome *c* the trend is the same, but it is less pronounced, as the reactivity varies only over a seven-fold range (Table 4a, page 76). For example, Phe82Gly and Phe82Ser are 15 to 17 times more reactive than wild type cytochrome *c* towards $Fe(edta)^{2-}$ but only 2.6 to 3 times more reactive towards $Co(phen)_3^{3+}$. The difference in results obtained for cytochrome oxidation and reduction is likely a consequence of the difference in the sizes of the two inorganic complexes used. The smaller radius of $Fe(edta)^{2-}$ (4 Å) compared to $Co(phen)_3^{3+}$ (7 Å) (Wherland & Gray, 1976) allows the former reagent to probe the surface of cytochrome *c* more intimately, allowing shorter distances between the metal centres.

The higher reactivities of Phe82Ser and Phe82Gly toward $Fe(edta)^{2-}$ may also be caused by a difference in the orientation of this electron transfer partner with respect to the surface of cytochrome *c*. As noted by Wherland & Gray (1976), $Fe(edta)^{2-}$ can present two faces to cytochrome *c*: a polar face bearing the carboxyls of the edta ligand, or a more hydrophobic face consisting of the ethylene backbone of the ligand. The hydrophilic face would be more favourable for electron transfer because of the

opportunity for π-π overlap of the carboxyl orbitals with the corresponding heme orbitals. However, this orientation of the hydrophilic face of $Fe(edta)^{2-}$ with the hydrophobic Phe82 residue would not be favourable. Instead, $Fe(edta)^{2-}$ would present its more hydrophobic face to the surface of wild type cytochrome *c*. In both Phe82Gly and Phe82Ser the surface of the protein in the mutation site would be more hydrophilic, allowing $Fe(edta)^{2-}$ to present its more reactive face to the protein.

In addition to altering the nature of the precursor complex by changes in the relative orientation of the reactants and shortening of the distance between electron transfer sites, Phe82Gly and Phe82Ser may increase reactivity by lowering the reorganization energy of cytochrome *c*. In the reduced structures of both proteins, WAT166 is 1 Å closer to the heme than it is in the wild type protein, giving the reduced structure some characteristics of the oxidized structure.

Although most position 82 mutants are more reactive toward $Fe(edta)^{2-}$ than $Co(phen)_3^{3+}$, one exception is Phe82Ile. The heme crevice of this mutant is structurally unstable, as described previously, and may allow the hydrophobic $Co(phen)_3^{3+}$ to penetrate the protein surface. This interaction could be described as an encounter between a hard sphere ($Co(phen)_3^{3+}$) and a soft sphere (Phe82Ile). In contrast to the behaviour of Phe82Ile, the electron transfer reactivity of its Phe82Leu isomer is closer to that of the wild type protein.

4.3.3 Water Switch Variants

The reactivity exhibited by the water switch mutants towards $Fe(edta)^{2-}$ and $Co(phen)_3^{3+}$ demonstrates that the specific arrangement of the hydrogen bond network in the region of the mutated residues is not a prerequisite for rapid electron transfer. Variants in which critical residues of this network have been removed all have similar or even greater reactivity than the wild type cytochrome. In at least two of the mutants studied, replacement of a hydrogen bonding side chain by a second buried water molecule allows electron transfer reactivity to be increased.

The case of Tyr67Phe clearly illustrates the need to take into account driving force differences through the application of the relative Marcus theory when comparing the electron transfer rates. The cross reaction rate of Tyr67Phe with $Fe(edta)^{2-}$ is similar to that of wild type. Without consideration of the 55 mV difference in reduction potential between these two proteins, the conclusion would be drawn that the mutation has no significant effect on the electron transfer properties of cytochrome *c*. One would then be hard pressed to explain the reason why the cross reaction rate of Tyr67Phe with $Co(phen)_3^{3+}$ is ten times that observed for the wild type protein. When the cross reaction rates and the reduction potentials are used with the relative Marcus equation to calculate the self exchange rate for each protein, one finds that Tyr67Phe is eleven times more reactive than the wild type cytochrome towards both electron transfer partners.

The observation that the electron transfer reactivity of Tyr67Phe relative to the wild type protein is independent of the identity of the electron transfer partner is true for all of the water switch variants examined (Figure 36). This finding indicates that these substitutions do not influence the nature of the precursor complex as do the position 82 replacements. Rather, the differences in reactivity that are observed with the water switch variants are caused by adjustments in the reorganization energy of the protein.

The Ile75Met variant has the same reactivity in both reactions as the wild type cytochrome. Its lower cross reaction rate with $Fe(edta)^{2-}$ and higher cross reaction rate with $Co(phen)_3^{3+}$ can be accounted for almost completely by the relatively low reduction potential of this variant. Thus the reorganization energy of Ile75Met is the same as that of the wild type protein. As this mutation likely does not remove any hydrogen bonding partners to WAT166, it is likely that the hydrogen bond network is intact in Ile75Met and that this protein undergoes oxidation state-linked conformational changes similar to those observed for the wild type protein. In contrast, the mutants Thr78Gly, Asn52Ala, and Tyr67Phe, each of which removes one of the hydrogen bond partners to WAT166, are all more reactive than the wild type protein. For Asn52Ala and Tyr67Phe, it is known that a second buried water molecule replaces the

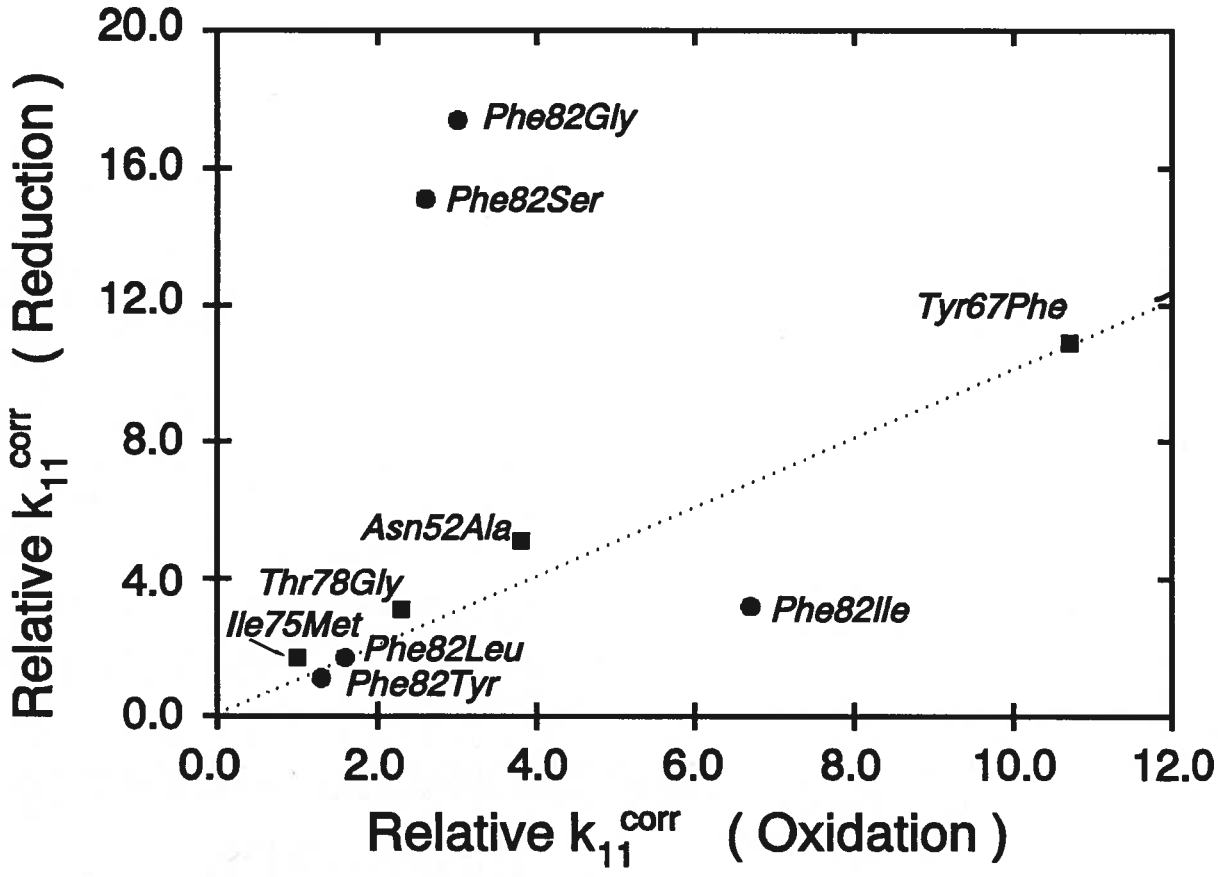

Figure 36 Comparison of the relative self exchange rates obtained for the reactions of the variant cytochromes with $Fe(edta)^{2-}$ (vertical axis) and $Co(phen)_3^{3+}$ (horizontal axis). The line corresponds to equal values for the two relative self exchange rates.

lost hydrogen bonding group (Figure 35; Guillemette *et al.*, submitted; Berghuis *et al.*, unpublished results). Although there is no structural evidence that a similar compensatory change in solvation occurs in the Thr78Gly variant, it is reasonable to suggest that a similar replacement does takes place. Notably, the Tyr67Phe mutant, with the second water molecule closest to the heme, has the highest reactivity, while the mutants Asn52Ala and Thr78Gly are less reactive than Tyr67Phe. The new water molecule in the Asn52Ala variant is further removed from the heme than that of the Tyr67Phe variant, and the Asn52Ala variant has a reactivity more similar to the wild type protein. The reactivity of the Thr78Gly variant is between those of Tyr67Phe and Asn52Ala variants. A proposed second water molecule that replaces the lost Thr78 side chain in Thr78Gly would be closer to the heme than the additional water molecule in the Asn52Ala variant, but it would be further from the heme than the new water molecule in the Tyr67Phe variant.

The lower reorganization energies of the Tyr67Phe, Asn52Ala, and possibly the Thr78Gly variants may be caused by smaller movements in the protein surrounding the heme and greater movement of the internal water molecules. In wild type cytochrome *c*, reorganization in the hydrogen bond network about WAT166 requires movement of hydrogen bonding side chains that are held in place to the protein backbone. In the three water switch variants, the second internal water molecule should have more freedom to move than the hydrogen bonding side chain that it replaces. Reorganization may simply involve facile movement of internal water molecules rather than movement of somewhat constrained side chain residues. Internal water molecules closest to the heme would be expected to have the largest effect, which would diminish as their distance from the heme increases. This possibility would explain the order of reactivity of the three internal site mutants.

The electron transfer properties of the water switch variants suggest that one of the roles of the hydrogen bond network of WAT166 is to lower the reorganization energy of cytochrome *c* by promoting movement of one or more internal solvent molecules so that movement of the surrounding polypeptide is minimized. Recently the structure of another water switch mutant, Asn52Ile of yeast iso-1-

cytochrome *c*, has been reported (Hickey *et al.*, 1991). This mutant completely lacks internal solvent molecules, including WAT166. Despite the absence of internal water molecules, this mutant appears to be fully functional and thermodynamically more stable than the wild type protein. Electron transfer kinetics of Asn52Ile with inorganic complexes have not yet been reported. The absence of internal water molecules requires that the reorganization energy of Ile52 prior to electron transfer is due solely to movement of the polypeptide chain in the vicinity of the heme. The results obtained in this work suggest that the reactivity of Ile52 will be lower than those of Tyr67Phe, Asn52Ala, and Thr78Gly.

4.3.4 Temperature Dependence of Electron Transfer Kinetics

Transition state theory has been applied to the analysis of the temperature dependences of the electron transfer reactions of the cytochrome *c* variants studied here to calculate their activation parameters, which are presented on pages 69 and 76. Results of this type must be interpreted cautiously for two reasons. First, the error inherent in collecting data over a short temperature interval and obtaining activation parameters by extrapolation to a point far removed from the data points is significant. A difference in free energy of activation of less than 1 kcal/mol can have a dramatic effect on the observed rates. The most striking example of this is the similarity of the activation parameters for reduction by $Fe(edta)^{2-}$ of the Phe82Gly variant and of the wild type protein. The difference in activation entropies and enthalpies for the two proteins are 2 eu and 0.8 kcal/mol respectively, yet the cross reaction rate constant of the Phe82Gly variant is almost twice that of the wild type protein at 25 °C. A second consideration is that the activation parameters are derived from the cross reaction and are not corrected for differences in driving force and the nature of the reactants. Such factors tend to dominate the activation parameters and may obscure the contributions of the mutations. For example, the lower activation enthalpy of the reaction of wild type cytochrome *c* with $Fe(edta)^{2-}$ compared to $Co(phen)_3^{3+}$ is due mainly to the higher driving force and electrostatic attraction in the former reaction. By comparison, the higher activation entropy associated with the oxidation of wild type by $Co(phen)_3^{3+}$ compared to $Fe(edta)^{2-}$ is a consequence

of the more symmetrical nature of the structure of the oxidant, which increases the number of ways that the specific geometry of the precursor complex can be reached. For these reasons, the differences between the activation parameters of mutant and wild type cytochromes *c* with a particular electron transfer partner tend to be small, even when there are clear differences in the cross reaction rates.

Comparison of the activation parameters for the reduction of Phe82Ala and Phe82Ser variants by $Fe(edta)^{2-}$ supports the proposal that the enhanced reduction rate of Phe82Ser is due in part to reorientation of the inorganic complex with respect to the protein surface. As discussed previously, the two variants should have a similar indentation in the protein surface. However, the activation parameters of Phe82Ala are within experimental error of those determined for the wild type protein. The lower activation enthalpy and more negative activation entropy of Phe82Ser are what would be expected for formation of a precursor complex with more effective orbital overlap with fewer ways of producing electron transfer active precursor complexes.

4.4 Alkaline Isomerization

Stopped flow pH-jump experiments were used by Davis *et al.* (1974) to characterize the mechanism of the alkaline isomerization of ferricytochrome *c*, as described in the Introduction. The results of these experiments were consistent with a two-step process consisting of an initial deprotonation characterized by pK_H, followed by a conformational change in which the axial Met80 is replaced by another ligand supplied by the protein. The second step is characterized by the equilibrium constant $K_c = k_f/k_b$. The alkaline isomerization pK_a measured by spectrophotometric titration is equal to $pK_H + pK_c$. Spectroscopic measurements on the alkaline isomer and comparisons with heme complexes of known ligation suggest that the alkaline isomer possesses His-Lys axial ligation, as previously discussed. It should be noted that the titrating group responsible for the observed pK_H need not be the group that replaces methionine as one of the axial ligands to the heme, although this possibility represents the simplest mechanism. Thus,

deprotonation of a heme propionate (Tonge *et al.*, 1989), WAT166 (Takano & Dickerson, 1981b) and His18 (Gadsby *et al.*, 1987) have each been proposed as the group responsible for the observed pK_H.

The equilibrium and kinetics of the alkaline isomerization of several position 82 variants of yeast iso-1-cytochrome *c* have been studied previously (Pearce et al., 1989). Although position 82 variants showed large differences in their alkaline pK_as and rate parameters, all behaved in a manner consistent with the mechanism described above. Replacement of Phe82 by a nonaromatic side chain destabilizes the native conformation by lowering pK_H by 1 to 1.4 pK units. The equilibrium constant K_c is either unaffected (Phe82Leu and Phe82Ile) or slightly lowered (Phe82Ser and Phe82Gly). A lower pK_c partially offsets the effect of the lower pK_H on the pK_a for the overall process.

The alkaline isomerization is also sensitive to mutations at residues that hydrogen bond to WAT166 (Table 5, page 80). The Thr78Gly variant destabilizes the native ligation state and has the lowest pK_a measured for any water switch or position 82 mutant. This behaviour results entirely from a lowering of the pK_H of the titrating group by 2 pH units. The equilibrium constant K_c is also lower for Thr78Gly than in the case of the wild type protein. This lower value for pK_c partially compensates the effect of the lower pK_H, as previously reported for the Phe82Gly and Phe82Ser variants.

Although the Asn52Ala variant has an alkaline pK_a within experimental error of that determined for wild type cytochrome *c* (Guillemette, unpublished), the kinetic data for the alkaline isomerization of this variant are inconsistent with the mechanism described above. Similar kinetic behaviour has been recorded for the alkaline isomerization of Tyr67Phe (Guillemette *et al.*, in preparation). The spectrophotometric pH titration curve of Asn52Ala indicates the release of one proton upon isomerization to the alkaline form. To be consistent with both the kinetic and equilibrium experiments, the mechanism of the alkaline isomerization of this variant would require at least four steps: two deprotonations, a protonation, and a conformational change. A possible mechanism is shown in Figure 37. The following equation for the observed rate constant is derived from this mechanism:

$$k_{obs} = \frac{k_b K_{H3}}{K_{H3} + [H^+]} + \frac{k_f K_{H1} K_{H2}}{K_{H1} K_{H2} + K_{H1}[H^+] + [H^+]^2} \qquad (29)$$

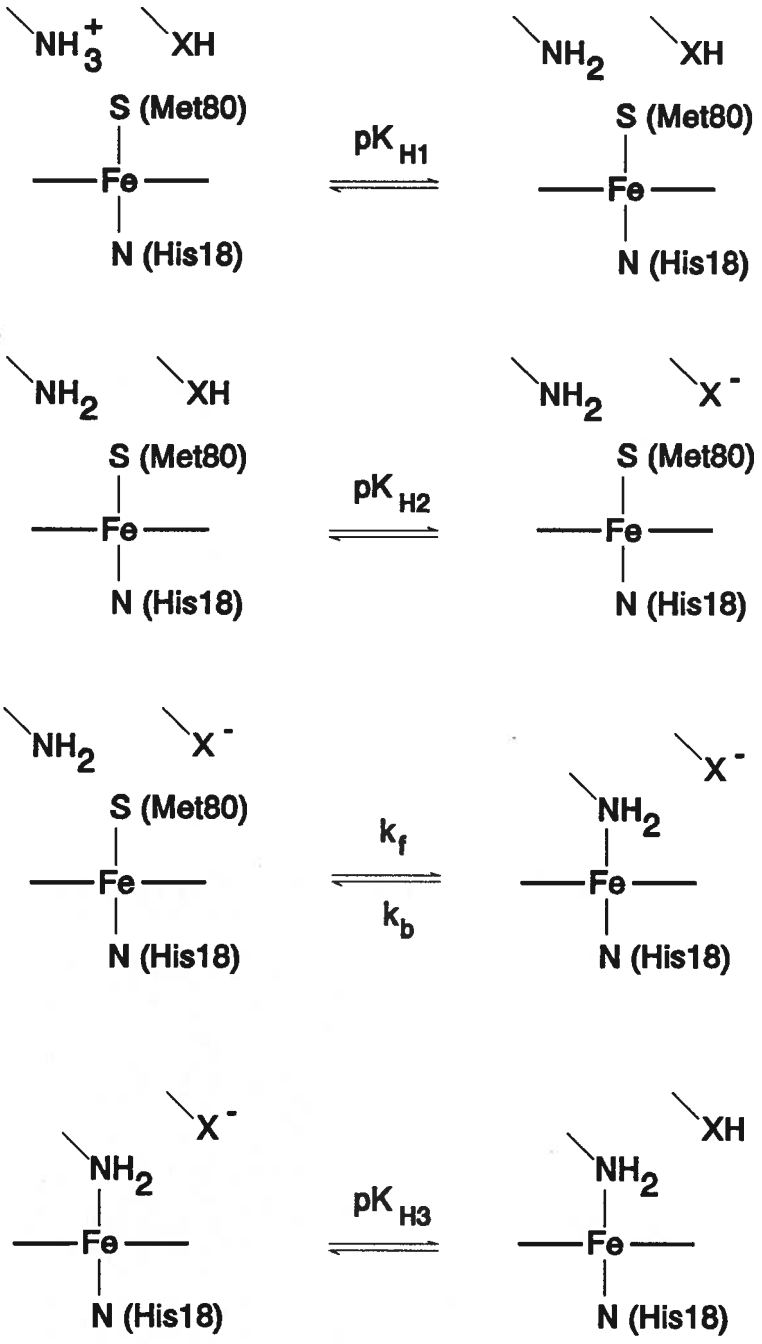

Figure 37 A possible minimal mechanism for the alkaline isomerization of the Asn52Ala variant of ferricytochrome *c*. For simplicity, this mechanism is presented with a lysine as one of the titrating groups as well as being the replacing ligand. Among groups proposed as the titrating residue responsible for pK_{H1} are a heme propionate (Tonge *et al.*, 1989) and WAT166 (Takano & Dickerson, 1981b). The porphyrin plane is symbolized by the horizontal line through the symbol for iron.

The initial deprotonation may be similar to that of the wild type protein. The second deprotonation may involve the disruption of a stabilizing interaction, such as a hydrogen bond. After the second deprotonation, the protein becomes sufficiently flexible to undergo the conformational change to the alkaline form. A subsequent protonation event may then stabilize the alkaline isomer.

The presence of a protonation following the conformational change to the alkaline isomer is consistent with the observed rate constant for the pH jump from high to low pH, which in the Asn52Ala is an order of magnitude smaller than observed for wild type. This behaviour suggests a pH dependent reverse rate. The rate of conversion from alkaline to native ligation state upon lowering the pH would depend on the concentration of alkaline isomer present without the proposed stabilizing hydrogen bond. At low pH, this interaction will be strengthened, resulting in only a small concentration of alkaline isomer without this stabilizing interaction that is capable of forming the native species. The kinetic data can be fitted well to an equation that describes such a mechanism. However, attempts to determine these parameters by use of a non-linear least squares analysis were not successful, as the calculated parameters were highly dependent on the initial estimates used in the calculation.

The strong influence on the alkaline isomerization of ferricytochrome *c* by mutations at positions 52, 67 and 78 suggests that the trigger for this process resides within the protein, rather than on a surface group such as the N-ϵ amino group of a lysine residue. It is unlikely that mutations at these internal positions influence the ionization of the replacing lysine residue(s) on the protein surface. This reasoning supports the proposal that a heme propionate, Tyr67, or WAT166 is the titrating group responsible for triggering the alkaline isomerization. Which one of these three possibilities is ultimately responsible cannot be determined from the results of this work, as the mutation sites occur at or close to all three potential candidates.

The mutation of Ile75 to Met has no effect on the alkaline isomerization. This finding suggests no significant structural changes within the hydrogen bonding network about WAT166 result from this

substitution. This observation argues against the possibility that the Ile75Met side chain is directed into the space occupied by WAT166 as it is unlikely that such a large change in the heme environment would have no effect on the alkaline isomerization.

In stopped-flow experiments performed above pH 10.5, biphasic kinetics were observed with the Asn52Ala variant and the wild type protein. The observed rate constant for this second kinetic phase was 37 to 45 s^{-1} for both proteins, and its contribution to the total absorbance change increased with pH. Biphasic kinetics of the alkaline isomerization of horse heart ferricytochrome *c* above pH 10 were observed using stopped flow pH jump experiments by Kihara and coworkers (1976), who attributed the faster kinetic phase to the formation of a transient intermediate species on an alternate pathway to the alkaline isomer. This pathway represents a 'short-cut' to the alkaline form, but only becomes available after a second deprotonation (Figure 38). An alternative explanation for the biphasic kinetics is that the faster phase represents the rate of conversion of the native protein to a second alkaline isomer with a different lysine residue as the axial ligand than the alkaline isomer observed below pH 10. This mechanism is consistent with a 2D NMR investigation that provides evidence for two distinct alkaline species of horse heart ferricytochrome *c* (Hong & Dixon, 1989). The second lysine residue may have a higher pK_H, but once it is deprotonated it may be able to displace Met80 more rapidly than the lysine residue that forms an alkaline isomer below pH 10.5.

4.5 Ligand Substitution

Azide binds to cytochrome *c* by displacing Met80 sulphur as one of the axial ligands, a process which can be monitored by the loss of absorbance at 695 nm with increasing azide concentration (Sutin & Yandell, 1972; Saigo, 1986). The binding isotherms determined here are consistent with one ligand molecule binding per molecule of cytochrome *c*, except for the Tyr67Phe mutant, where binding was incomplete even at ligand concentrations greater than 2 M.

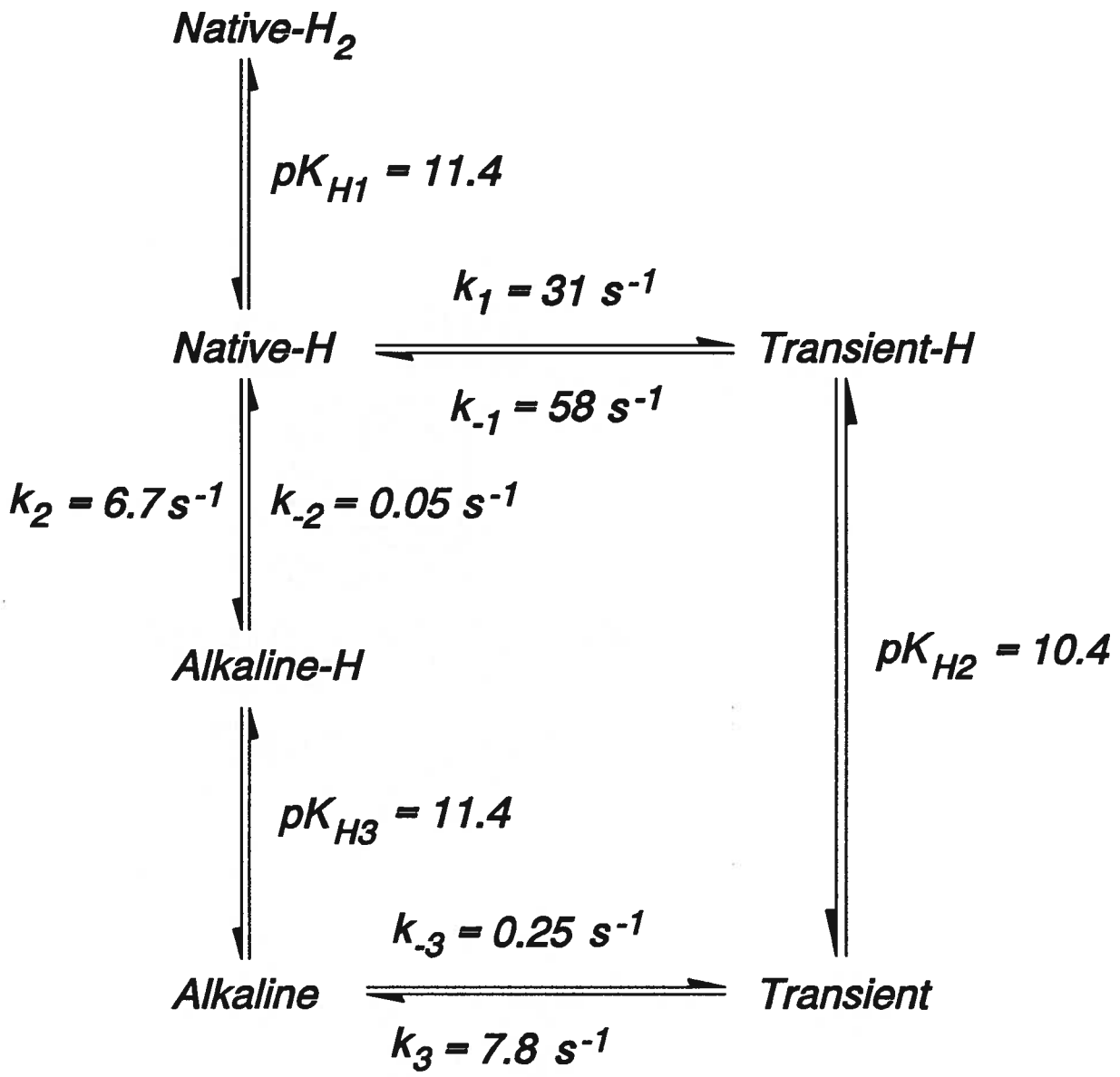

Figure 38 A mechanism proposed by Kihara and coworkers to account for the alkaline isomerization of horse heart ferricytochrome *c* between pH 9 and 12 (Kihara *et al.*, 1976). 'Native' refers to ferricytochrome *c* with histidine-methionine axial ligation to the iron; 'Alkaline' refers to the alkaline isomer of ferricytochrome *c* in which methionine has been replaced as one of the axial ligands. 'Transient' refers to a proposed intermediate of unknown ligation. The protonation state of each species is indicated by the number of H's which follow the name of each component. Note that the portion of the mechanism defined by pK_{H1}, k_2, and k_{-2} is identical to the mechansim proposed by Davis *et al.* (1974).

Although the stereochemistry of azidoferricytochrome *c* is not precisely known, structural studies of coordinated azides and knowledge of the electronic structure of the ligand predict several features that will be exhibited by this complex (Dori & Ziolo, 1973). The lone pair of electrons that azide donates to iron(III) are from an sp^2 hybridized orbital, giving an Fe-N1-N2 angle of 125° and a coordinate bond length of 1.93 Å in the complex of azido(pyridine)tetraphenylporphyrinatoiron(III) (Adams *et al.*, 1976). Azide methemoglobin possesses similar geometry, but the low resolution of the crystal structure of this complex did not allow precise calculation of the bond lengths and angles (Deatherage *et al.*, 1979). It is highly likely that azide will bind to ferricytochrome *c* in a similar fashion. The short azide-iron bond length (compared to the 2.43 Å iron-sulphur bond of the native protein (Louie & Brayer, 1990)) and the preference of azide for a bent coordinate bond are factors that favour minimal structural perturbation upon azide binding to cytochrome *c*.

The orientation of coordinated azide with respect to the plane of the heme in ferricytochrome *c* is unknown. Steric considerations suggest an orientation that places bound azide along the line defined by pyrrole rings II and IV. The side chain of Met80 lies over pyrrole rings I and III in native ferricytochrome *c* and, barring movement of the polypeptide backbone, would continue to occupy a similar position after disruption of the iron-sulphur bond. Additionally, the azide nitrogen atom that is coordinated to the iron bears a second lone pair in an sp^2 hybridized orbital that could potentially hydrogen bond to the hydroxyl group of Tyr67, as does the Met80 sulphur atom in ferrocytochrome *c*. This would place the azide mainly over pyrrole ring II. Formation of a Tyr67-OH / azide hydrogen bond would require a shortening of the distance between the potential hydrogen bonding partners.

Ligand substitution at the heme of ferricytochrome *c* is sensitive to the structure of the heme environment. If Phe82 is replaced by nonaromatic residues, K_{az} increases three to six fold. The results of the stopped-flow kinetics experiments show that the increase in azide binding affinity is caused by a 2.5 to 5-fold increase in k_1, the forward rate constant, and by an increase in the tendency of the

intermediate state to proceed to the azide bound form, characterized by an increase in the ratio of k_2/k_{-1}. These kinetic parameters are similar for Leu, Ser, and Gly mutants at position 82. The increase in k_1 for Phe82Ser and Phe82Gly is consistent with greater exposure of the heme to solvent, the former because of a solvent channel extending from the surface to Met80, the latter because of flexibility of the polypeptide chain in residues 81 through 84 (Louie & Brayer, 1988, 1989). The causes of the elevated k_1 for the Phe82Leu and Phe82Ile variants are not obvious, but the increased affinity of these species for azide is consistent with their lower alkaline pK_as, which also indicates a weakened heme crevice. Instability of the heme crevice in the Phe82Leu and Phe82Ile variants may be caused by an absence of hydrophobic contacts that the wild type Phe82 side chain normally makes with nearby residues or by disruption in packing against neighbouring side chains caused by replacing the planar aromatic ring of phenylalanine with branched aliphatic side chains.

Differences in the rate constant k_2 contribute to the difference in the observed azide binding constants of the Ser and Gly variants. The variation in k_2 observed here implies structural differences in the azido-cytochrome *c* complexes of these species. Both variants have similar forward rate constants that are at least three-fold greater than that of the wild type protein. The solvent channel of Phe82Ser allows ready access of the ligand to the heme, but it also offers no hindrance to the release of azide. Thus this variant has the largest rate constant for dissociation of azide from ferricytochrome *c*. In contrast, the Phe82Gly mutant has a greater forward rate constant and a smaller reverse rate constant that of the Ser variant, giving Phe82Gly a greater overall affinity for azide. Because azide binding to ferricytochrome *c* neutralizes the positive heme charge, it is possible that the protein undergoes conformational changes upon azide binding similar to those that occur upon reduction. Such a change would explain the lower k_2 for the Phe82Gly variant relative to Phe82Ser variant as in the former protein a conformational change in the reduced protein reduces heme solvent accessibility by movement of the polypeptide backbone toward the heme. This movement would sterically hinder the release of bound azide.

The mechanism by which azide association occurs is not known with certainty. This process may be dominated by the inherent strength of the iron(III)-sulphur bond, by the flexibility of the polypeptide around the heme, or by a combination of the two. The ratio of the rate constants leading away from the active intermediate is calculated indirectly from the value of the binding constant (K_{az}) and the forward (k_1) and reverse (k_{-2}) rate constants. The magnitude of this ratio will depend on the nature of this active intermediate and on the position of the incoming/outbound azide molecule. The accuracy with which this ratio can be determined will thus be dependent on the accuracy of the parameters from which it is derived. The lower ratio of k_2 /k_{-1} determined for the wild type protein relative to the position-82 variants reflects the greater tendency of the former to re-form the native ligation state and suggests that even when the heme crevice opens that the azide still has only limited access to the heme. The higher ratios of the Gly, Ser, Leu, and Ile variants indicate an increased tendency of the active intermediate to form the azido-cytochrome *c* complex.

In contrast to the position 82 mutants, the water switch mutants Tyr67Phe, Asn52Ala and Ile75Met all have lower affinities for azide than does wild type yeast cytochrome *c*. Tyr67Phe is highly resistant to ligand substitution, with a binding constant for azide of 1 M^{-1} or less. Consequently, it was not possible to extrapolate a rate of heme crevice opening from the rate data as there was no evidence of rate saturation up to azide concentrations of 0.5 M. However, the rate data indicate that low azide affinity results from a combination of a high reverse rate constant k_{-2} and a low ratio of k_2/k_{-1}. This suggests that the rate of heme crevice opening (k_1) may be little changed from the native protein. Unfavourable steric interactions in the azide bound species may increase k_{-2}. Additionally, the Met80 sulphur may be in a more favourable position to compete with azide for the axial coordination site, causing a decrease in the ratio of k_2/k_{-1}.

The lower affinity of Asn52Ala for azide is entirely caused by an increase in k_{-2}, indicating destabilization of the azide bound complex. There are no significant differences in the other rate parameters between Asn52Ala and the wild type protein. In all experiments where the properties of

Tyr67Phe and Asn52Ala mutants are compared to those of the wild type protein, the mutation closer to the heme always has the larger affect. Thus both mutants have lower reduction potentials, but that of Tyr67Phe is lower; both undergo electron transfer with inorganic complexes more readily, but Tyr67Phe is more reactive; both have altered alkaline isomerization kinetics, but Tyr67Phe has the higher alkaline pK_a. The azide binding affinities of these two mutants also follow this trend.

The rate data for the Ile75Met variant best fit a simple two state equilibrium model characterized by a forward and reverse rate constants k_f and k_b, respectively. Although this variant exhibits a strong dependence of the observed rate on azide concentration, it shows no indication of rate saturation. The equilibrium constant determined from the ratio k_f/k_b is in excellent agreement with that found by titration (Table 6). The means by which this substitution changes the mechanism of azide binding to cytochrome *c* is unknown. A similar mechanism has been proposed for the binding of imidazole to *Candida krusei* ferricytochrome *c* (Creutz & Sutin, 1974), which possesses isoleucine at position 75. Both *S. cerevisiae* iso-1 and *C. krusei* cytochromes *c* have high sequence homology among the residues defining the heme environment and have identical sequences between residues 71 and 87. Residue Ile75 shields the hydrogen bond network about WAT166 from exposure to solvent. The lower reduction potential of the Ile75Met variant may suggest that the heme is more solvent accessible in this variant, though other origins for this behaviour are also possible. A new route for azide to the active site through the mutation site might explain the kinetic properties of ligand substitution in this mutant.

Comparison of various species of cytochrome *c* led Saigo (1986) to note a correlation between the alkaline isomerization pK_a of a cytochrome *c* and its affinity for exogenous ligands such as imidazole and azide. A similar correlation has been observed in this work (Figure 39). The common feature of both processes is the disruption of the iron(III)-sulphur bond and the native heme crevice structure. The observation that the rates of substitution by exogenous ligands are faster than the rates of conformational change in the alkaline isomerization reflects the difference in the degree of freedom of the free azide ligand compared to the lysyl residue, which is constrained by its attachment to the rest of the protein.

The correlation does point out the inherent weakness of the iron(III)-sulphur coordination. This weakness is demonstrated by the observation that oxidized heme octapeptide requires 2 M N-acetylmethionine to form the iron(III)-Met complex (Harbury, 1965). Thus one of the functions of the protein environment around the heme of cytochrome *c* is to stabilize the intrinsically unstable axial ligation of the heme iron by Met80 in the ferricytochrome.

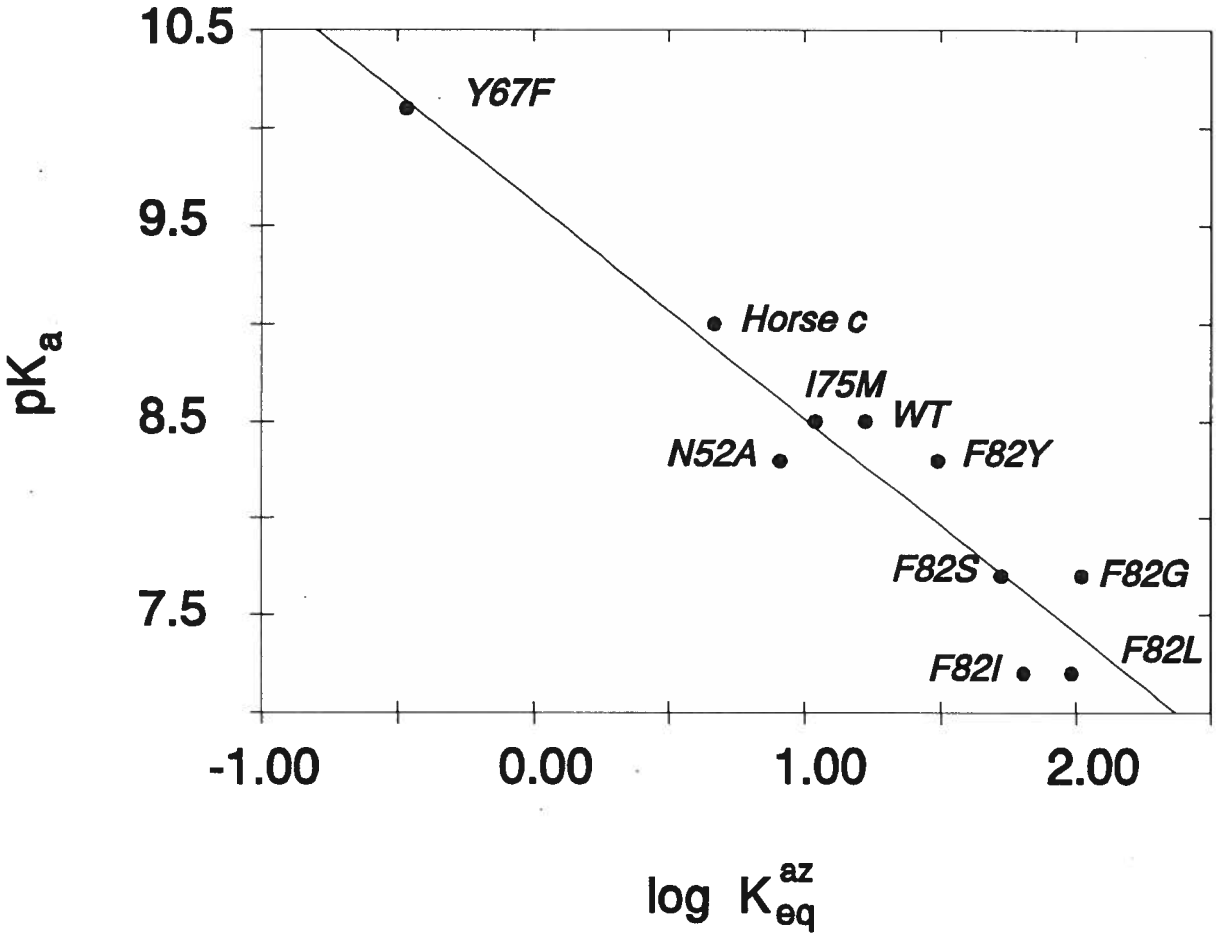

Figure 39 Correlation of azide binding with the alkaline pK_a for cytochromes *c*.

4.6 Summary

In this work, the effect of mutation at residues within the heme environment of yeast iso-1-cytochrome *c* on reduction potential, electron transfer reactivity, and stability of the native coordination state has been examined. From the results obtained in these experiments, several conclusions can be drawn regarding the roles of the residues occurring at these positions in the wild type protein.

The invariant residue Phe82 serves two major roles. First, it is required to maintain a high reduction potential. Except for the Phe82Leu variant, the reduction potentials of all other mutants at this position were 10 to 45 mV lower than wild type. Second, Phe82 stabilizes the iron(III)-Met80 sulphur bond by limiting the access of solvent to the heme. Phe82 is not essential for electron transfer activity. All of the position 82 mutants studied were capable of transferring electrons with inorganic complexes at rates similar to or greater than those exhibited by the wild type protein.

A major role of the water switch residues in the environment of WAT166 is to maintain a high reduction potential. All of the substitutions in this region lowered the reduction potential by at least 33 mV. The wild type residues are not required for efficient electron transfer, as several variants are more reactive than wild type. Nor are these residues essential for maintaining the iron(III)-Met80 sulphur ligation, as the results of ligand substitution and alkaline isomerization experiments for Tyr67Phe, Asn52Ala and Ile75Met demonstrate. One avenue that was not explored in this work was the influence of these residues on the stability of the folded structure of the protein. However, the instability of Thr78Val and Thr78Gln variants, and the lowered alkaline pK_a of Thr78Gly indicates that Thr78 plays a role in maintaining a folded conformation of the protein that is compatible with function.

REFERENCES

Abrams, R., Altschul, A.M., & Hogness, T.R. (1942) Cytochrome *c* Peroxidase II: The Peroxidase-Hydrogen Peroxide Complex, *J. Biol. Chem.* **142**, 303.

Adams, K., Ramussen, P.G., & Scheidt, W.R. (1976) In *Porphyrins and Metalloporphyrins*, (K.M. Smith, ed.)(unpublished results quoted by J.L. Hoard, pp 317-380, Elsevier, N.Y., 1975).

Allen, P.M., Hill, H.A.O, & Walton, N.J. (1984) Surface Modifiers for the Promotion of Direct Electrochemistry of Cytochrome *c*, *J. Electroanal. Chem.* **178**, 69.

Altschul, A.M., Abrams, R., & Hogness, T.R. (1940) Cytochrome *c* Peroxidase, *J. Biol. Chem.* **136**, 777.

Armstrong, F.A., Hill, H.A.O., & Oliver, B.N. (1984) Surface Selectivity in the Direct Electrochemistry of Redox Proteins: Contrasting Behavior at Edge and Basal Planes of Graphite, *J. Chem. Soc. Chem. Commun.*, 976.

Armstrong, G.D., Chapman, S.K, Sisley, M.J., Sykes, A.G., Aitken, A., Osherhoff, N., & Margoliash, E. (1986a) Preferred Sites on Cytochrome *c* for Electron Transfer with Two Positively Charged Blue Copper Proteins, *Anabaena variabilis* Plastocyanin and Stellacyanin, *Biochemistry* **25**, 6947.

Armstrong, G.D., Chambers., J.A., & Sykes, A.G. (1986b) Preferred Sites for Electron Exchange between Cytochrome *c* and $[Fe(edta)]^{2-}$ and $[Co(sep)]^{2+}$ Complexes, *J. Chem. Soc. Dalton. Trans.*, 755.

Augustin, M.A., Chapman, S.K., Davies, D.M., Sykes, A.G., Speck, S.H., & Margoliash, E. (1983) Interaction of Cytochrome *c* with the Blue Copper Proteins, Plastocyanin and Azurin, *J. Biol. Chem.* **258** 6405.

Bach, S.J., Dixon, M., & Keilin, D. (1942a) A New Soluble Cytochrome Component From Yeast, *Nature* **149**, 21.

Bach, S.J., Dixon, M., & Zerfas, L.G. (1942b) Lactic Dehydrogenase of Yeast, *Nature* **149**, 48.

Baker, B.R., Basolo, F., & Neumann, H.M. (1959) Electron Transfer in the System Tris-(1,10-Phenanthroline)-Cobalt(II) - Tris-(1,10-Phenanthroline)-Cobalt(III), *J. Phys. Chem.* **63**, 371.

Bard, A.J., & Faulkner, L.R. (1980) *Electrochemical Methods*, John Wiley & Sons, New York.

Barker, P.D., & Mauk, A.G. (1992) *J. Am. Chem. Soc.*, in press.

Berroteran, R.W., & Hampsey, M. (1991) Genetic Analysis of Yeast Iso-1-cytochrome *c* Structural Requirements: Suppression of Gly 6 Replacements by an Asn 52→Ile Replacement, *Arch. Biochem. Biophys.* **288**, 261.

Bond, A.M., Hill, H.A.O., Page, D.J, Psalti, I., & Walton, N.J. (1990) Evidence for Fast and Discriminatory Electron Transfer of Proteins at Modified Gold Electrode Surfaces, *Eur. J. Biochem.* **191**, 737.

Bosshard, H.R. (1979) Mapping of Contact Areas in Protein-Nucleic Acid and Protein-Protein Complexes by Differential Chemical Modification, *Methods Biochem. Analysis* **25**, 273, D. Glick, ed.

Bottomly, L.A., Olson, L., & Kadish, M. (1982) Redox Tuning of Iron Porphyrins *in* Electrochemical and Spectrochemical Studies of Biological Redox Components, K.M. Kadish, ed., *Adv. Chem. Ser.* **201**, 51.

Brautigan, D.L., Feinberg, B.A., Hoffmann, B.M., Margoliash, E., Peisach, J., & Blumberg, W.E. (1977) Multiple Low Spin Forms of the Cytochrome *c* Ferrihemochrome, *J. Biol. Chem.* **252**, 574.

Brautigan, D.L., Ferguson-Miller, S., & Margoliash, E. (1978a) Mitochondrial Cytochrome *c*: Preparation and Activity of Native and Chemically Modified Cytochromes *c*, *Methods Enzymol.* **53**, 128.

Brautigan, D.L., Ferguson-Miller, S., & Margoliash, E. (1978b) Definition of Cytochrome *c* Binding Domains by Chemical Modification. I. Reaction with 4-Chloro-3,5-Dinitrobenzoate and Chromatographic Separation of Singly Substituted Derivatives, *J. Biol. Chem.* **253**, 130.

Brautigan, D.L., Ferguson-Miller, S., & Margoliash, E. (1978c) Definition of Cytochrome *c* Binding Domains by Chemical Modification. II. Identification and Properties of Singly Substituted Carboxydinitrophenyl Cytochromes *c* at Lysines 8, 13, 22, 27,39,60,72,87 and 99, *J. Biol. Chem.* **253**, 140.

Burch, A.M., Rigby, S.E.J., Funk, W.D., MacGillivray, R.T.A., Mauk, M.R., Mauk, A.G., & Moore, G.R. (1990) NMR Characterization of the Surface Interactions in the Cytochrome b_5-Cytochrome *c* Complex, *Science* **247**, 831.

Bushnell, G.W., Louie, G.V., & Brayer, G.D. (1990) High Resolution Structure of Horse Heart Cytochrome *c*, *J. Mol. Biol.* **214**, 585.

Butler, J., Chapman, S.K., Davies, D.M., Sykes, A.G., Speck, S.H., Osheroff, N., & Margoliash, E. (1983) Preferred Sites for Electron Transfer Between Cytochrome *c* and Iron and Cobalt Complexes, *J. Biol. Chem.* **258**, 6400.

Churg, A.K., & Warshel, A. (1986) Control of the Redox Potential of Cytochrome *c* and Microscopic Dielectric Effects in Proteins, *Biochemistry* **25**, 1675.

Cohen, H.J., & Fridovich I. (1971) Hepatic Sulfite Oxidase: Purification and Properties, *J. Biol. Chem.* **246**, 359.

Concar, D.W., Whitford, D., Pielak, G.J., & Williams, R.J.P. (1991) The Role of Phe82 in Electron Exchange Reactions of Eukaryotic Cytochromes *c*, *J. Am. Chem. Soc.* **113**, 2401.

Connors, K.A. (1987) *Binding Constants*, John Wiley & Sons, New York.

Corradin, G., & Harbury, H.A. (1971) Reconstitution of Horse Heart Cytochrome *c*: Interaction of the Components Obtained Upon Cleavage of the Peptide Bond following Methionine Residue 65, *Proc. Natl. Acad. Sci. USA*, **68**, 3036.

Corradin, G., & Harbury, H.A. (1974) Reconstitution of Horse Heart Cytochrome *c*: Reformation of the Peptide Bond Linking Residues 65 and 66, *Biochem. Biophys. Res. Commun.* **61**, 1400.

Creutz, C., and Sutin, N. (1974) Kinetics of Ligand Binding and Oxidation-Reduction Reactions of Cytochrome *c* from Horse Heart and *Candida krusei*, *J. Biol. Chem.* **249**, 6788.

Cutler, R.L., Pielak, G.J., Mauk, A.G., & Smith, M. (1987) Replacement of Cysteine-107 of *Saccharomyces cerevisiae* Iso-1-cytochrome *c* with Threonine: Improved Stability of the Mutant Protein, *Protein Engineering* **1**, 95.

Cutler, R.L., Davies, A.M., Creighton, S., Warshel, A., Moore, G.R., Smith, M., & Mauk, A.G. (1989) Role of Arginine-38 in Regulation of the Cytochrome *c* Oxidation-Reduction Equilibrium, *Biochemistry* **28**, 3188.

Das, G., Hickey, D.R., McLendon, D., McLendon, G., & Sherman, F. (1989) Dramatic Thermostabilization of Yeast Iso-1-cytochrome *c* by an Asn52→Ile52 Replacement, *Proc. Natl. Acad. Sci. USA*, **86**, 496.

Davis, L.A., Schejter, A., Hess, G.P. (1974) Alkaline Isomerization of Oxidized Cytochrome *c*, *J. Biol. Chem.* **249**, 2624.

Dayhoff, M. (1972) *Atlas of Protein Sequence and Structure*, Volume 5, National Biomedical Research Foundation.

Deatherage, J.F., Obendorf, S.K., & Moffat, K. (1979) Structure of Azide Methemoglobin, *J. Mol. Biol.* **134**, 419.

Devault D. (1984) *Quantum-Mechanical Tunnelling in Biological Systems*, second edition, Cambridge University Press, Cambridge.

Dickerson, R.E., & Timkovitch, R. (1975) Cytochromes *c*, in *The Enzymes*, **XI**, P.D. Boyer, editor.

Dimaria, P., Polastro, E., Delange, R.J., Kim, S., & Paik, W.K. (1979) Studies on Cytochrome *c* Methylation in Yeast, *J. Biol. Chem.* **254**, 4645.

Dori, Z., & Ziolo, R.F. (1973) The Chemistry of Coordinated Azides, *Chem. Rev.* **73**, 247.

Eddowes, M.J., & Hill, H.A.O. (1977) Novel Method for the Investigation of the Electrochemistry of Metalloproteins: Cytochrome *c*, *J. Chem. Soc. Chem. Commun.*, 771.

Endo, S., Nagayama, K., & Wada, A. (1985) Comparision of Protease Suceptibility and Thermal Stability of Cytochrome *c*, *J. Biol. Structure & Dynamics* **3**, 409.

Evans, D.H., O'Connell, K.M., Petersen, R.A., & Kelly, M.J. (1983) Cyclic Voltammetry, *J. Chem. Ed.* **60**, 290.

Ewall, R.X., & Bennett, L.E. (1974) Reactivity Characteristics of Cytochrome *c*(III) Adduced from its Reduction by Hexaammineruthenium(II) Ion, *J. Am. Chem. Soc.* **96**, 940.

Eyring, H. (1935) The Activated Complex in Chemical Reactions, *J. Chem. Phys.* **3**, 107.

Frew, J.E., & Hill, H.A.O. (1988) Direct and Indirect Electron Transfer Between Electrodes and Redox Proteins, *Eur. J. Biochem.* **172**, 261.

Gadsby, P.M.A, Peterson, J., Foote, N., Greenwood, C., & Thompson, A.J. (1987) Identification of the Ligand-Exchange Process in the Alkaline Transition of Horse Heart Cytochrome *c*, *Biochem. J.* **246**, 43.

George, P., & Tsou, C.L. (1952) Reaction Between Hydrocyanic Acid, Cyanide Ion, and Ferricytochrome *c*, *Biochem. J.* **50**, 440.

Greenwood, C., & Palmer, G. (1965) Evidence for the Existence of Two Functionally Distinct Forms of Cytochrome *c* Monomer at Alkaline pH, *J. Biol. Chem.* **240**, 3660.

Gupta, R.K., & Koenig, S.H. (1971) Some Aspects of pH and Temperature Dependence of the NMR Spectra of Cytochrome *c*, *Biochem. Biophys. Res. Commun.* **45**, 1134.

Gupta, R.K., Koenig, S.H., & Redfield, A.G. (1972) On the Electron Transfer Between Cytochrome *c* Molecules as Observed by Nuclear Magnetic Resonance, *J. Magn. Resonance* **7**, 66.

Gupta, R.K. (1973) Electron Transfer in Cytochrome *c*. Role of the Polypeptide Chain, *Biochim. Biophys. Acta* **292**, 291.

Hampsey, D.M., Das, G., Sherman, F. (1986) Amino Acid Replacements in Yeast Iso-1-cytochrome *c*, *J. Biol. Chem.* **261**, 3259.

Harbury, H.A., Cronin, J.R., Fanger, M.W., Hettinger, T.P., Murphy, A.J., Myer, Y.P., Vinogradov, S.N. (1965) Complex Formation between Methionine and a Heme Peptide from Cytochrome *c*, *Proc. Natl. Acad. Sci. USA* **54**, 1658.

Hartshorn, R.T., & Moore, G.R. (1989) A Denaturation-Induced Proton-Uptake Study of Horse Ferricytochrome *c*, *Biochem. J.* **258**, 595.

Hennig, B., & Neupert, W. (1981) Assembly of Cytochrome *c* - Apocytochrome *c* is bound to Specific Sites on the Mitochondria before it is Converted to Holocytochrome *c*, *Eur. J. Biochem.* **121**, 203.

Hennig, B., Koehler, H., & Neupert, W. (1983) Receptor Sites Involved in Post-Translational Transport of Apocytochrome *c* into Mitochondria - Specificity and Number of Sites, *Proc. Natl. Acad. Sci. USA*, **80**, 4963.

Hickey, D.R., Berghuis, A.M., Lafond, G., Jaeger, J.A., Cardillo, T.S., McLendon, D., Das, G., Sherman, F., Brayer, G.D., & McLendon, G. (1991) Enhanced Thermodynamic Stabilities of Yeast Iso-1-cytochromes *c* with Amino Acid Replacements at Positions 52 and 102, *J. Biol. Chem.* **266**, 11686.

Hill, G.C., & Pettigrew, G.W. (1975) Evidence for the Amino Acid Sequence of *Crithidia fasciculata* cytochrome c_{555}, *Eur. J. Biochem.* **57**, 265.

Hodges, H.L., Holwerda, R.A., & Gray, H.B. (1974) Kinetic studies of the Reduction of Ferricytochrome *c* by $Fe(EDTA)^{2-}$, *J. Am. Chem. Soc.* **96**, 3132.

Holwerda, R.A., Knaff, D.B., Gray, H.B., Clemmer, J.D., Crowley, R., Smith, J.M, & Mauk, A.G. (1980) Comparision of the Electron-Transfer Reactivities of Tris(oxalato)cobalt(III) ($Co(ox)_3^{3-}$) and Tris(1,10-phenathroline)cobalt(III) ($Co(phen)_3^{3+}$) with Metalloproteins, *J. Am. Chem. Soc.* **102**, 1142.

Hong, X., & Dixon, D.W. (1989) NMR Study of the Alkaline Isomerization of Ferricytochrome *c*, *FEBS Lett.* **246**, 105.

Inglis, S.C., Guillemette, J.G., Johnson. J.A., & Smith, M. (1991) Analysis of the Invariant Phe82 Residue of Yeast Iso-1-cytochrome *c* by Site-Directed Mutagenesis using a Phagemid Yeast Shuttle Vector, *Protein Engineering*, **4**, 569.

Ito, A. (1980a) Cytochrome b_5-like Hemoprotein of Outer Mitochondrial Membrane I: O.M. Cyt *b*, *J. Biochem. (Japan)* **87**, 63.

Ito, A. (1980b) Cytochrome b_5-like Hemoprotein of Outer Mitochondrial Membrane II: Contribution of O.M. Cyt *b* to Rotenone Insensitive NADH-Cyt *c* Reductase Activity, *J. Biochem. (Japan)* **87**, 73.

Jörnvall, H. (1975) Acetylation of Protein N-Terminal Amino Groups. Structural Observations on α-Amino Acetylated Proteins, *J. Theor. Biol.* **55**, 1.

Kaminsky, L.S., Yong, F.C., & King, T.E. (1972) Circular Dichroic Studies of the Perturbations of Cytochrome *c* by Alcohols, *J. Biol. Chem.* **247**, 1354.

Kassner, R.J. (1972) Effects of Nonpolar Environments on the Redox Potentials of Heme Complexes, *Proc. Natl. Acad. Sci. USA* **69**, 2263.

Kassner, R.J. (1973) A Theoretical Model for the Effects of Local Nonpolar Heme Environments on the Redox Potentials in Cytochromes, *J. Am. Chem. Soc.* **95**, 2674.

Kihara, H., Saigo, S., Nakatani, H., Hiromi, K., Ikeda-Saito, M., Ilzuka, T., (1976) Kinetic Study of Isomerization of Ferricytochrome *c* at Alkaline pH, *Biochim. Biophys. Acta* **430**, 225.

Koul, A.K., Nasserman, G.F., & Warme, P.K. (1979) Semisynthetic Analogs of Cytochrome *c* at Positions 67 and 74, *Biochem. Biophys. Res. Commun.* **89**, 1253.

Kunkel, T.A. (1985) Rapid and Efficient Site Specific Mutagenesis without Phenotypic Selection, *Proc. Natl. Sci. USA* **82**, 488.

Latimer, W.M. (1952) *Oxidation Potentials*, 2nd Edition, Prentice-Hall, New York.

Latimer, W.M., Pitzer, K.S., & Smith, W.V. (1938) The Entropies of Aqueous Ions, *J. Am. Chem. Soc.* **60**, 1829.

Lederer, F., Ghrir, R., Guiard, B., Cortial, S., & Ito, A. (1983) Two Homologous Cytochromes b_5 in a Single Cell, *Eur. J. Biochem.* **132**, 95.

Libby, W.F. (1952) Theory of Electron Exchange Reactions in Aqueous Solutions, *J. Phys. Chem.* **56**, 863.

Louie, G.V. (1990) Ph.D. Dissertation, University of British Columbia.

Louie, G.V., & Brayer, G.D. (1988) Role of Phenylalanine 82 in Yeast Iso-1-Cytochrome *c* and Remote Conformational Changes Induced by a Serine Residue at This Position, *Biochemistry* **27**, 7870.

Louie, G.V., & Brayer, G.D. (1989) A Polypeptide Chain-refolding Event Occurs in the Phe82Gly Variant of Yeast-Iso-1-cytochrome *c*, *J. Mol. Biol.* **209**, 313.

Louie, G.V., & Brayer, G.D. (1990) High-resolution Refinement of Yeast Iso-1-Cytochrome *c* and Comparisions With Other Eukaryotic Cytochromes *c* , *J. Mol Biol.* **214**, 527.

Maloy, J.T. (1983) Factors Affecting the Shape of Current-Potential Curves, *J. Chem. Ed.* **60**, 285.

Marcus, R.A. (1964) Chemical and Electrochemical Electron Transfer Theory, *Ann. Rev. Phys. Chem.* **15**, 155.

Marcus, R.A. (1965) On the Theory of Electron Transfer Reactions. VI. Unified Treatment For Homogeneous and Electrode Reactions, *J. Chem. Phys.* **43**, 679.

Marcus, R. A., & Sutin, N. (1985) Electron Transfers in Chemistry and Biology, *Biochim. Biophys. Acta* **811**, 265.

Margoliash, E., & Frohwirt, N. (1959) Spectrum of Horse-Heart Cytochrome *c*, *Biochem. J.* **71**, 570.

Mauk, A.G., Coyle, C.L., Bordignon, E., & Gray, H.B. (1979) Bis(picolinate) Complexes of Cobalt(III) and Iron(II) as New Probes of Metalloprotein Electron Transfer Reactivity. Analysis of Reactions Involving Cytochrome *c* and Cytochrome c_{551}, *J. Am. Chem. Soc.* **101**, 5054.

Mauk, M.R., Mauk, A.G., Weber, P.C., & Matthew, J.B. (1986) Electrostatic Analysis of the Interaction of Cytochrome *c* with Native and Dimethyl Ester Heme Substituted Cytochrome b_5, *Biochemistry* **25**, 7085.

Michel, B., Mauk, A.G., & Bosshard, H.R. (1989) Binding and Oxidation of Mutant Cytochromes *c* by Cytochrome *c* Oxidase, *FEBS Lett.* **243**, 149.

McArdle, J.V., Gray, H.B., Creutz, C., & Sutin, N. (1974) Kinetic Studies of the Oxidation of Ferrocytochrome *c* from Horse Heart and *Candida krusei* by Tris(1,10-phenanthroline)cobalt(III), *J. Am. Chem. Soc.* **96**, 5737.

McLeod, R.M., Farkas, W., Fridovich, I., & Handler, P. (1961) Purification and Properties of Hepatic Sulfite Oxidase, *J. Biol. Chem.* **236**, 1841.

Moore, G.R. (1983) Control of Redox Properties of Cytochrome *c* by Special Electrostatic Interactions, *FEBS Lett.* **161**, 171.

Moore, G.R., Harris, D.E., Leitch, F.A., & Pettigrew, G.W. (1984) Characterization of the Ionizations that Influence the Redox Potential of Mitochondrial Cytochrome *c* and Photosynthetic Bacterial Cytochromes c_2, *Biochim. Biophys. Acta.* **764**, 331.

Moore, G.R., Pettigrew, G.W., & Rogers, N.K. (1986) Factors Influencing Redox Potentials of Electron Transfer Proteins, *Proc. Natl. Acad. Sci. USA* **83**, 4998.

Moore, G.R., & Pettigrew, G.W. (1990) *Cytochromes c: Evolutionary, Structural and Physicochemical Aspects*, Springer-Verlag, Heidelberg.

Moore, G.R., & Williams, R.J.P. (1977) Structural Basis For the Variation in Redox Potential of Cytochromes, *FEBS Lett.* **79**, 229.

Moore, G.R., & Williams, R.J.P. (1980) NMR Studies of Eukaryotic Cytochrome *c*: Assignment of Resonances of Aromatic Amino Acids, *Eur. J. Biochem.* **103**, 493.

Morton, R.A., Overnell, J., & Harbury, H.A. (1970) Electron Transfer between Cytochromes *c* from Horse and *Pseudomonas*, *J. Biol. Chem.* **245**, 4653.

Murray, R.W., Heineman, W.R., O'Dom, G.W. (1967) An Optically Transparent Thin Layer Electrochemical Cell, *Anal. Chem.* **39**, 1666.

Myer, Y.P. (1968) Conformation of Cytochromes. Effect of Urea, Temperature, Extrinsic Ligands and pH Variation on the Conformation of Horse Ferricytochrome *c*, *Biochemistry* **7**, 765.

Narita, K., & Titani, K. (1969) The Complete Amino Acid Sequence in Baker's Yeast Cytochrome *c*, *J. Biochem.* **65**, 226.

Nix, P.T., & Warme, P.K. (1979) Semisynthetic Analogs of Cytochrome *c* Reconstituted from Natural and Synthetic Peptides, *Biochem. Biophys. Acta.* **578**, 413.

Northrup, S.H., Boles, J.O., & Reynolds, J.C.L. (1988) Brownian Dynamics of Cytochrome *c* and Cytochrome *c* Peroxidase Association, *Science* **241**, 67.

Nozaki, M., Mizushima, H., Horio, T., & Okunuki, T. (1958) Further Studies on Proteinase Digestion of Baker's Yeast Cytochrome *c*, *J. Biochem.* **45**, 815.

Ochi, H., Hata, Y., Tanaka, N., Kakudo, M., Sakurai, T., Aihara, S., & Morita, Y. (1983) Structure of Rice Ferricytochrome *c* at 2.0 Å Resolution, *J. Mol. Biol.* **166**, 407.

Pearce, L.L., Gärtner, A.L., Smith, M., & Mauk, A.G. (1989) Mutation-Induced Perturbation of the Cytochrome *c* Alkaline Transition, *Biochemistry* **28**, 3152.

Perrin, D.D., & Dempsey, B. (1974) Buffers for pH and Metal Ion Control, Chapman & Hall, London.

Pettigrew, G.W. (1972) The Amino Acid Sequence of a Cytochrome *c* from a Protozoan, *Crithidia Oncopelti* , *FEBS Letters* **22**, 64.

Pettigrew, G.W., Aviram, I., & Schejter, A. (1975) Physicochemical Properties of Two Atypical Cytochromes *c*, *Crithidia* Cytochrome *c*-557 and *Euglena* Cytochrome *c*-558, *Biochem. J.* **149**, 155.

Pettigrew, G.W., & Moore, G.R. (1987) *Cytochromes c: Biological Aspects*, Springer-Verlag, Heidelberg, 1987.

Pielak, G.J., Mauk, A.G., & Smith, M.S. (1985) Site Directed Mutagenesis of Cytochrome *c* Shows that an Invariant Phe is not Essential for Function, *Nature* **313**, 152.

Polastro, E.T., Deconnick, M.M., DeVogel, M.R., Mailier, E.L., Looze, Y.R., Schneck, A.G., & Leonis, J. (1978) Evidence that Trimethylation of Iso-1-cytochrome *c* from *Saccharomyces cerevisiae* affects Interaction with the Mitochondrion, *FEBS Lett.* **86**, 17.

Poulos, T.L., & Kraut, J. (1980) A Hypothetical Model of the Cytochrome *c* Peroxidase - Cytochrome *c* Electron Transfer Complex, *J. Biol. Chem.* **255**, 10322.

Przystas, T.J., & Sutin, N. (1973) Kinetic Studies of Anion Assisted Outer-Sphere Electron Transfer Reactions, *J. Am. Chem. Soc.* **95**, 5545.

Raphael A.L., & Gray, H.B. (1991) Semisynthesis of Axial Ligand (Position-80) Mutants of Cytochrome *c*, *J. Am. Chem. Soc.* **113**, 1038.

Reichlin, M., Fogel, S., Nisonhoff A., & Margoliash E. (1966) Antibodies against Cytochromes *c* from Vertebrates, *J. Biol. Chem.* **241**, 251.

Reid, L.S. (1984) Ph.D. Dissertation, University of British Columbia.

Reid, L.S., & Mauk, A.G. (1982) Kinetic Analysis of Cytochrome b_5 Reduction by $Fe(EDTA)^{2-}$, *J. Am. Chem. Soc.* **104**, 841.

Reid, L.S., Taniguchi, V.T., Gray, H.B., & Mauk, A.G. (1982) Oxidation-Reduction Equilibrium of Cytochrome b_5, *J. Am. Chem. Soc.* **104**, 7516.

Rieder, R., & Bosshard, H.R. (1980) Comparision of the Binding Sites for Cytochrome *c* Oxidase, Cytochrome bc_1, and Cytochrome c_1, *J. Biol. Chem.* **255**, 4732.

Rigby, S.E.J., Moore, G.R., Gray, J.C., Gadsby, P.M.A., George, S.J., & Thomson, A.J. (1988) NMR, EPR, and Magnetic-C.D. Studies on Cytochrome *f*: Identity of the Haem Axial Ligands, *Biochem. J.* **256**, 571.

Robinson, M.N., Boswell, A.P., Huang, Z., Eley, C.G.S., & Moore, G.R. (1983) The Conformation of Eukaryotic Cytochrome *c* around Residues 39, 57, 59 and 74, *Biochem. J.* **213**, 687.

Saigo, S. (1986) Isomerization and Denaturation of Homologous Cytochromes *c*; Correlation Between Local and Gross Conformational Changes, *J. Biochem (Japan)* **100**, 157.

Salemme, F.R. (1976) An Hypothetical Structure for an Intermolecular Electron Transfer Complex of Cytochrome *c* and Cytochrome b_5, *J. Mol. Biol.* **102**, 563.

Schejter, A., & Aviram, I. (1969) The Reaction of Cytochrome *c* with Imidazole, *Biochemistry* **8**, 149.

Schejter, A., Plotkin, B., & Vig, I. (1991) The Reactivity of Cytochrome *c* with Soft Ligands, *FEBS Letters* **280**, 199.

Schweingruber, M.E., Stewart, J.W., & Sherman, F. (1978) Amino Acid Replacements of the Evolutionarily Invariant Tryptophan at Position 64in Mutant Forms of Iso-1-cytochrome *c* from *Saccharomyces cerevisiae, J. Mol. Biol.* **118**, 481.

Scott, R.A., Mauk, A.G., & Gray, H.B. (1985) Experimental Approaches to Studying Biological Electron Transfer, *J. Chem. Ed.* **62**, 932.

Shechter, E., & Saludjian, P. (1967) Conformation of Ferricytochrome *c*. IV. Relationship Between Optical Absorption and Protein Conformation, *Biopolymers* **5**, 788.

Sherman, F., Stewart, J.W., Margoliash, E., Parker, J., & Campbell, W. (1966) The Structural Gene for Yeast Cytochrome *c*, *Proc. Natl. Acad. Sci. USA* **55**, 1498.

Sherman, F., Stewart, J.W., Jackson, M., Gilmore, R. A., & Parker, J.H. (1974) Mutants of Yeast Defective in Iso-1-cytochrome *c*, *Genetics* **77**, 255.

Shporer, M., Ron, G., Loewenstein, A., & Navon, G. (1965) Study of Some Cyano-Metal Complexes by Nuclear Magnetic Resonance. II. Kinetics of Electron Transfer between Ferri- and Ferrocyanide Ions, *Inorg. Chem.* **4**, 361.

Simpkin, D., Palmer, G., Devlin, F.J., McKenna, M.C., Jensen, G.M., & Stephens, P.J. (1989) The Axial Ligands of Heme in Cytochromes: A Near-I.R. Magnetic Circular Dichroism Study of Yeast Cytochromes *c*, c_1, and *b* and Spinach Cytochrome, *Biochemistry*, **28**, 8033.

Smith, M., Leung, D.W., Gillam., S., Astell, C.R., Montgomery, D.L., & Hall, B.D. (1979) Sequence of the Gene for Iso-1-cytochrome *c* in *Saccharomyces Cerevisiae*, *Cell* **16**, 753.

Stellwagen, E., Babul, J., & Wilgus, H. (1975) The Alkaline Isomerization of Lysine Modified Ferriytochrome *c*, *Biochim. Biophys. Acta* **405**, 115.

Sutin, N. (1973) Oxidation-Reduction in Coordination Compounds, in: *Inorganic Biochemistry*, G.I. Eichhorn, ed., Elsevier, Amsterdam.

Sutin, N., & Yandell, J.K. (1972) Mechanisms of the Reactions of Cytochrome *c*: Rate and Equlibrium Constants for Ligand Binding to Horse Heart Ferricytochrome *c*, *J. Biol. Chem.* **247**, 6932.

Takano, T. & Dickerson, R.E. (1981a) Conformation Change of Cytochrome *c*. I: Ferrocytochrome *c* Structure Refined at 1.5 Å Resolution *J. Mol. Biol.* **153**, 79.

Takano, T. & Dickerson, R.E. (1981b) Conformation Change of Cytochrome *c*. II: Ferricytochrome *c* Refinement at 1.8 Å and Comparision with the Ferrocytochrome Structure, *J. Mol. Biol.* **153**, 95.

Taniguchi, I., Toyosawa, K., Yamaguchi H., & Yasukouchi, K. (1982a) Voltammetric Response of Horse Heart Cytochrome *c* at a Gold Electrode in the Presence of Sulfur Bridged Bipyridines, *J. Electroanal. Chem.* **140**, 187.

Taniguchi, V.T., Ellis, W.R., Cammarata, J., Webb, J., Anson, F.C., & Gray, H.B. (1982b) Spectroelectrochemical Determination of the Temperature Dependence of Reduction Potentials, In *Electrochemical and Spectrochemical Studies of Biological Redox Components*, K.M. Kadish, ed., *Adv. Chem. Ser.* **201**, 51.

Theorell, H., & Åkesson, Å. (1941) Studies on Cytochrome *c* II. The Optical Properties of Pure Cytochrome *c* and Some of Its Derivatives, *J. Am. Chem. Soc.* **63**, 1812.

Tonge, P., Moore, G.R., & Wharton, C.W. (1989) Fourier-Transform Infra-Red Studies of the Alkaline Isomerization of Mitochondrial Cytochrome *c* and the Ionization of Carboxylic Acids, *Biochem. J.* **258**, 599.

Tsunasawa, S., & Sakujama, F. (1984) Amino-Terminal Acetylation of Proteins - an Overview, *Methods Enzymol.* **106**, 165.

Tuppy, H., & Paleus, S. (1955) Study of a Peptic Degradation Product of Cytochrome *c*. I. Purification and Chemical Composition, *Acta Chem. Scand.* **9**, 353.

Ulmer, D.D., & Kagi, J.H.R. (1968) Hydrogen-Deuterium Exchange of Cytochrome *c* I. Effect of Oxidation State, *Biochemistry* **7**, 2710.

Urry, D.W. (1965) Protein-Heme Interactions in Heme Proteins - Cytochrome *c*, *Proc. Natl. Acad Sci. USA* **54**, 640.

Vickery, L., Nozawa, T., & Sauer, K. (1976) MCD Studies of Low Spin Cytochromes. Temperature Dependence and Affects of Axial Coordination on the Spectra of Cytochrome *c* and Cytochrome b_5, *J. Am. Chem. Soc.* **98**, 351.

Vogel, A. (1978) Textbook of Practical Organic Chemistry, 4th Edition, Longman Group Ltd., London.

Wallace, C.J.A., Mascagni, P., Chait, B.T., Collawn, J.F., Paterson, Y., Proudfoot, A.E.I., & Kent S.B.H. (1989), Substitutions Engineered by Chemical Synthesis at Three Conserved Sites in Mitochondrial Cytochrome *c*; Thermodynamic and Functional Consequences, *J. Biol. Chem.* **264**, 15199.

Wallace, C.J.A., Guillemtte, J.G., Hibaya, Y., & Smith, M. (1991) Enhancing Protein Engineering Capabilities by Combining Mutagenesis and Semisynthesis, *J. Biol. Chem.* **266**, 21355.

Wendoloski, J.J., Matthew, J.B., Weber, P.C., & Salemme, F.R. (1987) Molecular Dynamics of a Cytochrome *c*-Cytochrome b_5 Electron Transfer Complex, *Science* **238**, 794.

Wherland, S., Holwerda, R.A., Rosenberg, R.C., & Gray, H.B. (1975) Kinetic Studies of the Reduction of Blue Copper Proteins by $Fe(EDTA)^{2-}$, *J. Am. Chem. Soc.* **97**, 5260.

Wherland, S., & Gray, H.B. (1976) Metalloprotein Electron Transfer Reactions: Analysis of Reactivity of Horse Heart Cytochrome *c* with Inorganic Complexes, *Proc. Natl. Acad. Sci. USA* **73**, 2950.

Wilkins, R.G., & Yelin, R.E. (1968) Electron Transfer Rate Studies of Metal Complexes of Ethylenediaminetetraacetate and *trans*-1,2-diaminocyclohexanetetraacetate, *Inorg. Chem.* **7**, 2667.

Williams, G., Moore, G.R., & Williams, R.J.P. (1985) Biological Electron Transfer: The Structure, Dynamics and Reactivity of Cytochrome *c*, *Comments Inorg. Chem.* **IV**, 55.

Wilson, M.T., & Greenwood, C. (1971) Studies on Ferricytochrome *c*. 2: A Correlation between Reducibility and the Possession of the 695 nm Absorption Band of Ferricytochrome *c*, *Eur. J. Biochem.* **22**, 11.

Wooten, J.B., Cohen, J.S., Vig, I., Schejter, A. (1981) pH Induced Conformational Transitions of Ferricytochrome *c*: A Carbon-13 and Deuterium NMR Study, *Biochemistry* **20**, 5394.

Yamanaka, T., Mizushima, H., Nozaki, M., Horio, T., Okunuki, K. (1959) Studies on Cytochrome *c*, *J. Biochem.* **46**, 121.

Yandell, J.K., Fay, D.P., & Sutin, N. (1973) Mechanisms of the Reactions of Cytochrome *c*. II. The Rate of Reduction of Horse-Heart Ferricytochrome *c* by Cr(II), *J. Am. Chem. Soc.* **95**, 1131.

Yee, E., Cave, R.J., Guyer, K.L., Tyma, P.D., & Weaver, M.J. (1979) A Survey of Ligand Effects upon the Reaction Entropies of Some Transition Metal Redox Complexes, *J. Am. Chem. Soc.* **101**, 1131.

Yeh, P., & Kuwana, T. (1977) Reversible Electrode Reaction of Cytochrome *c*, *Chem. Lett.*, 1145.

Zoller, M.J., & Smith, M. (1983) Oligonucleotide-Directed Mutagenesis, *Methods Enzymol.* **100**, 468.

APPENDIX A: ***Reduction Potential Measurements***

Protein	pH	Temperature (Kelvin)	E^0 (mV *vs* SHE)	ΔE_p (mV)
Horse heart cytochrome *c*	7.00	283.2	275.9	65
			276.9	65
		288.0	275.9	63
			274.9	63
		292.8	272.9	61
			272.9	61
		297.7	270.4	61
			269.9	61
		303.1	268.9	61
			268.9	61
		308.0	266.4	62
			267.4	62
		314.0	263.9	65
			262.9	63
Yeast iso-1-cytochrome *c*	5.50	298.0	290.9	63
			292.4	60
	6.00	283.0	295.9	59
		287.8	294.4	56
		293.0	292.4	58
		297.8	290.9	55
		297.8	287.9	58
		303.1	287.9	54
		307.9	285.9	55
		313.4	284.4	54
	7.00	298.0	277.0	56
			277.5	57
	7.00	298.0	281.5	61

Protein	pH	Temperature (Kelvin)	E^0 (mV *vs* SHE)	ΔE_p (mV)
Yeast iso-1 cytochrome *c*	7.41	298.0	272.4	68
	7.43		274.9	57
	7.78		271.9	55
	7.86		270.4	54
	7.89		269.9	55
Asn42Lys/Ala43His	5.46	298.0	279.4	56
	6.01		276.4	56
	6.47		272.4	60
	7.00		266.9	67
	7.49		263.4	61
	8.00		262.4	68
	8.46		261.4	70
Asn52Ala	5.50	298.0	262.4	60
			261.9	54
	6.00	282.9	262.4	54
			262.4	54
		287.9	260.9	55
		292.8	258.4	54
		297.9	257.4	54
			257.4	54
			257.4	56
		303.2	254.9	54
		307.9	253.4	54
		313.2	252.4	56
	6.48	298.0	253.4	54
	6.97		249.9	55
	7.36		246.4	56
	7.90		243.9	54

Protein	pH	Temperature (Kelvin)	E^0 (mV *vs* SHE)	ΔE_p (mV)
Ile75Met	5.57	298.0	249.4	60
	6.00	282.3	255.4	64
			254.4	62
		287.6	249.9	57
			250.4	58
		292.8	247.4	56
			247.9	55
		298.0	245.4	54
			244.9	54
			244.9	83
		303.0	243.4	58
			244.9	57
		308.1	241.4	56
			240.9	57
		313.7	237.4	60
			237.4	60
	6.52	298.0	242.9	63
	7.02		235.9	71
	7.04		235.9	63
	7.47		231.4	66
	7.84		229.4	70
	8.16		228.4	80
Thr78Gly	6.00	281.5	254.9	59
		281.2	252.4	60
		288.0	252.4	62
			253.9	61
		293.0	251.4	62
		298.0	249.4	62
		302.9	248.9	63

Protein	pH	Temperature (Kelvin)	E^0 (mV *vs* SHE)	ΔE_p (mV)
Thr78Gly		307.9	247.4	62
		314.4	244.4	76
Phe82Ala	6.00	283.1	265.9	63
			266.9	61
		288.2	264.4	60
			263.9	61
		293.1	261.9	61
			261.9	61
		298.0	260.4	60
			260.4	60
		307.9	257.4	72
			257.9	73
Phe82Gly	6.00	283.2	252.4	54
			253.4	54
		288.0	251.4	54
			251.4	54
		293.2	249.4	54
			249.4	54
		298.1	247.9	54
			248.4	54
		303.0	245.4	54
		303.0	246.9	54
		307.8	243.9	55
			244.9	54
		313.4	242.9	59
			241.9	57

Protein	pH	Temperature (Kelvin)	E^0 (mV *vs* SHE)	ΔE_p (mV)
Phe82Ile	6.00	283.0	282.9	59
			282.4	64
			282.4	60
		288.0	278.9	55
			287.9	57
		293.0	276.4	54
			276.4	56
		298.0	273.4	54
			273.4	56
		303.0	271.4	54
			271.9	55
		307.9	268.9	55
			269.4	56
		313.3	265.4	54
			266.4	56
Phe82Leu	6.00	283.0	292.9	61
		287.9	290.9	61
		290.6	290.4	60
		293.0	289.4	60
		295.5	287.4	60
		298.1	286.9	59
		303.1	284.4	60
		308.1	280.4	62
		313.2	277.4	69
Phe82Ser	6.00	283.1	263.4	58
		287.9	260.9	57
		292.9	257.9	53
		297.7	255.9	57

Protein	pH	Temperature (Kelvin)	E^0 (mV *vs* SHE)	ΔE_p (mV)
Phe82Ser		298.0	254.4	56
		303.5	252.9	54
	6.00	307.8	252.4	76
		313.2	246.4	56
	6.48	298.0	248.4	54
	6.99		239.9	55
			241.4	56
	7.42	298.0	236.4	60
			237.4	60
	7.88		234.4	54
			231.4	54
	8.17		231.9	55
Phe82Tyr	6.00	283.0	286.4	54
		287.9	284.4	56
		292.9	292.9	57
		297.8	280.4	54
		303.0	279.4	54
		307.9	277.4	54
		313.2	275.4	62

APPENDIX B *Fe(edta)$^{2-}$ Reduction Kinetic Data*

Protein	Temperature (Kelvin)	[Fe(edta)2-] (mM)	k_{obs} (s^{-1})
Horse Heart cytochrome *c*	298.0	0.05	1.36 ± 0.01
		0.10	2.93 ± 0.01
		0.15	4.43 ± 0.01
		0.20	6.05 ± 0.02
		0.25	7.53 ± 0.04
		0.50	13.6 ± 0.1
Yeast iso-1-cytochrome *c*	283.0	0.20	10.12 ± 0.04
	290.2		11.11 ± 0.04
	298.0	0.05	2.72 ± 0.01
		0.10	7.08 ± 0.03
		0.15	10.25 ± 0.07
	298.0	0.20	13.49 ± 0.05
		0.20	13.72 ± 0.04
		0.25	18.68 ± 0.08
		0.50	32.6 ± 0.4
	303.2	0.20	15.94 ± 0.06
	308.6		17.83 ± 0.06
	313.8		19.96 ± 0.05
Asn52Ala	282.8	0.05	2.18 ± 0.02
			2.32 ± 0.02
	287.8		2.46 ± 0.02
			2.72 ± 0.03
	293.2		3.10 ± 0.02
			3.23 ± 0.02
	298.0	0.05	3.69 ± 0.03
			3.53 ± 0.03

Protein	Temperature (Kelvin)	[Fe(edta)2-] (mM)	k_{obs} (s^{-1})
Asn52Ala	298	0.05	4.06 ± 0.01
		0.10	8.72 ± 0.05
		0.15	14.04 ± 0.07
		0.20	18.6 ± 0.1
		0.25	22.7 ± 0.2
		0.50	42.9 ± 0.4
	303.2	0.05	4.77 ± 0.03
			4.81 ± 0.04
	308.8		5.63 ± 0.04
			5.76 ± 0.04
Ile75Met	283.5	0.10	1.65 ± 0.01
	287.7		2.07 ± 0.01
	292.7		2.57 ± 0.02
	298.0	0.05	2.07 ± 0.01
		0.10	3.77 ± 0.02
			3.50 ± 0.02
		0.15	6.23 ± 0.02
		0.20	8.94 ± 0.04
		0.25	11.83 ± 0.07
		0.50	19.7 ± 0.1
	302.8	0.10	4.17 ± 0.04
	308.0	0.10	4.91 ± 0.03
Thr78Gly	283.8	0.20	6.58 ± 0.05
	288.4		8.2 ± 0.1
	294.0		10.1 ± 0.2
	298.0	0.05	2.36 ± 0.02
		0.10	5.2 ± 0.1

Protein	Temperature (Kelvin)	[Fe(edta)2-] (mM)	k_{obs} (s^{-1})
Thr78Gly	298.0	0.15	9.1 ± 0.1
		0.20	13.1 ± 0.2
		0.20	12.2 ± 0.2
		0.25	15.2 ± 0.1
		0.50	29.3 ± 0.3
	303.4	0.20	13.1 ± 0.2
	308.4		14.6 ± 0.2
	316.4		15.6 ± 0.2
Phe82Ala	283.0	0.20	13.99 ± 0.05
	288.0		15.30 ± 0.04
	293.0		16.97 ± 0.06
	298.0	0.05	4.84 ± 0.02
		0.10	9.84 ± 0.05
		0.15	14.83 ± 0.07
		0.20	19.75 ± 0.05
			21.06 ± 0.08
		0.25	25.1 ± 0.1
		0.50	47.5 ± 0.1
	303.4	0.20	20.8 ± 0.1
	309.4		21.4 ± 0.1
Phe82Gly	283.4	0.20	19.76 ± 0.04
	288.2		21.67 ± 0.08
	293.0		23.76 ± 0.05
	298.0	0.05	6.46 ± 0.04
		0.10	13.71 ± 0.05
		0.15	21.41 ± 0.06
		0.20	28.24 ± 0.05
		0.20	26.72 ± 0.06

Protein	Temperature (Kelvin)	[Fe(edta)2-] (mM)	k_{obs} (s^{-1})
Phe82Gly	298.0	0.25	32.86 ± 0.07
		0.50	65.9 ± 0.2
	303.8	0.20	29.19 ± 0.07
	308.6		31.6 ± 0.1
Phe82Ile	283.6	0.20	12.39 ± 0.04
	288.7		14.09 ± 0.04
	293.0		16.60 ± 0.04
	298.0	0.05	4.28 ± 0.02
		0.10	8.87 ± 0.04
		0.15	14.62 ± 0.04
		0.20	18.58 ± 0.06
			18.99 ± 0.05
		0.25	24.68 ± 0.04
		0.50	45.33 ± 0.07
	304.0	0.20	19.1 ± 0.3
	308.2		19.3 ± 0.2
Phe82Leu	283.0	0.20	10.31 ± 0.04
	289.2		12.48 ± 0.03
	294.6		15.55 ± 0.07
	298.0	0.05	3.71 ± 0.07
		0.10	7.5 ± 0.1
		0.15	14.5 ± 0.1
		0.20	18.9 ± 0.1
		0.25	23.8 ± 0.3
		0.50	44.4 ± 0.4
	299.8	0.20	18.26 ± 0.09
	305.0		19.5 ± 0.2
			20.2 ± 0.2

Protein	Temperature (Kelvin)	[Fe(edta)2-] (mM)	k_{obs} (s^{-1})
Phe82Leu	311.2	0.20	22.2 ± 0.2
Phe82Ser	283.2	0.20	24.1 ± 0.2
	289.8		25.9 ± 0.3
	293.2		27.4 ± 0.2
	298.0	0.05	7.51 ± 0.09
		0.10	14.8 ± 0.1
		0.20	30.0 ± 0.3
			28.9 ± 0.3
		0.25	37.5 ± 0.4
		0.50	73.9 ± 0.6
	304.4	0.20	31.5 ± 0.3
	308.8		32.9 ± 0.2
Phe82Tyr	283.6	0.20	7.39 ± 0.04
	289.6		9.53 ± 0.04
	298.0	0.05	2.84 ± 0.01
		0.10	6.07 ± 0.03
		0.15	8.96 ± 0.05
		0.20	12.21 ± 0.06
		0.25	15.31 ± 0.08
		0.50	30.0 ± 0.2
	298.6	0.20	11.79 ± 0.05
			12.53 ± 0.04
	303.8		13.67 ± 0.05
			14.05 ± 0.06
	309.6		15.64 ± 0.06
			15.83 ± 0.06

APPENDIX C *$Co(phen)_3Cl_3$ Oxidation Kinetic Data*

Protein	Temperature (Kelvin)	$[Co(phen)_3Cl_3]$ (mM)	k_{obs} (s^{-1})
Horse Heart cytochrome *c*	298.0	0.20	0.299 ± 0.0003
			0.301 ± 0.0003
		0.40	0.599 ± 0.0003
			0.599 ± 0.0003
		0.80	1.197 ± 0.001
			1.204 ± 0.002
		1.00	1.487 ± 0.002
		1.20	1.771 ± 0.001
			1.771 ± 0.002
		1.40	2.064 ± 0.002
			2.089 ± 0.002
		1.60	2.350 ± 0.003
			2.390 ± 0.003

Protein	Temperature (Kelvin)	$[Co(phen)_3Cl_3]$ (mM)	k_{obs} (s^{-1})
Yeast iso-1-cytochrome *c*	283.5	1.00	0.597 ± 0.0003
			0.593 ± 0.0003
	288.3		0.775 ± 0.0004
			0.788 ± 0.0005
	293.0	1.00	1.073 ± 0.001
			1.088 ± 0.001
	298.0	0.20	0.310 ± 0.0003
			0.317 ± 0.0003
		0.40	0.695 ± 0.001
			0.705 ± 0.001
		0.80	1.350 ± 0.002
			1.377 ± 0.002
		1.00	1.702 ± 0.002
			1.741 ± 0.002
			1.523 ± 0.001
			1.529 ± 0.001
		1.20	2.027 ± 0.003
			2.061 ± 0.003
			2.024 ± 0.004
		1.40	2.404 ± 0.003
			2.417 ± 0.003
		1.60	2.729 ± 0.004
			2.762 ± 0.004
	303.3	1.00	2.206 ± 0.002
			2.250 ± 0.002
	308.3		2.910 ± 0.009
			3.160 ± 0.005
			3.178 ± 0.005
	313.3		4.21 ± 0.01
			4.415 ± 0.005

Protein	Temperature (Kelvin)	$[Co(phen)_3Cl_3]$ (mM)	k_{obs} (s^{-1})
Asn52Ala	283.0	1.00	2.483 ± 0.003
	288.0		3.308 ± 0.004
			3.314 ± 0.004
	293.0		4.370 ± 0.003
			4.365 ± 0.004
	298.0	0.20	1.233 ± 0.001
			1.221 ± 0.001
		0.40	2.505 ± 0.002
			2.516 ± 0.002
		0.80	5.093 ± 0.006
			4.987 ± 0.005
		1.00	6.031 ± 0.005
			5.985 ± 0.009
	298.0	1.00	5.663 ± 0.005
			5.707 ± 0.006
		1.20	7.49 ± 0.01
			7.45 ± 0.01
		1.40	8.52 ± 0.01
			8.54 ± 0.01
		1.60	9.87 ± 0.02
			9.81 ± 0.02
	303.0	1.00	7.75 ± 0.01
			7.73 ± 0.01
	308.2		9.96 ± 0.03
			10.94 ± 0.02
	313.0		14.46 ± 0.04
			13.74 ± 0.04

Protein	Temperature (Kelvin)	$[Co(phen)_3Cl_3]$ (mM)	k_{obs} (s^{-1})
Tyr67Phe	283.5	1.00	6.139 ± 0.005
	288.4		8.384 ± 0.01
			8.159 ± 0.01
	293.1		10.84 ± 0.01
			10.89 ± 0.01
	298.0	0.20	2.952 ± 0.005
			3.006 ± 0.004
		0.40	5.716 ± 0.01
			6.156 ± 0.02
		0.80	11.92 ± 0.05
			12.38 ± 0.04
		1.00	14.79 ± 0.05
			15.10 ± 0.05
			14.42 ± 0.03
			14.18 ± 0.03
	298.0	1.00	14.75 ± 0.05
		1.20	18.47 ± 0.06
			18.55 ± 0.06
		1.40	20.55 ± 0.07
			22.04 ± 0.09
		1.60	25.23 ± 0.09
			25.1 ± 0.1
	303.2	1.00	20.3 ± 0.1
	308.2		27.7 ± 0.1
			27.6 ± 0.1
	313.2		36.8 ± 0.1
			36.8 ± 0.1

Protein	Temperature (Kelvin)	$[Co(phen)_3Cl_3]$ (mM)	k_{obs} (s^{-1})
Ile75Met	283.0	1.00	1.374 ± 0.002
	288.0		1.876 ± 0.002
			1.871 ± 0.002
	293.0		2.646 ± 0.003
			2.605 ± 0.004
			2.725 ± 0.002
	298.0	0.20	0.767 ± 0.001
			0.772 ± 0.001
		0.40	1.558 ± 0.003
			1.576 ± 0.004
		0.80	3.237 ± 0.005
			3.257 ± 0.005
		1.00	3.997 ± 0.007
			3.985 ± 0.009
			3.882 ± 0.004
			3.887 ± 0.006
		1.20	4.72 ± 0.01
			4.77 ± 0.01
		1.40	5.60 ± 0.01
			5.65 ± 0.01
		1.60	6.21 ± 0.02
			6.62 ± 0.02
	303.0	1.00	5.45 ± 0.01
			5.43 ± 0.01
	308.0		7.37 ± 0.02
			7.78 ± 0.02
	313.0		10.31 ± 0.05
			11.48 ± 0.04
			11.61 ± 0.04

Protein	Temperature (Kelvin)	$[Co(phen)_3Cl_3]$ (mM)	k_{obs} (s^{-1})
Thr78Gly	283.0	1.00	1.936 ± 0.005
	288.5		2.708 ± 0.003
			2.820 ± 0.005
	293.2		3.556 ± 0.008
			3.572 ± 0.009
	298.0	0.20	1.099 ± 0.003
			1.105 ± 0.002
		0.40	2.156 ± 0.007
			2.189 ± 0.005
		0.80	4.30± 0.01
			4.56 ± 0.01
		1.00	5.67 ± 0.02
			5.55 ± 0.02
			4.99 ± 0.02
			4.96 ± 0.02
		1.20	6.49 ± 0.02
			6.75 ± 0.03
		1.40	7.96 ± 0.03
			7.87 ± 0.03
		1.60	8.65 ± 0.04
			9.20 ± 0.04
	303.0	1.00	6.40 ± 0.02
			6.63 ± 0.02
			6.53 ± 0.03

Protein	Temperature (Kelvin)	$[Co(phen)_3Cl_3]$ (mM)	k_{obs} (s^{-1})
Phe82Gly	283.5	1.00	2.729 ± 0.004
			2.815 ± 0.006
	288.5		3.529 ± 0.006
			3.526 ± 0.006
	293.1		4.64 ± 0.01
			4.623 ± 0.008
	298.0	0.20	1.141 ± 0.004
			1.173 ± 0.003
		0.40	2.596 ± 0.006
			2.620 ± 0.007
		0.80	5.05 ± 0.01
			5.20 ± 0.01
		1.00	6.60 ± 0.02
			6.35 ± 0.02
			6.08 ± 0.01
			6.16 ± 0.01
		1.20	7.97 ± 0.02
			7.61 ± 0.03
		1.40	8.60 ± 0.04
			9.19 ± 0.03
		1.60	9.76 ± 0.04
			10.20 ± 0.04
	303.5	1.00	7.96 ± 0.02
			7.80 ± 0.03
	308.2		9.79 ± 0.05
			9.79 ± 0.06
			9.79 ± 0.06
	313.3		13.54 ± 0.05
			12.96 ± 0.06

Protein	Temperature (Kelvin)	$[Co(phen)_3Cl_3]$ (mM)	k_{obs} (s^{-1})
Phe82Ile	283.5	1.00	2.137 ± 0.003
			2.184 ± 0.004
	288.0		2.941 ± 0.007
			2.956 ± 0.007
	293.0		4.032 ± 0.007
			4.068 ± 0.007
	298.0	0.20	1.050 ± 0.002
			1.079 ± 0.002
		0.40	2.335 ± 0.006
			2.361 ± 0.007
		0.80	4.68 ± 0.01
			4.87 ± 0.01
		1.00	5.72 ± 0.02
			5.87 ± 0.01
			5.70 ± 0.01
			5.78 ± 0.01
		1.20	7.12 ± 0.02
			7.09 ± 0.02
		1.40	8.38 ± 0.02
			8.41 ± 0.02
		1.60	9.59 ± 0.02
			9.78 ± 0.02
	303.3	1.00	7.94 ± 0.01
			7.95 ± 0.02
	308.4		11.17 ± 0.02
			11.53 ± 0.03
			11.37 ± 0.03
	313.1		15.21 ± 0.05
			14.75 ± 0.05

Protein	Temperature (Kelvin)	$[Co(phen)_3Cl_3]$ (mM)	k_{obs} (s^{-1})
Phe82Leu	283.5	1.00	0.784 ± 0.002
			0.761 ± 0.002
	288.2		1.089 ± 0.002
			1.059 ± 0.002
	293.0		1.472 ± 0.002
			1.491 ± 0.002
	298.0	0.20	0.425 ± 0.001
			0.438 ± 0.001
		0.40	0.933 ± 0.005
			0.973 ± 0.006
		0.80	1.895 ± 0.008
			1.895 ± 0.008
		1.00	2.23 ± 0.01
			2.30 ± 0.01
			2.09 ± 0.004
			2.153 ± 0.004
		1.20	2.84 ± 0.02
			2.77 ± 0.02
		1.40	3.19 ± 0.03
			2.93 ± 0.03
	303.0	1.00	3.130 ± 0.007
			3.014 ± 0.006
			3.108 ± 0.007
	308.0		4.11 ± 0.01
			4.24 ± 0.01
			4.16 ± 0.01
	313.3		5.87 ± 0.02
			5.83 ± 0.02
			6.15 ± 0.02

Protein	Temperature (Kelvin)	$[Co(phen)_3Cl_3]$ (mM)	k_{obs} (s^{-1})
Phe82Ser	283.5	1.00	2.048 ± 0.002
			2.045 ± 0.003
	288.0		2.673 ± 0.005
			2.684 ± 0.005
	293.2		3.947 ± 0.009
			4.010 ± 0.006
			3.917 ± 0.007
	298.0	0.20	0.951 ± 0.002
			0.938 ± 0.002
		0.40	2.184 ± 0.004
			2.143 ± 0.004
		0.80	4.151 ± 0.009
			4.224 ± 0.009
		1.00	4.95 ± 0.01
			5.01 ± 0.01
			5.35 ± 0.01
			5.36 ± 0.01
		1.20	5.93 ± 0.02
			6.20 ± 0.02
		1.40	7.30 ± 0.02
			7.54 ± 0.01
		1.60	8.54 ± 0.02
			8.61 ± 0.02
	303.0	1.00	7.281 ± 0.02
			7.307 ± 0.009
	308.2		9.63 ± 0.02
			9.68 ± 0.02
			9.94 ± 0.02
	313.3		13.18 ± 0.04
			13.82 ± 0.03

Protein	Temperature (Kelvin)	$[Co(phen)_3Cl_3]$ (mM)	k_{obs} (s^{-1})
Phe82Tyr	283.4	1.00	0.866 ± 0.001
			0.836 ± 0.001
	288.3		1.097 ± 0.001
			1.105 ± 0.001
	293.0		1.512 ± 0.001
			1.539 ± 0.001
	298.0	0.20	0.423 ± 0.001
			0.432 ± 0.001
		0.40	0.963 ± 0.002
			0.954 ± 0.002
		0.80	1.898 ± 0.002
			1.900 ± 0.002
		1.00	2.313 ± 0.003
			2.379 ± 0.003
			2.168 ± 0.002
			2.193 ± 0.002
		1.20	2.788 ± 0.006
			2.822 ± 0.003
		1.40	3.215 ± 0.006
			3.245 ± 0.005
		1.60	3.772 ± 0.007
			3.747 ± 0.005
	303.1	1.00	3.031 ± 0.006
			3.07 ± 0.01
	308.0		4.269 ± 0.004
			4.278 ± 0.007
			4.280 ± 0.006
	313.4		5.88 ± 0.02

APPENDIX D ***pH Jump Kinetic Data***

Protein	pH	k_{obs} (s^{-1})
Horse Heart cytochrome *c*	6.1	0.035 ± 0.001
	8.99	0.071 ± 0.001
	9.18	0.083 ± 0.001
		0.086 ± 0.001
	9.50	0.136 ± 0.002
	9.70	0.192 ± 0.003
	9.99	0.328 ± 0.005
	10.5	0.89 ± 0.01
Yeast iso-1-cytochrome *c*	5.9	0.043 ± 0.001
	8.99	0.150 ± 0.001
	9.53	0.445 ± 0.002
	10.01	1.47 ± 0.01
	10.51	4.7 ± 0.03 (61 %) 45 ± 1 (39 %)
	10.88	7.2 ± 0.2 (32 %) 37 ± 1 (68 %)
Thr78Gly	6.00	0.047 ± 0.001
	7.45	0.148 ± 0.003
	7.65	0.199 ± 0.003
	7.95	0.333 ± 0.003
	8.14	0.508 ± 0.004
	8.53	1.03 ± 0.01
	8.72	1.345 ± 0.006
	8.98	1.90 ± 0.02

Protein	pH	k_{obs} (s^{-1})
Asn52Ala	6.00	0.007 ± 0.001
	9.55	0.204 ± 0.002
	9.72	0.387 ± 0.002
	9.74	0.364 ± 0.002
	9.82	0.435 ± 0.003
	9.90	0.633 ± 0.003
	10.03	0.761 ± 0.004
	10.10	0.989 ± 0.005
	10.23	1.586 ± 0.009
	10.32	1.817 ± 0.006
	10.46	3.27 ± 0.01
	10.64	5.25 ± 0.03 50 ± 2
	10.83	7.35 ± 0.04 45 ± 1
Ile75Met	6.08	0.041 ± 0.001
	8.48	0.074 ± 0.001
		0.086 ± 0.001
	8.98	0.177 ± 0.001
		0.167 ± 0.001
	9.43	0.392 ± 0.002
		0.396 ± 0.002
	9.88	1.080 ± 0.007
		1.114 ± 0.008
	10.27	2.18 ± 0.02
		2.10 ± 0.02

APPENDIX E ***Azide Binding Kinetic Data***

Protein	[Azide] (M)	k_{obs} (s^{-1})
Horse Heart cytochrome *c*	0.05	7.31 ± 0.08
		7.42 ± 0.08
	0.10	9.23 ± 0.06
		8.83 ± 0.06
	0.20	10.23 ± 0.09
		11.15 ± 0.07
	0.25	12.27 ± 0.08
		12.22 ± 0.06
	0.30	12.82 ± 0.08
		13.03 ± 0.06
	0.40	14.82 ± 0.05
		14.77 ± 0.06
	0.50	16.76 ± 0.07
		17.37 ± 0.06
Yeast iso-1-cytochrome *c*	0.05	3.20 ± 0.02
	0.10	4.31 ± 0.02
	0.20	6.77 ± 0.03
	0.25	7.85 ± 0.04
	0.30	8.48 ± 0.05
	0.40	11.00 ± 0.04
	0.50	13.13 ± 0.07

Protein	[Azide] (M)	k_{obs} (s^{-1})
Asn52Ala	0.05	4.94 ± 0.02
		5.22 ± 0.02
	0.10	6.63 ± 0.02
		6.53 ± 0.03
	0.20	8.94 ± 0.03
		8.83 ± 0.03
	0.25	9.95 ± 0.04
		9.81 ± 0.04
	0.30	10.98 ± 0.04
		11.20 ± 0.04
	0.40	13.03 ± 0.04
		13.18 ± 0.04
	0.50	15.09 ± 0.04
		15.04 ± 0.04
Tyr67Phe	0.10	11.7 ± 0.2
		11.9 ± 0.2
	0.20	12.7 ± 0.1
	0.25	13.1 ± 0.1
	0.30	13.6 ± 0.1
	0.40	14.7 ± 0.1
	0.50	15.7 ± 0.1
Ile75Met	0.05	5.12 ± 0.07
	0.10	6.45 ± 0.04
	0.20	10.33 ± 0.06
	0.25	10.84 ± 0.07
	0.30	13.1 ± 0.1
	0.40	16.34 ± 0.07
	0.50	19.7 ± 0.1

Protein	[Azide] (M)	k_{obs} (s^{-1})
Phe82Gly	0.05	26.3 ± 0.3
		27.1 ± 0.3
	0.10	44.3 ± 0.4
		44.1 ± 0.4
	0.20	83 ± 1
		80.4 ± 0.6
	0.30	106 ± 1
		102 ± 1
	0.40	131 ± 2
		139 ± 2
	0.5	142 ± 2
		140 ± 2
Phe82Leu	0.05	16.1 ± 0.2
		15.5 ± 0.2
	0.10	27.2 ± 0.5
		25.7 ± 0.2
	0.20	40.2 ± 0.3
		40.4 ± 0.3
	0.30	53.9 ± 0.5
		55.8 ± 0.5
	0.40	68.6 ± 0.7
		71.0 ± 0.8
	0.50	82 ± 1
		88 ± 1
Phe82Ile	0.05	9.6 ± 0.1
		9.6 ± 0.1

Protein	[Azide] (M)	k_{obs} (s^{-1})
Phe82Ile	0.10	14.5 ± 0.1
		15.4 ± 0.1
		14.8 ± 0.1
	0.15	18.6 ± 0.1
		18.9 ± 0.1
	0.25	27.6 ± 0.2
		26.6 ± 0.2
	0.30	34.6 ± 0.3
		32.3 ± 0.2
	0.40	45.3 ± 0.5
		44.0 ± 0.5
	0.50	44.7 ± 0.4
		52.0 ± 0.5
Phe82Ser	0.05	22.6 ± 0.2
		24.0 ± 0.1
	0.10	37.7 ± 0.2
		37.3 ± 0.3
	0.20	60.5 ± 0.6
		58.2 ± 0.6
	0.30	77.9 ± 0.5
		78.3 ± 0.6
	0.40	96 ± 1
		102 ± 1
	0.50	117 ± 2
		115 ± 1
Phe82Tyr	0.05	6.46 ± 0.07
		6.70 ± 0.06
	0.10	9.30 ± 0.06
		9.44 ± 0.08

Protein	[Azide] (M)	k_{obs} (s^{-1})
Phe82Tyr	0.20	13.90 ± 0.07
		12.99 ± 0.08
	0.30	17.39 ± 0.08
		16.76 ± 0.09
	0.40	20.4 ± 0.1
		21.0 ± 0.2
	0.50	23.7 ± 0.1
		23.7 ± 0.2